Testing Stationarity and Change Point Detection in Reinforcement Learning

Mengbing Li[1], Chengchun Shi[2], Zhenke Wu[3], and Piotr Fryzlewicz[4]

[1,3]University of Michigan, Ann Arbor
[2,4]London School of Economics and Political Science

Abstract

We consider reinforcement learning (RL) in possibly nonstationary environments. Many existing RL algorithms in the literature rely on the stationarity assumption that requires the state transition and reward functions to be constant over time. However, this assumption is restrictive in practice and is likely to be violated in a number of applications, including traffic signal control, robotics and mobile health. In this paper, we develop a model-free test to assess the stationarity of the optimal Q-function based on pre-collected historical data, without additional online data collection. Based on the proposed test, we further develop a change point detection method that can be naturally coupled with existing state-of-the-art RL methods designed in stationary environments for online policy optimization in nonstationary environments. The usefulness of our method is illustrated by theoretical results, simulation studies, and a real data example from the 2018 Intern Health Study. A Python implementation of the proposed procedure is publicly available at https://github.com/limengbinggz/CUSUM-RL.

1 Introduction

Reinforcement learning [RL, see Sutton and Barto, 2018, for an overview] is a powerful machine learning technique that allows an agent to learn and interact with a given environment, to maximize the cumulative reward the agent receives. It has been one of the most popular research topics in the machine learning and computer science literature over the past few years. Significant progress has been made in solving challenging problems across various domains using RL, including games, recommender systems, finance, healthcare, robotics, transportation, among many others [see Li, 2019, for an overview]. In contrast, statistics as a field has only begun to engage with RL both in depth and in breadth. Most RL works in the statistics literature focused on developing data-driven methodologies for precision medicine [see e.g., Murphy, 2003, Robins, 2004, Chakraborty et al., 2010, Qian and Murphy, 2011, Zhang et al., 2013, Zhao et al., 2015, Wallace and Moodie, 2015, Song et al., 2015, Luedtke and van der

Laan, 2016, Zhu et al., 2017, Zhang et al., 2018, Shi et al., 2018a,b, Wang et al., 2018, Qi et al., 2020, Nie et al., 2021, Fang et al., 2023]. See also Tsiatis et al. [2019] and Kosorok and Laber [2019] for overviews. These aforementioned methods were primarily motivated by applications in precision medicine with only a few treatment stages. They require a large number of patients in the observed data to achieve consistent estimation and become ineffective in the long- or infinite-horizon setting where the number of decision stages diverges with the number of observations. The latter setting is widely studied in the RL literature to formulate many sequential decision making problems in games, robotics, ridesharing, etc. Recently, several algorithms have been proposed in the statistics literature for policy optimization or evaluation in long horizon settings [Ertefaie and Strawderman, 2018, Liao et al., 2021, Luckett et al., 2020, Hu et al., 2021, Ramprasad et al., 2021, Liao et al., 2022, Shi et al., 2022, Hu and Wager, 2023, Liu et al., 2023, Wang et al., 2023a, Chen et al., 2024, Li et al., 2024, Shi et al., 2024a, Zhou et al., 2024, Bian et al., 2025].

Central to the empirical validity of most existing state-of-the-art RL algorithms is the stationarity assumption that requires the state transition and reward functions to be constant functions of time. Although this assumption is valid in online video games, it can be violated in a number of other applications, including traffic signal control [Padakandla et al., 2020], robotic navigation [Niroui et al., 2019], mobile health [mHealth, Liao et al., 2020], e-commerce [Chen et al., 2020] and infectious disease control [Cazelles et al., 2018]. According to Sutton and Barto [2018], "*nonstationarity is the case most commonly encountered in reinforcement learning*". It is also a key challenge in lifelong RL where the tasks presented to the agent change over time [Silver et al., 2013]. We consider a few examples to elaborate the violation of the stationarity assumption.

One motivating example considered in our paper comes from the Intern Health Study [IHS; NeCamp et al., 2020]. The period of medical internship, which marks the initial phase of professional medical training in the United States, is a highly demanding and stressful time for physicians. During this phase, residents are confronted with challenging decisions, extended work hours, and sleep deprivation. In this ongoing prospective longitudinal study, one primary objective is to determine the optimal timing for providing smartphone-delivered interventions. These interventions send mobile prompts through a customized study app, aimed at offering timely tips to encourage interns to adopt anti-sedentary routines that may enhance their physical well-being. Nonstationarity poses a significant challenge within the context of the mHealth study. Specifically, as individuals receive mobile-delivered interventions for longer duration, they may habituate to the prompts or become overwhelmed, resulting in reduced responsiveness to the contents of the suggestions [Klasnja et al., 2019, Qian et al., 2022]. Consequently, the treatment effect of activity suggestions may transition from positive to negative over time. To maximize the effectiveness of interventions, ideal treatment policies would be those adapting swiftly to the current circumstances of the subjects based on the most recent data collected. Failing to recognize potential nonstationarity in treatment effects over time may lead to policies that overburden medical interns, resulting in app deletion and study dropouts.

As another example, the coronavirus disease 2019 (COVID-19) emerged as one of the most severe global pandemics in history and infected hundreds of millions of people worldwide. In

response to this crisis, there was a growing interest in utilizing RL to develop data-driven intervention policies to contain the spread of the virus [see e.g., Eftekhari et al., 2020, Kompella et al., 2020, Wan et al., 2020]. However, the dynamics of COVID-19 transmission were highly intricate and exhibited nonstationary over time. Initially, strict lockdown measures were proven to be highly effective in controlling the spread of the virus [Kharroubi and Saleh, 2020]. However, these measures had significant economic costs [Eichenbaum et al., 2020]. As effective vaccines were developed and a substantial proportion of the population became vaccinated, a natural inclination was to ease these lockdown restrictions. Nonetheless, the efficacy of the vaccine was likely to diminish over time, particularly in the presence of new viral variants. To summarize, policymakers needed to dynamically adapt public health policies by taking the nonstationary nature of the COVID-19 spread into consideration, in order to enhance global health outcomes while carefully balancing the negative impacts on the economy and society.

In this paper, we consider situations where the optimal Q-function Q^{opt} (the expected cumulative reward under the optimal policy, see Section 2.3 for its detailed definition) is possibly nonstationary, as a result of potential changes in the state transition or reward functions. These functions can change at an arbitrarily unknown time point (referred to as a change point), and the changes can be abrupt or smooth. A number of time series works have focused on testing the stationarity of a given time series and detecting the change point locations in various models, ranging from the simple piecewise-constant signal plus noise setting [Killick et al., 2012, Fryzlewicz, 2014] to complex high-dimensional panel data and time series [Cho and Fryzlewicz, 2015, Wang and Samworth, 2018]; see Aminikhanghahi and Cook [2017] and Truong et al. [2020] for comprehensive reviews. Different from the aforementioned works in time series, Q^{opt} takes a state-action pair as input. To test its stationarity, we need to check whether it is constant over time, for each possible value of the state-action pair.

Our methodological contributions are summarized as follows:

1. We propose a novel test to assess the stationarity of the optimal Q-function. To the best of our knowledge, this is the first work on developing statistically sound tests for stationarity in offline RL – a domain where policies are learned from previously collected datasets, instead of actively collected data in real-time as in online RL. Our proposal is an example of harnessing the power of classical statistical inferential tools such as hypothesis testing to help address an important practical issue in RL.

2. We apply our proposed test to compute p-values and identify the most recent historical change point location from a set of potential change point candidates for subsequent online policy learning in nonstationary environments.

Our technical contributions are summarized as follows:

1. We present and systematically examine various types of stationarity assumptions, analyzing their interrelationships.

2. We establish the size and power properties of the proposed tests under a bidirectional asymptotic framework that allows either the number of data trajectories or the number of

decision points per trajectory to diverge to infinity. This is useful for different types of applications. For example, disease management studies using registry data [e.g., Cooperberg et al., 2004] or infectious disease control studies [e.g., Lopes-Júnior et al., 2020] often involve a large number of subjects and the objective is to develop an optimal policy at the population level to maximize the overall long-term reward. Conversely, there are other applications where the number of subjects is limited yet the number of decision points is large [see e.g., Marling and Bunescu, 2020].

3. We develop a matrix concentration inequality for nonstationarity Markov decision processes in order to establish the consistency of the proposed test. The derivation is nontrivial and naively applying the concentration inequality designed for scalar random variables [Alquier et al., 2019] would yield a loose error bound; see Section B.4 for detailed illustrations.

4. We derive the limiting distribution of the estimated optimal Q-function computed via the fitted Q-iteration [FQI, Ernst et al., 2005] algorithm, one of the most popular Q-learning type algorithms. See Equation (3.5).

The proposed test and change point detection procedure are useful in practical situations. In particular, the proposed test is useful in identifying nonstationary environments. Existing RL algorithms designed for stationary environments are no longer valid in nonstationary environments. While some recent proposals [Lecarpentier and Rachelson, 2019, Cheung et al., 2020, Fei et al., 2020, Domingues et al., 2021, Wei and Luo, 2021, Xie et al., 2021, Zhong et al., 2021, Feng et al., 2023] allow for nonstationarity, they may be less efficient in stationary settings. By examining the stationarity assumption, our proposed test provides valuable insights into the system's dynamics, enabling practitioners to select the most suitable state-of-the-art RL algorithms for implementation. Specifically, if the stationarity assumption is not rejected, standard RL algorithms (e.g., Q-learning, policy gradient methods) can be implemented to ensure efficiency of policy learning. Otherwise, RL algorithms designed for nonstationary environments, such as those mentioned above, should be preferred.

Additionally, the proposed change point detection procedure identifies the most recent "best data segment of stationarity". It can be integrated with state-of-the-art RL algorithms for online policy learning in nonstationary environments. We apply this procedure to both synthetic and real datasets in Sections 5 and 6, respectively. Results show that the estimated policy based on our constructed data segment is comparable or often superior to those computed by (i) stationary RL algorithms that ignore nonstationarity, (ii) nonstationary RL algorithms that do not perform change point detection and (iii) nonstationary RL algorithms that employ alternative tests for identifying change points. In the motivating IHS study, the proposed method reveals the benefit of nonstationarity detection for optimizing population physical activities for interns in some medical specialties. The promotion of healthy behaviors and the mitigation of negative chronic health outcomes typically require continuous monitoring over a long term where nonstationarity is likely to occur. As RL continues to drive development of optimal interventions in mHealth studies, this paper substantiates the need and effectiveness of incorporating a classical statistical inferential tool to accommodate nonstationarity.

The rest of the paper is organized as follows. In Section 2, we introduce the offline RL problem and review some existing algorithms. In Section 3, we detail our procedures for hypothesis testing and change point detection. We establish the theoretical properties of our procedure in Section 4, conduct simulation studies in Section 5, and apply the proposed procedure to the IHS data in Section 6.

2 Problem Formulation

We start by introducing the data generating process and the concept of policy in RL. We next review Q-learning [Watkins and Dayan, 1992], a widely used RL algorithm that is closely related to our proposal. Finally, we discuss five types of stationarity assumptions and introduce our testing hypotheses.

2.1 Data

We consider an offline setting to learn an optimal policy based on a pre-collected dataset from a randomized trial or observational study. The offline dataset is summarized as $\mathcal{D} = \{(S_{i,t}, A_{i,t}, R_{i,t})\}_{1\le i\le N, 0\le t\le T}$, where $(S_{i,t}, A_{i,t}, R_{i,t})$ denotes the state-action-reward triplet of the ith subject at time t. Without loss of generality, we assume all subjects share the same termination time T, which is reasonable in many mHealth studies. In Section A.2, we extend our proposal to settings where subjects have different termination times. In IHS, the state corresponds to some time-varying covariates associated with each medical intern, such as their mood score, step counts, and sleep minutes. The action is a binary variable, corresponding to whether to send a certain text message to the intern or not. The immediate reward is the step counts. We assume all rewards are uniformly bounded, as commonly adopted in the RL literature to simplify theoretical analysis [see e.g., Fan et al., 2020]. These N trajectories are assumed to be i.i.d copies of an infinite horizon Markov decision process [MDP, Puterman, 2014] $\{(S_t, A_t, R_t)\}_{t\ge 0}$ whose data generating process can be described as follows:

1. **State Presentation**: At each time t, the environment (represented as an intern in our example) is in a state $S_t \in \mathcal{S}$ where $\mathcal{S} \in \mathbb{R}^d$ denotes the state space and d denotes the dimension.

2. **Action Selection**: The agent (or decision maker) then selects an action A_t from the action space $\mathcal{A}$ based on the observed data history H_t including S_t and the state-action-reward triplets up to time $t-1$.

3. **Reward Generation**: The agent receives an immediate reward $R_t \in \mathbb{R}$ with its expected value specified by an unknown reward function r_t:

$$\mathbb{E}(R_t|H_t, A_t) = r_t(A_t, S_t). \tag{2.1}$$

4. **State Transition**: Subsequently, the environment transitions to the next state S_{t+1}, determined by an unknown transition function $\mathcal{T}_t$:

$$S_{t+1} = \mathcal{T}_t(A_t, S_t, \delta_t), \tag{2.2}$$

where $\{\delta_t\}_t$ is a sequence of i.i.d. random noises, with each δ_t being independent of $\{(S_j, A_j, R_j)\}_{j \le t}$.

Remark 1. *By definition, $\mathcal{T}_t$ specifies the conditional distribution of the future state given the current state-action pair, and r_t is the conditional mean function of the reward. Both (2.1) and (2.2) impose certain Markov or conditional independence assumptions on the data trajectories, implying that the future state and the conditional mean of the current reward are independent of the H_t given the current state-action pair. These assumptions are testable from the observed data [Chen and Hong, 2012, Shi et al., 2020b, Zhou et al., 2023].*

2.2 Policy

A policy defines how actions are chosen at each decision time. In particular:

1. A **history-dependent policy** π is a sequence of decision rules $\{\pi_t\}_{t \ge 0}$ such that each π_t takes H_t as input, and outputs a probability distribution on the action space, denoted by $\pi_t(\bullet|H_t)$. Under π, the agent will set $A_t = a$ with probability $\pi_t(a|H_t)$ at time t.

2. A **Markov policy** π is a special history-dependent policy where each π_t depends on H_t only through the current state S_t.

3. A **stationary policy** π is a special Markov policy where $\{\pi_t\}_t$ are time-invariant, i.e., there exists some function π^* such that $\pi_t(\bullet|H_t) = \pi^*(\bullet|S_t)$ almost surely for any t, and we use $\pi(\bullet|S_t)$ to denote the resulting decision rule.

4. An **optimal policy** $\pi^{opt} = \{\pi_t^{opt}\}_t$ maximizes the expected γ-discounted cumulative reward $J_\gamma(\pi) = \sum_{t \ge 0} \gamma^t \mathbb{E}^\pi(R_t)$ among all history-dependent policies π, given a discount factor $0 < \gamma \le 1$ which balances the trade-off between the immediate and future rewards. The expectation $\mathbb{E}^\pi$ is calculated under the assumption that the agent makes decisions in accordance with the policy π.

5. The **behavior policy** $b = \{b_t\}_t$ denotes the policy the agent adopted for all individuals in the offline dataset. This policy is not necessarily optimal and may be a purely random policy in scenarios like sequential multiple assignment randomized trials [SMARTs, Collins et al., 2007].

Remark 2. *Under (2.1) and (2.2), there exists an optimal Markov policy π^{opt} whose $J_\gamma(\pi^{opt})$ is no worse than that of any history-dependent policy; see Theorem 6.2.10 of Puterman [2014]. This substantially simplifies the calculation of the optimal policy. Hence, throughout this paper, 'optimal policy' specifically refers to the optimal Markov policy, meaning that each π_t^{opt} is a*

function of the current state S_t only. Note that the proof in Puterman [2014] relies on the assumption that the reward is a deterministic function of the state-action-next-state triplet. However, this assumption can be effectively relaxed to (2.1) while still preserving the validity of the proof.

2.3 Q-Learning

We review Q-learning, one of the most popular RL algorithms. It is model-free in that the optimal policy is derived without directly estimating the MDP model (i.e., transition and reward functions). Central to Q-learning is the state-action value function, commonly known as the Q-function. Given a policy π, its Q-function $Q^\pi = \{Q_t^\pi\}_{t\geq 0}$ is defined such that each Q_t^π is the expected cumulative reward given a state-action pair following π, i.e., $Q_t^\pi(a,s) = \mathbb{E}^\pi\left(\sum_{k\geq 0}\gamma^k R_{t+k}|A_t=a, S_t=s\right)$. The optimal Q-function, denoted by $Q^{\pi^{opt}}$ or simply Q^{opt}, corresponds to the Q-function under the optimal policy. The optimal Q-function possesses two key properties[1]: (i) π^{opt} is greedy with respect to Q^{opt}, i.e., for any $t \geq 0$,

$$\pi_t^{opt}(a|s) = \begin{cases} 1, & \text{if } a = \arg\max_{a'} Q_t^{opt}(a', s); \\ 0, & \text{otherwise.} \end{cases} \tag{2.3}$$

(ii) The Bellman optimality equation holds, stating that the expected Q-value at time t equals the immediate reward plus the maximum Q-value of the next state:

$$\mathbb{E}\left\{R_t + \gamma \max_a Q_{t+1}^{opt}(a, S_{t+1})|A_t, S_t\right\} = Q_t^{opt}(A_t, S_t), \qquad \forall t \geq 0. \tag{2.4}$$

Equations (2.3) and (2.4) form the basis of Q-learning, which estimates $\{Q_t^{opt}\}_t$ by solving the Bellman optimality equation (2.4) and computes π^{opt} based on the estimated optimal Q-function using (2.3). Assuming the stationarity of the optimal Q-function, i.e., $Q_t^{opt} = Q^{opt}$ for any t, various algorithms have been developed under this framework, such as tabular Q-learning [Watkins and Dayan, 1992], FQI, greedy gradient Q-learning [Maei et al., 2010, Ertefaie and Strawderman, 2018], double Q-learning [Hasselt, 2010] and deep Q-network [DQN, Mnih et al., 2015]. In particular, FQI, which our paper implements, iteratively updates the optimal Q-function estimator based on (2.4). Beginning with an initial Q-function estimator $Q^{(0)}$ (typically set to zero), we compute $Q^{(k+1)}$ by minimizing

$$Q^{(k+1)} = \arg\min_Q \sum_{i,t}\left\{R_{i,t} + \gamma \max_a Q^{(k)}(a, S_{i,t+1}) - Q(A_{i,t}, S_{i,t})\right\}^2, \tag{2.5}$$

during the kth iteration. The above optimization can be cast into a supervised learning problem with $\{R_{i,t}+\gamma\max_a Q^{(k)}(a, S_{i,t+1})\}_{i,t}$ as the responses and $\{(A_{i,t}, S_{i,t})\}_{i,t}$ as the predictors. We will establish the limiting distribution of the resulting Q-function estimator when employing the method of sieves for function approximation.

[1]Typically, these properties are verified in a stationary setting, see e.g., Theorem 1.8 of Agarwal et al. [2019]. However, by simply incorporating the time index into the state definition, the proofs of these theorems can be readily adapted to nonstationary MDPs defined in Section 2.1 as well.

2.4 The Stationarity Assumption

Starting from a given time point $T_0 \geq 0$, we introduce five types of stationarity assumptions:

SA1 (**Stationary MDPs**): The transition function $\mathcal{T}_t$ and the reward function r_t remain constant over time, for all $t \geq T_0$.

SA2 (**Stationary Q-functions**): For any stationary policy π (see the definition in Section 2.2), the associated Q-function Q_t^π is constant as a function of t, for all $t \geq T_0$.

SA3 (**Stationary optimal Q-functions**): $Q_{T_0}^{opt} = Q_{T_0+1}^{opt} = \cdots = Q_t^{opt} = \cdots$.

SA4 (**Stationary optimal policies**): $\pi_{T_0}^{opt} = \pi_{T_0+1}^{opt} = \cdots = \pi_t^{opt} = \cdots$.

SA5 (**Stationary behavior policies**): $b_{T_0} = b_{T_0+1} = \cdots = b_t = \cdots$.

The following theorem discusses the relationships among these assumptions.

Theorem 2.1 (Stationarity relationships)**.** *Assume both the state space and the action space are finite, and the rewards are uniformly bounded. Then SA1 implies SA2, SA2 implies SA3, and SA3 implies SA4.*

Remark 3. *Throughout this paper, stationary MDPs refer to MDP models with stationary transition and reward functions. Therefore, SA1 represents a "model-based" stationarity assumption, as it directly relates to the MDP model. It is the most prevalently employed form of stationarity in the literature [Sutton and Barto, 2018]. Importantly, this concept does not require the stationarity of the behavior policy (SA5), which characterizes the decisions or strategies put forth by the agent and operates independently of the environmental factors. Nor does SA5 imply SA2 – SA4. As a result, the optimal policy may be stationary or nonstationary, regardless of whether the behavior policy is stationary or not.*

Remark 4. *SA2 and SA3 are characterized as model-free stationarity assumptions, as they are defined without direct reference to the state transition or reward functions. Theorem 2.1 suggests that these assumptions are automatically satisfied under SA1. Furthermore, it is well-known that in stationary MDPs, the optimal policy is stationary as well [Puterman, 2014]. The proof that SA2 leads to SA3, however, is not straightforward. Drawing inspiration from the policy iteration algorithm [Sutton and Barto, 2018, Section 4.3], we define a sequence of policies whose Q-functions converge to the optimal Q-function. This enables us to establish the connection between a non-optimal Q-function and the optimal one, thus proving the stationarity of the optimal Q-function in a potentially nonstationary MDP (i.e., when SA2 holds, but SA1 does not). We refer readers to Section B.1 for details.*

2.5 Hypothesis Testing under Nonstationarity

As commented in the introduction, the stationarity assumption can be restrictive in practice. This motivates us to test stationarity based on the offline dataset. Given the five different types of stationarity assumptions we have identified, there are correspondingly five different hypotheses to test. In this paper, we focus on testing SA3 due to the following considerations:

- Testing SA1 poses considerable challenges in scenarios with moderate to high-dimensional states, as the transition function's outputs are multidimensional with dimension matching that of the state.
- Testing SA2 is extremely difficult due to the need to enumerate over all possible policies, whose number increases exponentially with the cardinality of the state space.
- Based on (2.3), the optimal policy is intrinsically tied to the optimal Q-function. Theorem 2.1 further implies that SA4 follows from SA3. Thus, by testing SA3, we can effectively assess the stationarity of the optimal policy.
- Optimal testing of SA4 is complex since the optimal policy is a highly nonlinear functional of the observed data, complicating the derivation of its estimator's limiting distribution. Moreover, π^{opt} may lack uniqueness even when $\{Q_t^{opt}\}_t$ is uniquely determined.
- Testing SA5 is meaningless because the stationarity of the behavior policy does not influence that of the optimal policy.

Thus, our testing hypotheses are formulated as follows:

$$\mathcal{H}_0 : Q_t^{opt} = Q^{opt},\ \forall t \geq T_0,\ \text{ versus } \mathcal{H}_1 : Q_t^{opt} \text{ has at least one smooth or abrupt change point for } t \geq T_0 \text{ (see Figure 3.1).} \tag{2.6}$$

3 Proposed Stationarity Test and Change Point Detection

In this section, we start by proposing three types of test statistics for testing (2.6). Next, we present key computation steps in constructing these tests. Finally, we present our change point detection method, built upon the proposed test.

3.1 Test Statistics

All test statistics we propose require an estimated optimal Q-function, denoted as $\widehat{Q}_{[T_1,T_2]}(a,s)$ (here we drop the superscript opt in Q^{opt} for simplicity), using data collected in the interval $[T_1,T_2] \subseteq [T_0,T]$. For any candidate change point $u \in (T_0+\epsilon T, (1-\epsilon)T)$, where $\epsilon > 0$ is a pre-specified boundary-removal constant, we use $\widehat{Q}_{[u,T]}(a,s) - \widehat{Q}_{[T_0,u]}(a,s)$ to measure the difference in the optimal Q-function after and before the candidate. Based on this measure, we

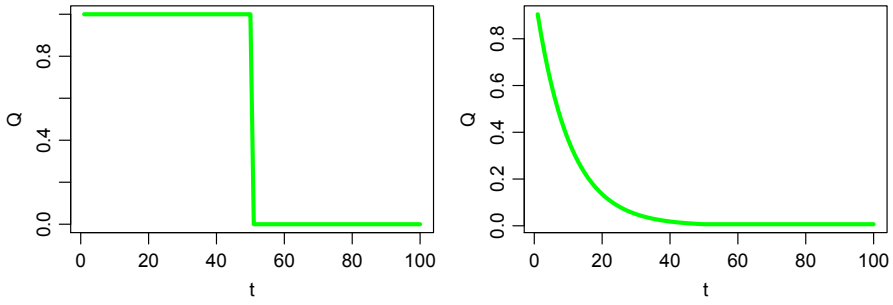

Figure 3.1: Examples of Q^{opt} at a given state-action pair, with an abrupt change point (left panel) and a gradual change point (right panel) at $t = 50$. $T_0 = 0$ in both examples.

Algorithm 1 Testing Stationarity of the Optimal Policy via the Optimal Q-Function.

Input: The offline data $\{(S_{i,t}, A_{i,t}, R_{i,t})\}_{1\le i\le N, T_0\le t\le T}$, and the significance level $0 < \alpha < 1$.

Step 1. For each $u \in [T_0+\epsilon T, (1-\epsilon)T]$, employ the fitted Q-iteration algorithm to compute the estimated Q-functions $\widehat{Q}_{[T_0,u]}$ and $\widehat{Q}_{[u,T]}$ on separate time segments.

Step 2. Construct one of the CUSUM-type test statistics TS_1, TS_∞ or TS_n, according to (3.1), (3.2) or (3.3).

Step 3. Employ multiplier bootstrap to compute the bootstrapped test statistics TS_1^b, TS_∞^b or TS_n^b, and calculate the p-value according to (3.7).

Output: Reject the null hypothesis if the p-value is smaller than α.

introduce three test statistics: an ℓ_1-type, a maximum-type, and a normalized maximum-type, given by

$$\text{TS}_1 = \max_{T_0+\epsilon T<u<(1-\epsilon)T} \tau_u \Big[\frac{1}{N(T-T_0)} \sum_{i,t} |\widehat{Q}_{[T_0,u]}(A_{i,t}, S_{i,t}) - \widehat{Q}_{[u,T]}(A_{i,t}, S_{i,t})|\Big], \tag{3.1}$$

$$\text{TS}_\infty = \max_{T_0+\epsilon T<u<(1-\epsilon)T} \max_{a,s} \tau_u |\widehat{Q}_{[T_0,u]}(a,s) - \widehat{Q}_{[u,T]}(a,s)|, \tag{3.2}$$

$$\text{TS}_n = \max_{T_0+\epsilon T<u<(1-\epsilon)T} \max_{a,s} \tau_u \widehat{\sigma}_u^{-1}(a,s) |\widehat{Q}_{[T_0,u]}(a,s) - \widehat{Q}_{[u,T]}(a,s)|, \tag{3.3}$$

respectively, where $\tau_u = \sqrt{\frac{(u-T_0)(T-u)}{(T-T_0)^2}}$ is the scale factor being dependent on the proximity of u to the interval boundary, $\widehat{\sigma}_u^2(a,s)$ denotes a consistent variance estimator of $\widehat{Q}_{[T_0,u]}(a,s) - \widehat{Q}_{[u,T]}(a,s)$ whose detailed form is given in Section B.2.2.

Under a given significance level α, the critical values and p-values for TS_1, TS_∞ and TS_n are computed using a multiplier bootstrap method (detailed in Section 3.3) to approximate their

asymptotic distributions. This multiplier bootstrap is easy to implement. Unlike other methods such as the nonparametric bootstrap, it does not require to re-estimate the Q-function, thus simplifying the estimation. We reject the null hypothesis when the test statistic exceeds its corresponding critical value (or equivalently, the p-value falls below α).

Remark 5. *The three test statistics* (3.1)–(3.3) *are very similar to the classical cumulative sum (CUSUM) statistic in change point analysis [Csörgő et al., 1997]. The weight scale* τ_u *assigns smaller weights on data points near the boundary of the interval* $(T_0+\epsilon T, (1-\epsilon)T)$*. Removing the boundary is necessary as it is difficult to accurately estimate the Q-function when close to the boundary. Such practice is commonly employed in the time series literature for change point detection in non-Gaussian settings [see e.g., Cho and Fryzlewicz, 2012, Yu and Chen, 2021].*

Remark 6. *In addition, the three test statistics differ in how they aggregate the estimated changes* $|\widehat{Q}_{[T_0,u]} - \widehat{Q}_{[u,T]}|$ *across different state-action pairs. The* ℓ_1*-type test* (3.1) *computes the average of the changes, weighted by the empirical state-action distribution. The two maximum-type tests* (3.2) *and* (3.3) *focus on the largest change in the (normalized) absolute value. Normalization can enhance efficiency, especially in cases where some state-action pairs* (a, s) *are less frequently visited. In these cases, the standard error of the difference* $\widehat{Q}_{[T_0,u]}(a, s) - \widehat{Q}_{[u,T]}(a, s)$ *tends to be large. As a consequence, the estimated maximizer* $\arg\max_{a,s} |\widehat{Q}_{[T_0,u]}(a, s) - \widehat{Q}_{[u,T]}(a, s)|$ *may differ significantly from the oracle maximizer* $\arg\max_{a,s} |Q^{opt}_{[T_0,u]}(a, s) - Q^{opt}_{[u,T]}(a, s)|$*, leading to reduced power in the unnormalized test. We remark that such normalized supremum-type statistics have been commonly employed in the econometrics literature [see e.g., Belloni et al., 2015, Chen and Christensen, 2015, 2018]. On the other hand, the normalized test requires to compute the estimated variance* $\widehat{\sigma}^2_u$*, which introduces additional variability into the test statistic that might lower its type-I error control, and slightly increases computational time. Thus, we expect the normalized test to exhibit a larger type-I error and a larger power than the unnormalized and* ℓ_1*-type tests, despite all the three tests are consistent. This is confirmed by our theoretical and numerical studies, which we will demonstrate later.*

Remark 7. *To conclude this section, we remark that the proposed test is model-free, as it constructs the test statistic without directly estimating the reward and transition functions. Alternatively, one may consider model-based tests. We compare against an existing model-based test in Section 5.1 and provide a detailed discussion of model-free versus model-based tests in Section A.1.*

3.2 Estimation of the Q-Function

We provide more details on estimating Q^{opt} in this section. In particular, we focus on a discrete action space $\mathcal{A} = \{0, 1, \cdots, m-1\}$ with m available actions. We employ the sieve method [Grenander, 1981] to model Q^{opt}, primarily for two reasons. First, the sieve method ensures the resulting Q-estimator has a tractable limiting distribution, which allows us to derive the

asymptotic distribution of the test statistic. Second, the sieve method is useful in mitigating bias caused by model misspecification, achieved by increasing the number of basis functions.

Specifically, we propose to model $Q^{opt}(a,s)$ by $\phi_L^\top(a,s)\beta^*$ for some $\beta^* \in \mathbb{R}^{mL}$ where

$$\phi_L(a,s) = [\mathbb{I}(a=0)\Phi^\top(s), \mathbb{I}(a=1)\Phi^\top(s), \cdots, \mathbb{I}(a=m-1)\Phi^\top(s)]^\top, \tag{3.4}$$

is an mL-dimensional vector constructed using products between the action indicator $\mathbb{I}(a=\bullet)$ and a vector of L basis functions Φ on the state space. Several choices can be considered here for Φ. For continuous state spaces, options for Φ include power series, Fourier series, splines or wavelets [see e.g., Judd, 1998]. For discrete state spaces, one could use a lookup table and set $\phi_L(a,s) = [\mathbb{I}\{(a,s)=(a',s')\}; a' \in \mathcal{A}, s' \in \mathcal{S}]^\top$. In Section 4.2, we show that the proposed test is not overly sensitive to the choice of the number of basis functions L. In practice, we can determine L using cross-validation, as illustrated in our simulation studies.

For a given time interval $[T_1, T_2] \subseteq [T_0, T]$, we compute an estimator $\widehat{\beta}_{[T_1,T_2]}$ for β^* using data collected from this interval. Specifically, we employ FQI to iteratively update $\widehat{\beta}_{[T_1,T_2]}$ as outlined in (2.5). With a linear model, we perform ordinary least square regression at the kth iteration with $\{R_{i,t} + \gamma \max_a \phi^\top(a, S_{i,t+1})\beta^{(k-1)}\}_{1\le i\le N, T_1\le t<T_2}$ as the responses and $\{\phi(A_{i,t}, S_{i,t})\}_{1\le i\le N, T_1\le t<T_2}$ as the predictors to compute the regression coefficients $\beta^{(k)}$. The procedure stops after K iterations and we set $\widehat{\beta}_{[T_1,T_2]}$ to $\beta^{(K)}$.

3.3 Bootstrap Approach to Critical Value

We employ a multiplier bootstrap method [Wu, 1986, Chernozhukov et al., 2014] to obtain the p-values. The idea is to simulate Gaussian random noises to approximate the limiting distribution of the Q-function estimator, and subsequently to approximate that of the test statistic. A key observation is that, under the null hypothesis, when the Q-function is well-approximated and the optimal policy is unique, the estimated Q-function $\phi_L(a,s)^\top\widehat{\beta}_{[T_1,T_2]}$ has the following linear representation:

$$\begin{aligned}&\phi_L(a,s)^\top\widehat{\beta}_{[T_1,T_2]} - Q^{opt}(a,s)\\ =&\frac{1}{N(T_2-T_1)}\phi_L^\top(a,s)W_{[T_1,T_2]}^{-1}\sum_{i=1}^{N}\sum_{t=T_1}^{T_2-1}\phi_L(A_{i,t},S_{i,t})\delta_{i,t}^* + o_p(1),\end{aligned} \tag{3.5}$$

where

$$W_{[T_1,T_2]} = \frac{1}{T_2-T_1}\sum_{t=T_1}^{T_2-1}\mathbb{E}\phi_L(A_{i,t},S_{i,t})\{\phi_L(A_{i,t},S_{i,t}) - \gamma\phi_L(\pi^{opt}(S_{i,t+1}),S_{i,t+1})\}^\top,$$

$\delta_{i,t}^* = R_{i,t} + \gamma\max_a Q^{opt}(a,S_{i,t+1}) - Q^{opt}(A_{i,t},S_{i,t})$ is the temporal difference error. By the Bellman optimality equation (2.4), the leading term on the right-hand-side (RHS) of (3.5) forms a mean-zero martingale. When its quadratic variation process converges, it follows from the martingale central limit theorem [McLeish, 1974] that $\widehat{\beta}_{[T_1,T_2]}$ is asymptotically normal. As such, the estimated Q-function is asymptotically normal as well. Refer to Lemma B.2 for the formal statements.

Remark 8. *To the best of our knowledge, the limiting distribution of the Q-function estimated via FQI has not been established in the existing RL literature. Most papers focus on establishing non-asymptotic error bound of the estimated Q-function [see e.g., Munos and Szepesvári, 2008, Chen and Jiang, 2019, Fan et al., 2020, Uehara et al., 2021]. One exception is a recent proposal by Hao et al. [2021] that studied the asymptotics of Q-estimators computed via the fitted Q-evaluation [FQE, Le et al., 2019] algorithm. We note that FQE is similar to FQI but is designed for the purpose of policy evaluation.*

In addition, it follows from (3.5) that

$$\begin{aligned}\widehat{Q}_{[T_0,u]}(a,s)-\widehat{Q}_{[u,T]}(a,s)=&\frac{1}{N(u-T_0)}\phi_L^\top(a,s)W_{[T_0,u]}^{-1}\sum_{i=1}^{N}\sum_{t=T_0}^{u-1}\phi_L(A_{i,t},S_{i,t})\delta_{i,t}^*\\&-\frac{1}{N(T-u)}\phi_L^\top(a,s)W_{[u,T]}^{-1}\sum_{i=1}^{N}\sum_{t=u}^{T-1}\phi_L(A_{i,t},S_{i,t})\delta_{i,t}^*+o_p(1).\end{aligned}\tag{3.6}$$

This motivates us to construct B bootstrap samples to approximate the asymptotic distribution of the leading term on the RHS of (3.6). Specifically, at the bth iteration, $b=1,\ldots,B$, we compute a bootstrap sample $\widehat{Q}^b_{[T_0,u]}(a,s)-\widehat{Q}^b_{[u,T]}(a,s)$ where

$$\widehat{Q}^b_{[T_1,T_2]}(a,s)=\frac{1}{N(T_2-T_1)}\phi_L^\top(a,s)\widehat{W}_{[T_1,T_2]}^{-1}\sum_{i=1}^{N}\sum_{t=T_1}^{T_2-1}\phi_L(A_{i,t},S_{i,t})\delta_{i,t}(\widehat{\beta}_{[T_1,T_2]})e^b_{i,t},\ \forall T_1,T_2,$$

where $\widehat{W}_{[T_1,T_2]}$ denotes a consistent estimator for $W_{[T_1,T_2]}$ (refer to Lemma B.3 for a detailed upper bound on the estimation error) given by

$$\widehat{W}_{[T_1,T_2]}=\frac{1}{N(T_2-T_1)}\sum_{i=1}^{N}\sum_{t=T_1}^{T_2-1}\phi_L(A_{i,t},S_{i,t})\{\phi_L(A_{i,t},S_{i,t})-\gamma\phi_L(\pi_{\widehat{\beta}_{[T_1,T_2]}}(S_{i,t+1}),S_{i,t+1})\}^\top,$$

$\delta_{i,t}(\beta)=R_{i,t}+\gamma\max_a\beta^\top\phi_L(a,S_{i,t+1})-\beta^\top\phi_L(A_{i,t},S_{i,t})$, $\{e^b_{i,t}\}_{i,t}$ is a sequence of i.i.d. standard Gaussian random variables independent of the observed data, and $\pi_{\widehat{\beta}_{[T_1,T_2]}}$ denotes the greedy policy with respect to the estimated Q-function (see (2.3)), $\pi_{\widehat{\beta}_{[T_1,T_2]}}(s)=\arg\max_a\phi_L^\top(a,s)\widehat{\beta}_{[T_1,T_2]}$. This yields the bootstrapped statistics,

$$\begin{aligned}\mathrm{TS}_1^b&=\max_{T_0+\epsilon T<u<(1-\epsilon)T}\tau_u\Big[\frac{1}{N(T-T_0)}\sum_{i,t}|\widehat{Q}^b_{[T_0,u]}(A_{i,t},S_{i,t})-\widehat{Q}^b_{[u,T]}(A_{i,t},S_{i,t})|\Big],\\
\mathrm{TS}_\infty^b&=\max_{T_0+\epsilon T<u<(1-\epsilon)T}\max_{a,s}\tau_u|\widehat{Q}^b_{[T_0,u]}(a,s)-\widehat{Q}^b_{[u,T]}(a,s)|,\\
\mathrm{TS}_n^b&=\max_{T_0+\epsilon T<u<(1-\epsilon)T}\max_{a,s}\tau_u\widehat{\sigma}_u^{-1}(a,s)|\widehat{Q}^b_{[T_0,u]}(a,s)-\widehat{Q}^b_{[u,T]}(a,s)|.\end{aligned}$$

The random noise $e^b_{i,t}$ in $\widehat{Q}^b_{[T_1,T_2]}$ plays a crucial role in the approximation of the asymptotic distribution. In particular, in Step 3 of the proof of Theorem 4.1 (see Section B.2.1), we show

that the conditional variance of the difference in the bootstrap sample $\widehat{Q}^b_{[T_0,u]}(a,s) - \widehat{Q}^b_{[u,T]}(a,s)$ given the data, is asymptotically equivalent to the asymptotic variance of the difference in the actual Q-function estimator $\widehat{Q}_{[T_0,u]}(a,s) - \widehat{Q}_{[u,T]}(a,s)$. Meanwhile, $\widehat{Q}^b_{[T_0,u]}(a,s) - \widehat{Q}^b_{[u,T]}(a,s)$ follows a normal distribution given the data, due to the injected Gaussian noises $\{e^b_{i,t}\}_{i,t}$, while $\widehat{Q}_{[T_0,u]}(a,s) - \widehat{Q}_{[u,T]}(a,s)$ is asymptotically normal. These alignments justify the use of the multiplier bootstrap. We thus set the critical value of each test to the αth upper quantile of the bootstrapped samples. The p-values can be computed by

$$\frac{1}{B}\sum_{b=1}^{B}\mathbb{I}(\mathrm{TS}_1^b > \mathrm{TS}_1), \frac{1}{B}\sum_{b=1}^{B}\mathbb{I}(\mathrm{TS}_\infty^b > \mathrm{TS}_\infty) \text{ and } \frac{1}{B}\sum_{b=1}^{B}\mathbb{I}(\mathrm{TS}_n^b > \mathrm{TS}_n), \tag{3.7}$$

respectively.

3.4 Change Point Detection

Given the offline data collected from N subjects up to time T, we aim to learn an optimal "warm-up" policy, i.e., the optimal policy that maximizes these subjects' long-term rewards starting from time T, until the reward or transition function changes. This goal aligns with our motivating mHealth study setting where the researchers want to design the best policy based on pre-collected data and extends the policy to the same group of subjects after the study ends. To this end, we focus on identifying the most recent change point T^* such that $Q^{opt}_{T^*} = Q^{opt}_{T^*+1} = \cdots = Q^{opt}_T$ and apply state-of-the-art Q-learning to the data subset $\{(S_{i,t}, A_{i,t}, R_{i,t})\}_{1\le i\le N, T^*\le t\le T}$ to learn π^{opt}_T.

To estimate T^*, we apply any of the three proposed tests to a sequence of candidate change points from the back. We start by specifying a monotonically increasing sequence $\{\kappa_j\}_j \subseteq (0,T)$ and apply the test to intervals $[T-\kappa_j, T]$. The estimator $\widehat{T}^*$ is then set to the candidate change point before the first rejection, i.e., $\widehat{T}^* = T - \kappa_{j_0-1}$ where the test is first rejected at κ_{j_0}. If no changes are detected, we propose to use all the observed data for policy optimization.

Though offline, the proposed change point detection method is an integral part in batch online RL settings via the following strategy: Step 1) A behavior policy is used to collect experiences; 2) After certain amount of experiences is collected, apply the proposed approach to detect the most recent change point; 3) If there exists a change point, use the data after the most recent change point to update the policy; 4) The new policy, together with ϵ-greedy algorithm, is then used to collect more data; Repeat Steps 2) to 4) for a pre-specified or indefinitely long duration of interactions with the environment. See Section 5.2 for detailed simulation experiments that demonstrate this strategy and utility.

4 Consistency of the Test

We proceed by first investigating the size (i.e., the rejection probability or type-I error) of the proposed test, and next establishing its power property. To simplify the theoretical analysis,

we focus on the setting where the state space $\mathcal{S} = [0,1]^d$, and Φ denotes the tensor product of B-spline basis functions, motivated by their popularity in the sieve estimation literature [see e.g., Section 6 of Chen and Christensen, 2015, for a review]. We use $p_t(\bullet|a,s)$ to denote the probability density function of $\mathcal{T}_t(a,s,\delta_1)$. In other words, p_t corresponds to the density function of S_{t+1} given $(A_t,S_t)=(a,s)$. For each s and t, we use $\pi_t^{opt}(s)$ to denote the greedy action $\arg\max_a Q_t^{opt}(a,s)$ that π_t^{opt} picks (see (2.3)). Let δ_t^* denote the temporal difference error $R_t+\max_a Q_t^{opt}(a,S_{t+1})-Q_t^{opt}(A_t,S_t)$. As commented in the introduction, all the theories in this section are established under a bidirectional asymptotic framework, which is to say that they are valid as either N or T diverges to infinity.

4.1 Size of the Test

We introduce the following assumptions:

A1 (**CUSUM statistics**): The boundary removal parameter ϵ in the proposed test statistics (3.1), (3.2) and (3.3), is proportional to $\log^{-c_1}(NT)$ for some $c_1 \geq 0$.

A2 (**Realizability**): Assume that there exist some constants $p, c_2 > 0$, such that for any $a \in \mathcal{A}$ and $t \geq T_0$, the reward function $r_t(a,\bullet) \in \Lambda(p,c_2)$, where $\Lambda(p,\bullet)$ is the Hölder class with the smoothness parameter p; see the Supplementary Materials for its definition.

A3 (**Completeness**): For any $\beta \in \mathbb{R}^{mL}$ whose ℓ_2 norm $\|\beta\|_2$ is less than or equal to 1, there exists some β^* with $\|\beta^*\|_2 \leq 1$ such that the function $\mathcal{B}_t\phi_L^\top\beta$ can be uniformly approximated by $\phi_L^\top\beta^*$ with an approximation error $O(L^{-p/d})$, where $\mathcal{B}_t$ denotes the operator $(\mathcal{B}_t g)(a,s) = \mathbb{E}[\max_{a'} g(a', \mathcal{T}_t(a,s,\delta))]$.

A4 (**Transition**): (i) $\sup_{t,a}\mathbb{E}\|\mathcal{T}_t(a,s,\delta)-\mathcal{T}_t(a,s',\delta)\|_2 \leq \rho\|s-s'\|_2$ for some $0 \leq \rho < 1$, $\sup_{t,a,s}\|\mathcal{T}_t(a,s,\delta)-\mathcal{T}_t(a,s,\delta')\|_2 = O(\|\delta-\delta'\|_2)$; (ii) Suppose δ_1 has sub-exponential tails, i.e., for any jth element $\delta_{1,j}$, $\mathbb{E}|\delta_{1,j}|^k = O(k!c_3^{k-2})$ for some constant $c_3 > 0$; (iii) $p_t(s'|a,s)$ is bounded and is Lipschitz continuous as a function of s; (iv) $\inf_{t,a,s}\mathrm{Var}((1-\gamma)\delta_t^*|A_t=a,S_t=s)$ is bounded away from zero.

A5 (**Behavior policy**): (i) π^b is a Markov policy; (ii) $\inf_{t\geq T_0,0\leq\gamma'\leq\gamma}(1-\gamma')^{-1}\lambda_{\min}[\mathbb{E}\phi_L(A_t,S_t)\phi_L(A_t,S_t)^\top-(\gamma')^2\mathbb{E}\phi_L(\pi_{opt}(S_{t+1}),S_{t+1})\phi_L^\top(\pi_{opt}(S_{t+1}),S_{t+1})]$ is uniformly bounded away from zero where $\lambda_{\min}[\bullet]$ denotes the minimum eigenvalue of a given matrix.

A6 (**Optimal policy**): The optimal policy π_t^{opt} is unique for all t.

A7 (**Optimal Q-function**): The margin $Q_t^{opt}(\pi_t^{opt}(s),s)-\max_{a\in\mathcal{A}\setminus\pi_t^{opt}(s)}Q_t^{opt}(a,s)$ is bounded away from zero, uniformly for all s and t.

A8 (**Computation**): The number of FQI iterations K to produce the estimated Q-function $\widehat{Q}$ is much larger than $\log(NT)$.

A9 (**Basis functions**): L is proportional to $(NT)^{c_4}$ for some $0 < c_4 < 1/4$. Under the null SA3 (see (2.6)), we additionally require $c_4 > d/(2p)$ for all three types of tests.

Remark 9. *As commented earlier, assumptions similar to A1 are commonly adopted in the change point detection literature [Yu and Chen, 2021]. This assumption can be easily satisfied as the boundary removal parameter ϵ is user-specified.*

Remark 10. *The realizability and completeness assumptions are commonly imposed in the RL literature [see e.g., Chen and Jiang, 2019, Uehara et al., 2021]. In our context, realizability requires the Hölder class to be sufficiently rich to contain the reward functions. The completeness assumption requires the linear function class to be "approximately complete" in the sense that it remains closed under the operator $\mathcal{B}_t$ up to certain approximation error. It holds automatically when the transition density function p_t belongs to the Hölder class as well [see e.g., Fan et al., 2020, Shi et al., 2022]. Such smoothness conditions are commonly imposed in the sieve estimation literature as well [see e.g. Huang, 1998, Chen and Christensen, 2015]. They are mild as the smoothness parameter p remains unspecified and can be adjusted to be arbitrarily small to meet the two conditions.*

Remark 11. *Conditions A4(i) and (ii) are needed to establish concentration inequalities for nonstationary Markov chains [Alquier et al., 2019]. They allow us to develop a matrix concentration inequality with nonstationary transition functions, which is needed to prove the validity of the bootstrap method (see Lemma B.3 for details). These assumptions are automatically satisfied when the state satisfies a time-varying AR(1) process:*

$$S_{t+1} = \rho_t S_t + \beta_t A_t + \delta_t,$$

for some $\{\rho_t\}_t$ and $\{\beta_t\}$ such that $\sup_t |\rho_t| < 1$, and δ_t has sub-exponential tails. More generally, it also holds when the auto-regressive model is given by

$$S_{t+1} = f_t(A_t, S_t) + \delta_t,$$

with $\sup_{a,t} |f_t(a,s) - f_t(a,s')| \leq \rho \|s - s'\|_2$ for some $\rho < 1$. When the transition functions are stationary over time, it essentially requires the Markov chain to possess the exponential forgetting property [Dedecker and Fan, 2015]. Condition A4(iii) is automatically satisfied when p_t belongs to the Hölder class with the smoothness parameter $p \geq 1$. Condition A4(iv) requires the transition to be stochastic so that the variance of the temporal difference error remains strictly positive.

We also remark that the sub-exponential tail assumption in A4(ii) is generally met in mHealth studies, particularly in the IHS. This is because the state variable such as the mood score is bounded. Additionally, after cubic root transformation of weekly average step count and square root transformation of weekly average sleep minutes, these two variables exhibit light upper tails, as can be seen from Figure C.5.

Remark 12. *A5(i) allows the behavior policy that generates the data to be nonstationary over time. Assumptions to A5(ii) are commonly imposed in the statistics literature on RL [see e.g., Ertefaie and Strawderman, 2018, Luckett et al., 2020, Shi et al., 2022]. These assumptions are typically satisfied in mobile health where the behavior policy is usually a constant policy – as in the IHS study – which is thus Markovian (fulfilling A5(i)) and is expected to cover the optimal policy (fulfilling A5(ii)).*

Remark 13. *A6 is a necessary condition for establishing the limiting distribution of* $\widehat{\beta}_{[T_1,T_2]}$ *computed based on FQI. It is widely imposed in the statistics literature [Ertefaie and Strawderman, 2018, Luckett et al., 2020], but can be violated in nonregular settings where the optimal policy is not unique [Chakraborty et al., 2013, Luedtke and van der Laan, 2016, Shi et al., 2020a, Guo and He, 2021]. Our proposal could be further coupled with data splitting to derive a valid test in nonregular settings without A6. Specifically, we divide all trajectories into two parts: one to estimate the optimal policy and the other to construct the test. However, the resulting test might suffer from a loss of power, due to the use of data splitting.*

Remark 14. *The margin* $Q_t^{opt}(\pi_t^{opt}(s), s) - \max_{a\in\mathcal{A}\setminus\{\pi_t^{opt}(s)\}} Q_t^{opt}(a, s)$ *in A7 measures the difference between the state-action value under the best action and the second best action. This condition is imposed to simplify the theoretical analysis. It can be relaxed to require the probability that the margin approaches zero to converge to zero at certain rate [see e.g., Qian and Murphy, 2011, Luedtke and van der Laan, 2016, Shi et al., 2022, 2024b], when coupled with data splitting.*

Remark 15. *Both A8 and A9 are mild as* K *and* L *are user-specified. Meanwhile, it is also possible to remove the lower bound requirements on* c_4 *in A9 under SA1 and SA5. In such cases, it suffices for the sieve approximation error to simply tend towards zero, as opposed to being* $o\{(NT)^{-1/2}\}$*. The latter is required to ensure the bias of the Q-estimator converge to zero at a faster rate than its standard deviation. Consequently, our CUSUM-type test statistics ensure that the proposed tests remain valid under weaker assumptions about the approximation error and are not overly sensitive to the number of basis functions* L*. This is because at each hypothesized error location, the test statistics implement scaled differencing, requiring the difference in approximation errors, instead of these errors themselves, to converge at a specific order. Under SA1 and SA5, all the approximation errors are equal, and such an order requirement is automatically satisfied.*

Theorem 4.1 (Size)**.** *Recall that* $\mathcal{D}$ *denote the observed data. Suppose A1-A9 and the null hypothesis SA3 hold, we have*

$$\sup_z |\mathbb{P}(TS_1^b \le z|\mathcal{D}) - \mathbb{P}(TS_1 \le z)| = O\Big(\frac{\sqrt{L}\log^2(NT)}{(1-\gamma)^{3/4}(\epsilon NT)^{1/8}}\Big) + O\Big(\frac{L^{-p/d}\sqrt{NT\log(NT)}}{(1-\gamma)^2}\Big),$$

$$\sup_z |\mathbb{P}(TS_n^b \le z|\mathcal{D}) - \mathbb{P}(TS_n \le z)| = O\Big(\frac{L^{1/4}\log^2(NT)}{(1-\gamma)^{1/4}(\epsilon NT)^{1/8}}\Big) + O\Big(\frac{L^{-p/d}\sqrt{NT\log(NT)}}{(1-\gamma)^3}\Big),$$

$$\sup_z |\mathbb{P}(TS_\infty^b \le z|\mathcal{D}) - \mathbb{P}(TS_\infty \le z)| = O\Big(\frac{\sqrt{L}\log^2(NT)}{(1-\gamma)^{3/4}(\epsilon NT)^{1/8}}\Big) + O\Big(\frac{L^{-p/d}\sqrt{NT\log(NT)}}{(1-\gamma)^2}\Big),$$

with probability at least $1 - O(N^{-1}T^{-1})$.

Theorem 4.1 derives the upper error bounds on the differences in distribution between the proposed test statistics and the conditional distributions of the bootstrapped statistic given the data. In particular, the error bounds depend on five factors: (i) the minimal sample size ϵNT

in estimating the Q-function over specified time intervals; (ii) the number of basis functions L; (iii) the $(1-\gamma)^{-1}$ term which has a similar interpretation as the "horizon" in episodic tasks; (iv) the smoothness of the system dynamics, measured by p; (v) the dimension of the state space d. Under the given conditions in L, ϵ, p, d, and as γ remains bounded away from 1, these bounds decay to zero, implying that the size of the proposed test approaches the nominal level as the total number of observations diverges to infinity.

Additionally, it is important to note that the second error bound for the normalized test statistics depends more heavily on the horizon $(1-\gamma)^{-1}$ compared to the other two test statistics. Specifically, this error term for the normalized test statistics is proportional to $(1-\gamma)^{-3}$, while for the other two, it is $(1-\gamma)^{-2}$. This increased dependence is due to the estimation of variance in the normalized test procedure. As such, in settings where the system is not overly smooth – i.e., p is small – the second error term becomes the dominant factor in the error bound, leading to a higher type-I error for the normalized test. Such a finding aligns with our results in the real-data-based simulation; see Figure C.4.

Finally, as commented in the introduction, the derivation of the consistency of the proposed test is complicated due to that we allow L to grow with the number of observations. Specifically, when L is fixed, the test statistic's limiting distribution can typically be derived using classical weak convergence theorems [van der Vaart and Wellner, 1996]. However, these theorems become inapplicable as L diverges with the sample size. This complexity arises because the dimension of the estimator $\widehat{\beta}$ also expands with L. To prove its asymptotic normality, it is necessary to demonstrate that $\widehat{\beta}$ converges to a Gaussian vector despite the growth of its dimension. To address this challenge, we develop a matrix concentration inequality for nonstationary MDPs in Lemma B.3.

4.2 Power of the Test

We next establish the power property of the proposed test. In our theoretical analysis, we focus on a particular type of alternative hypothesis $\mathcal{H}_a$ where there is a single change point $T^* \in (T_0, T)$ such that

$$Q_{T_0}^{opt} = Q_{T_0+1}^{opt} = \cdots = Q_{T^*-1}^{opt} \neq Q_{T^*}^{opt} = Q_{T^*+1}^{opt} = \cdots = Q_T^{opt}. \tag{4.1}$$

Let $\Delta_1 = T^{-1}\sum_{t=0}^{T-1}\mathbb{E}|Q_{T_0}^{opt}(A_t, S_t) - Q_T^{opt}(A_t, S_t)|$ and $\Delta_\infty = \sup_{a,s}|Q_{T_0}^{opt}(a,s) - Q_T^{opt}(a,s)|$ characterize the degree of nonstationarity. Specifically, the null holds if Δ_1 or Δ_∞ equals zero and the alternative hypothesis $\mathcal{H}_a$ holds if Δ_1 or Δ_∞ is positive. However, we remark that the proposed test is consistent against more general alternative hypothesis as well. See Section 5 for details. For any two positive sequences $\{a_{N,T}\}_{N,T}$ and $\{b_{N,T}\}_{N,T}$, the notation $a_{N,T} \gg b_{N,T}$ means that $b_{N,T}/a_{N,T} \to 0$ as $NT \to \infty$.

A10 (Change point): $T_0 + \epsilon T < T^* < (1-\epsilon)T$ given the boundary removal parameter ϵ.

Theorem 4.2 (Power)**.** *Suppose A1-A10 hold.*

- *If* $\Delta_1 \gg (1-\gamma)^{-2}\sqrt{L(\epsilon NT)^{-1}\log(NT)} + (1-\gamma)^{-2}L^{-p/d}$*, then the power of the test based on* TS_1 (3.1) *is at least* $1 - O(N^{-1}T^{-1})$*;*

- *If* $\Delta_\infty \gg (1-\gamma)^{-2}\sqrt{L(\epsilon NT)^{-1}\log(NT)} + (1-\gamma)^{-2}L^{-p/d}$*, then the power of the test based on* TS_∞ (3.2) *is at least* $1 - O(N^{-1}T^{-1})$*;*
- *If* $\Delta_\infty \gg (1-\gamma)^{-2}\sqrt{L(\epsilon NT)^{-1}\log(NT)} + L^{-p/d}$*, then the power of the test based on* TS_n (3.3) *is at least* $1 - O(N^{-1}T^{-1})$.

Assumption A10 is reasonable as we allow ϵ to decay to zero as the number of observations grows to infinity (see A1). The conditions on Δ_1 and Δ_∞ essentially require the signal under $\mathcal{H}_a$ to be much larger than a certain lower bound to detect the change. In settings where the system is not overly smooth and p is small, the second term will dominate the lower bound. It is evident that the lower bounds for the ℓ_1-type and unnormalized maximum-type tests depend more heavily on the horizon $(1-\gamma)^{-1}$ than the normalized test. As such, when Δ_1 and Δ_∞ are of the same order of magnitude, both the ℓ_1-type test (3.1) and unnormalized maximum-type test (3.2) require stronger conditions on the signal strength to detect the alternative hypothesis than the normalized test. This observation aligns with our empirical study, where we find that the normalized test generally achieves better power properties than the other two tests (see Figure C.4). To further boost power, we use cross-validation to select the number of basis functions for all three tests, as discussed in Section C.1. This ensures the bias and standard deviation of the Q-function estimator are approximately of the same order of magnitude.

5 Simulations

In this section, we conduct simulation studies to evaluate the finite sample performance of the proposed method and compare against common alternatives. Section 5.1 presents results of the proposed offline testing and change point detection methods based on four generative models with different nonstationarity scenarios (see Table 5.1). Section 5.2 further demonstrates the usefulness of the proposed method in an online setting as data accumulate. In Section C.5 of the Supplementary Materials, we simulate data to mimic the data setup in the motivating application of IHS. All simulation results are aggregated over 100 replications.

5.1 Offline Testing and Change Point Detection

We consider four nonstationary data generating processes with one-dimensional states and binary actions where the nonstationarity occurs in either the state transition function or the reward function, as listed in Table 5.1. For nonstationary functions, both abrupt (e.g., the underlying function is piece-wise constant) and smooth changes are considered. Specifically, in the first two scenarios, the transition function $\mathcal{T}_t$ is stationary whereas the reward function r_t is piecewise constant or varies smoothly over time, respectively. The last two scenarios involve stationary reward functions and nonstationary transition functions. See Section C.3 for more details about the data generating processes in these four scenarios.

In all scenarios, we set T =100 and simulated offline data with sample sizes $N = 25, 100$. The true location of the change point T^* was set to 50. We first applied each of the proposed

	State transition function	Reward function
(1)	Time-homogeneous	Piecewise constant
(2)	Time-homogeneous	Smooth
(3)	Piecewise constant	Time-homogeneous
(4)	Smooth	Time-homogeneous

Table 5.1: Simulation scenarios with different types of nonstationarity in Sections 5.1 and 5.2.

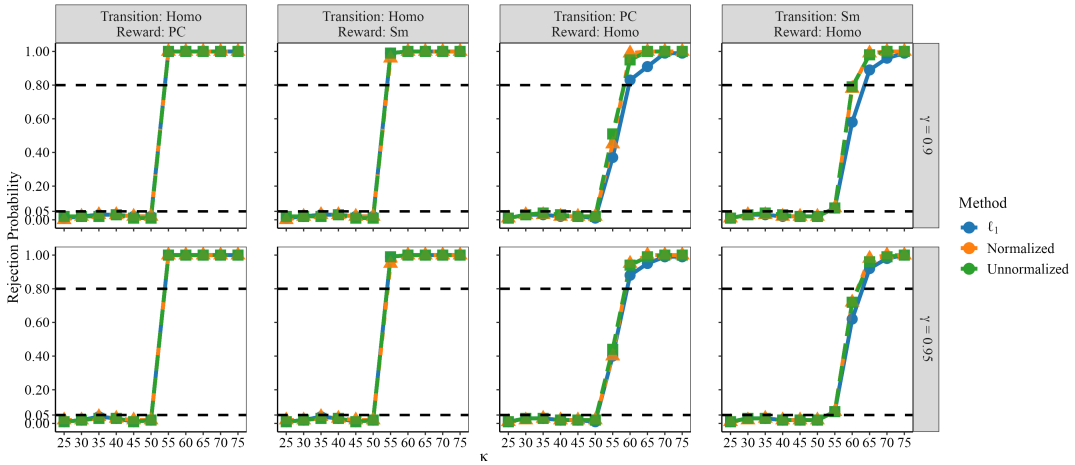

Figure 5.1: Empirical type-I errors and powers of the proposed test and their associated 95% confidence intervals under settings described in Section 5.1, with $N = 25$. Abbreviations: Homo for homogeneous, PC for piecewise constant, and Sm for smooth.

three tests to the time interval $[T - \kappa, T]$ to detect nonstationarity, where κ took value from a equally-spaced sequence between 25 and 75 with increments of 5. According to the true data generating mechanisms, when $\kappa \leq 50$, the null of no change point over $[T - \kappa, T]$ holds; the alternative hypothesis holds if $\kappa > 50$. The actions were generated i.i.d. according to a Bernoulli random variable with a success probability of 0.5.

Figures 5.1 and C.2(a) show the empirical rejection probabilities of each proposed test, when $N = 25$ and 100 respectively. First, in all settings, each test properly controls the type-I error. Second, the power increases with κ due to inclusion of more pre-change-point data into the interval $[T - \kappa, T]$. The power also increases with the sample size N, demonstrating the consistency of our tests. Third, as expected, gradual changes are more difficult to detect than abrupt changes. This is evident in Figure 5.1, where when $\kappa = 55$, the power of the proposed test in scenarios with a smooth reward or state transition function is smaller than scenarios with a piecewise constant function. Finally, the maximum-type tests (3.2) and (3.3) achieve slightly higher power than the ℓ_1-type test (3.1) when $N = 25$, whereas the powers of the three tests become indistinguishable when $N = 100$.

Next, we investigate the finite sample performance of the estimated change point location

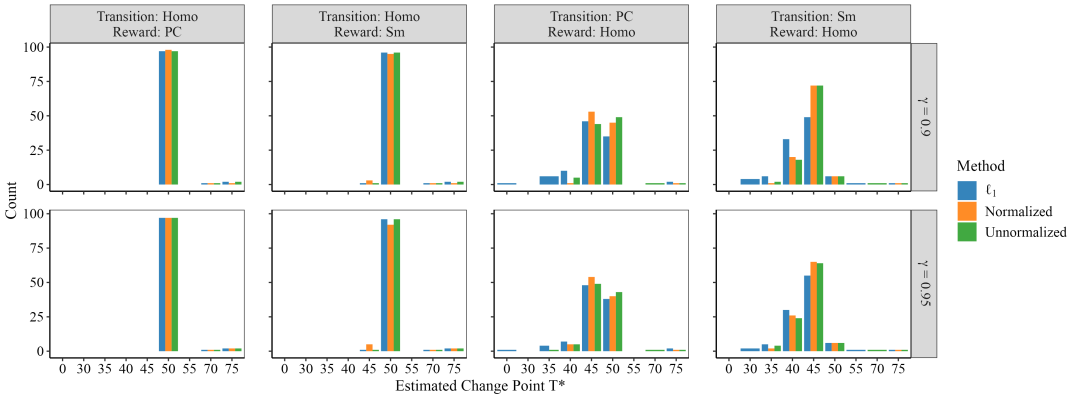

Figure 5.2: Distribution of detected change points under simulation settings in Section 5.1 with $N = 25$.

$\widehat{T}^*$. Figures 5.2 and C.2(b) depict the distribution of $\widehat{T}^*$ in each simulation scenario. It can be seen that in the first two scenarios with abrupt changes, the estimated change points concentrate on 50, which is the true change point location, yielding a minimal detection delay. In the last two scenarios with smooth changes, the estimated change points have a wider spread especially when $N = 25$. This results in a marginally extended detection delay. However, in the majority of cases, these estimators are still close to 50.

5.2 Online Evaluation

Finally, we illustrate how the proposed change point detection method can be coupled with existing state-of-the-art RL algorithms for policy learning in nonstationary environments. In each simulation, we first simulated an offline dataset as discussed earlier with $T = 100$ and $N = 200$. We next applied our proposal to identify the most recent change point location $\widehat{T}^*$ and estimated the optimal policy using the data subset $\{(S_{i,t}, R_{i,t}, A_{i,t}) : 1 \leq i \leq N, \widehat{T}^* \leq t \leq T\}$. As commented earlier, the resulting estimated policy can be used for treatment recommendation after study end time T. Specifically, we used a decision tree model [Myles et al., 2004] to approximate Q^{opt} to obtain interpretable policies for healthcare researchers. Through FQI, we transformed the estimation of Q^{opt} into an iterative regression problem (see (2.5)) and employed decision tree regression to update the Q-estimator at each iteration. The decision tree model involves hyperparameters such as the maximum tree depth and the minimum number of samples on each leaf node. We used 5-fold cross validation to select these hyperparameters from $\{3, 5, 6\}$ and $\{50, 60, 80\}$, respectively.

Next, for each of the 200 subjects, we sequentially applied our procedure for online policy learning as data accumulated to maximize their cumulative reward. Specifically, we assumed the number of change points after $T = 100$ followed a Poisson process with rate $1/50$. In other words, we expected a new change point to occur every 50 time points. We set the termination time $T_{end} = 300$, yielding 3 to 4 change points in most simulations. We similarly considered four different types of change points listed in Table 5.1. Whenever a new change point

occured, the effect of the action on the state transition or reward function was reversed. We further considered three different settings with strong, moderate and weak signals by varying the magnitude of treatment effect. For instance, suppose we have two change points T_1 and T_2 after $T = 100$. In Scenario (1) with a piecewise constant reward function, we set $r(s, a)$ to $1.5\delta as$ when $t \in [100, T_1)$ or $[T_2, 300]$ and $-1.5\delta as$ when $t \in (T_1, T_2]$ where δ measures the treatment effect equals $1, 0.5$ and 0.3 in strong-, moderate- and weak-signal settings, respectively.

Finally, we assumed that online data came in batches regularly at every $L = 15$ time points starting from $T = 100$. The first online data batch was generated according to an ϵ-greedy policy that selected actions using the estimated optimal policy $\widehat{\pi}$ computed based on the data subset in the time interval $[\widehat{T}^*, T]$ with probability $1 - \epsilon$ and a uniformly random policy with probability ϵ. Let $T^{*(0)} = \widehat{T}^*$. Suppose we have received k batches of data. We first apply the proposed change point detection method on the data subset in $[T^{*(d-1)}, T + dL]$ to identify a new change point $T^{*(d)}$. If no changes are detected, we set $T^{*(d)} = T^{*(d-1)}$. We next update the optimal policy based on the data subset in $[T^{*(d)}, T + dL]$ and use this estimated optimal policy (combined with the ϵ-greedy algorithm) to generate the $(k+1)$-th data batch. We repeat this procedure until the termination time T_{end} is reached and aggregate all immediate rewards obtained from time T to T_{end} over the 200 subjects to estimate the average value.

Comparison is made among the following methods:

Proposed: The proposed ℓ_1-type test (3.1) (the other two tests yield similar change points and policies. Their results are not reported to save space);

Oracle: The "oracle" policy optimization method that works as if the oracle change point location were known in advance;

Overall: Standard policy optimization method that uses all the data;

Random: Policy optimization with a randomly assigned change point location;

ODCP: The online Dirichlet change point approach proposed by Padakandla et al. [2020];

MBCD: The model-based RL context detection approach proposed by Alegre et al. [2021];

Kernel: The kernel-based approach developed by Domingues et al. [2021].

For fair comparisons, we used FQI and decision tree regression to compute the optimal Q-function for all methods. To implement the random method, after a new batch of data arrived, we randomly picked a time point uniformly from the new batch as the next change point location and computed the optimal Q-function based on the observations that occurred afterwards. The oracle method was implemented by repeatedly using observations that occurred after the oracle change point to update the optimal policy.

The last three methods – ODCP, MBCD and Kernel – are existing state-of-the-art nonstationary RL approaches. In particular, similar to ours, both ODCP and MBCP are change-point-based methods that apply stationary RL to the best data segment of stationarity identified by a change point detection algorithm. Among the two algorithms, MBCD is model-based, which uses neural networks for estimating the reward and transition functions, along with a likelihood ratio test for detecting change point. ODCP was originally proposed by Prabuchandran et al. [2022] for handling compositional multivariate data and later adapted by Padakandla et al. [2020] for RL in nonstationary environments. It is model-free. Specifically, it does not model the reward and transition functions, but applies the likelihood ratio test to detect changes in the

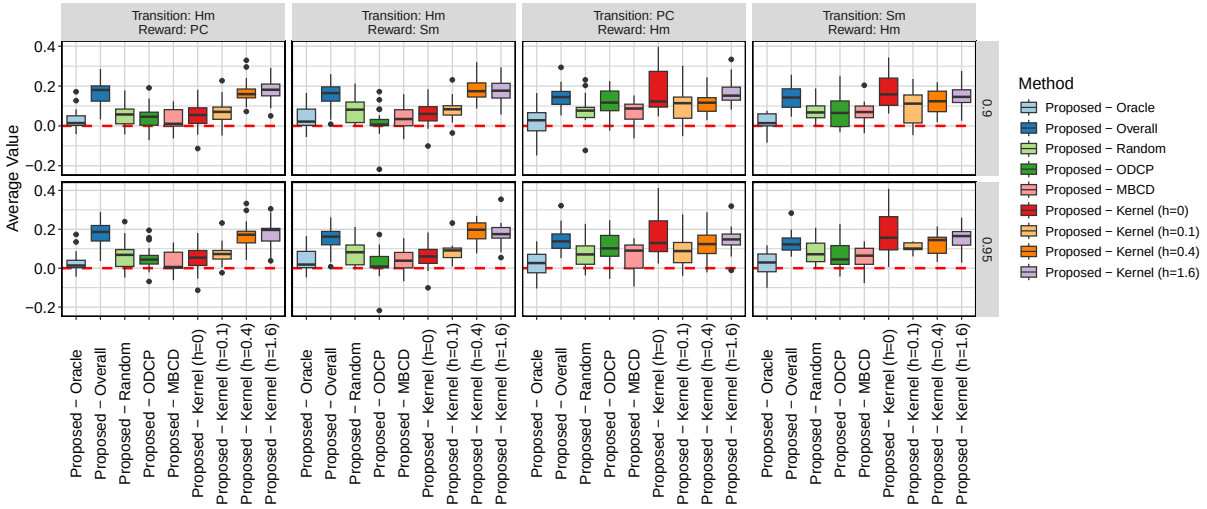

Figure 5.3: Distribution of the difference between the average value $(T_{end} - T)^{-1} \sum_{t=T+1}^{T_{end}} \mathbb{E} R_t$ under the proposed policy and those under policies computed by other baseline methods, under settings in Section 5.1 with strong signal-to-noise ratio. The proposed policy is based on the change point detected by the ℓ_1-type test (3.1). In all scenarios, we find the normalized or unnormalized tests (3.2) and (3.3) yield similar average values.

marginal state-reward distribution. As such, this algorithm is not consistent: it might detect changes in the behavior policy rather than in the Q- or transition function [Wang et al., 2023b]. Finally, the kernel-based method is non-change-point-based. It uses a kernel to assign larger weights to more recent observations, and smaller weights to past observations to deal with nonstationarity. To implement this method, we used the Gaussian RBF kernel with bandwidth parameters chosen from $\{0, 0.1, 0.4, 1.6\}$. More details about these three methods can be found in Section C.3.

Figure 5.3 reports the difference between the average value under the proposed policy and those under policies estimated based on these baseline methods in the "strong signal" setting (i.e., the treatment effect $\delta = 1$). Results with moderate and weak signals are available in Section C.4. We briefly summarize a few notable findings:

1. First, the proposed method achieves much larger average values compared to the "overall" method, demonstrating the inferiority of the best policy learned without acknowledging the nonstationarity.

2. Second, the proposed method is no worse and often better than kernel-based approaches in most cases. In addition, as shown in Figure 5.3, kernel-based method can be sensitive to the choice of the kernel bandwidth and it remains unclear how to determine this tuning parameter in practice. These results highlight the necessity of change point detection in policy learning, demonstrating the benefits of change-point-based methods in nonstationary RL.

3. Third, the proposed method outperforms the "random" method in almost all cases. It also achieves larger average values than ODCP in most cases. As ODCP is not guaranteed to consistently detect the change point, these results imply that correctly identifying the change point location is essential to policy optimization in nonstationary environment.

4. Finally, the model-based MBCD method produces smaller average rewards in general than the proposed method. This demonstrates the advantage of our model-free method, which is less prone to model misspecification.

6 Application to Intern Health Study

The 2018 Intern Health Study (IHS) is a micro-randomized trial (MRT) that seeks to evaluate the efficacy of push notifications sent via a customized study app upon proximal physical and mental health outcomes [NeCamp et al., 2020], a critical first step for designing effective just-in-time adaptive interventions. Over the 26 weeks, each study subject was re-randomized weekly to receive or not to receive activity suggestions; daily self-reported mood scores were assessed via ecological momentary assessments, a method repeatedly recording subjects' behaviors in real time and in their natural environment; step count and sleep duration were measured by Fitbit. In this paper, we focus on policy optimization for improving time-discounted cumulative step counts under the infinite horizon setting. As discussed in Section 1, determining the optimal policy for delivering prompts is challenging due to potential nostationarity that results in changes in treatment effects. Here we demonstrate how to use the proposed method to detect change point and perform optimal policy estimation in the presence of potential temporal nonstationarity.

6.1 Data and method: Setup

Let S_t denote a 4-dimensional state vector comprised of the following: (i) the square root of average step count in the previous week $t-1$; (ii) the cubic root of average sleep minutes in week $t-1$; (iii) the average mood score in week $t-1$; (iv) the square root of average step count in week $t-2$. All these variables are centered and scaled [NeCamp et al., 2020]. The binary action $A_t = 1$ (0) corresponds to pushing (not pushing) an activity message at the start of week t. The randomization probabilities are known under MRT: $\mathbb{P}(A_t = 1) = 1 - \mathbb{P}(A_t = 0) = 1/4$. The reward R_t is defined as the average step count in week t. To resemble a real-time evaluation scenario, we divide the data of 26 weeks into two trunks: we perform change point detection and estimate the optimal policy based on data collected in the first $T = 22$ weeks (training data batch), and then evaluate the estimated policy on data in the remaining 4 weeks (evaluation data batch) assuming that there is no change point in the final 4 weeks. To implement change point detection, we set the boundary removal parameter $\epsilon = 0.08$ and search for change points within $[5, 18]$. We focus on three specialties: emergency ($N = 141$), pediatrics ($N = 211$), and family practice ($N = 125$). One consideration is that work schedules and activity levels vary greatly across different specialties, and thus medical interns might

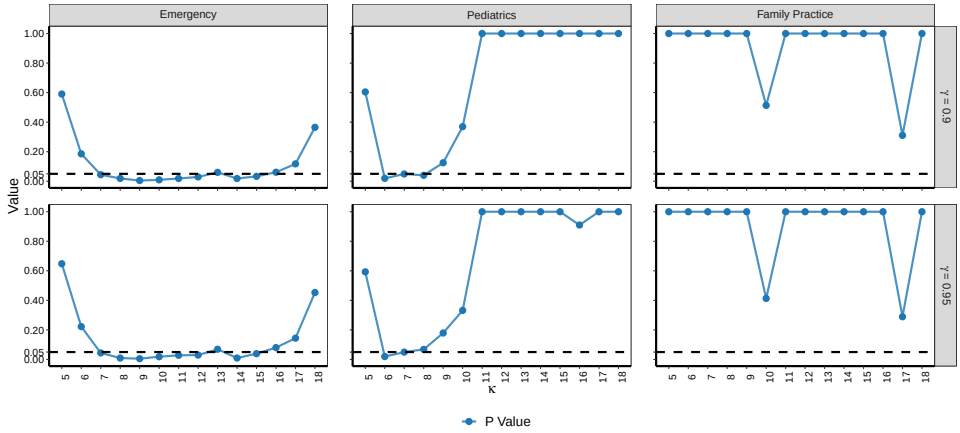

Figure 6.1: p-values over different values of κ (the number of time points from the last time point T) under $\gamma = 0.9$ (top) and 0.95 (bottom) among the three specialties considered in IHS.

experience distinct change points. Stratification by specialty may improve homogeneity of the study groups so that the assumption of a common change point is more plausible.

6.2 Results

Figure 6.1 plots the trajectories of p-values using ℓ_1-type test statistic (3.1); the results are similar when maximum-type tests (3.2) and (3.3) were applied to the data (not reported here). We consider $\gamma = 0.9$ or 0.95, which produce similar results. First, we notice that in the pediatrics and family practice specialties, many p-values are close to 1. This is due to the use of the p-value aggregation method [Meinshausen et al., 2009, see Section C.1 for details], which tends to increase insignificant p-values and reduce the type-I error. Second, the emergency specialty displays roughly monotonically decreasing p-values over time, whereas at the largest few κ values the p-values rise up due to the limited effective sample size at the boundary. Third, the U-shaped p-value trajectory of the pediatrics specialty shows evidence for multiple change points. Specifically, when only a single change point exists, the significant p-values are likely to decrease with κ. The U-shaped p-value trajectory can occur only when the data interval contains at least two change points and the system dynamics after the second change point is similar to that before the first change occurs, yielding a small CUSUM statistics. Because we focus on the latest detected change point (first κ_{j_0-1} where κ_{j_0} results in a rejection of the null) to inform the latest data segment to use for optimal policy estimation, we find $\kappa_{j_0-1} = 6$ for the emergency specialty and $\kappa_{j_0-1} = 5$ for the pediatrics specialty, for both choices of γ. Fourth, the p-value trajectories of the family practice specialty (mostly close to 1) are above the significance threshold, indicating the stationarity assumption is compatible with this data subset. We therefore estimate the optimal policy using data from all the time points for the family practice specialty.

We next compare the proposed policy optimization method with three other methods: 1) overall, 2) random, which were described in Section 5.1) and 3) behavior, which is the treat-

ment policy used in the completed MRT. The data of the first 22 weeks are used to learn an optimal policy $\widehat{\pi}^{opt}$ through FQI and decision tree regression. In particular, the proposed method uses data after the estimated change point location whereas the overall method uses all the training data. Similar to simulations, hyperparameters of the decision tree regression are selected via 5-fold cross-validation. Next, based on the evaluation data, we applied FQE to the testing data of the remaining 4 weeks to evaluate the γ-discounted values (i.e., $J_\gamma(\pi)$) of these estimated optimal policies. Results are reported in Table 6.2. It can be seen that the proposed method achieves larger values when compared to "random" and "behavior" in all cases, demonstrating the need for change point detection and data-driven decision making. In the following, we focus on comparing the proposed method against "overall". In the emergency specialty, the optimal policy estimated using data after the detected change point improves weekly average step count per day by about $130 \sim 170$ steps relative to the estimated policy based on the overall method. In the pediatrics specialty, however, the overall method achieves a larger weekly average step count by about $40 \sim 112$ steps per day. Recall that the proposed method only uses data on $t \in [T - \kappa_{j_0-1}, T] = [17, 22]$ for policy learning. As commented earlier, there are likely two change points in the pediatrics specialty and according to Fig 6.1, the system dynamics after the first most recent change point are very similar to those before the second most recent change point. As a result, the overall method pools over more data from similar dynamics, resulting in a better policy. This represents a bias-variance trade-off. In settings with a U-shaped p-value trajectory and the most recent change point is close to the second most recent one, it might be sensible to borrow more information from the historical data. Finally, the proposed and overall methods have equal values in the family practice specialty since no change point is identified.

Number of Change Points	Specialty	Method	$\gamma = 0.9$	$\gamma = 0.95$
≥ 1	Emergency	Proposed	8237.16	8295.99
		Overall	8108.13	8127.55
		Behavior	7823.75	7777.32
		Random	8114.78	8080.27
≥ 2	Pediatrics	Proposed	7883.08	7848.57
		Overall	7925.44	7960.12
		Behavior	7730.98	7721.29
		Random	7807.52	7815.30
0	Family Practice	Proposed	8062.50	7983.69
		Overall	8062.50	7983.69
		Behavior	7967.67	7957.24
		Random	7983.52	7969.31

Table 6.2: Mean value estimates using decision tree in analysis of IHS. Values are normalized by multiplying $1 - \gamma$. All values are evaluated over 10 splits of data.

7 Discussion

We propose three tests for assessing the stationarity assumption in RL, including an ℓ_1-type test, a maximum-type test and a normalized maximum-type test. In our numerical experiments, these tests generally lead to the same conclusions. To illustrate this, we calculate the percentage of times any of the two tests produce concordant results – either both rejecting or both not rejecting the null hypothesis – across 100 simulation replications and visualize them in Figure A.1. The agreement rates exceed 95% for any two tests in most scenarios. Specifically, the ℓ_1-type and unnormalized maximum-type tests exhibit particularly high consistency, with agreement rates over 97.5% in the majority of cases. Most inconsistencies primarily arise between the normalized test and the other two. This behavior is expected since our theoretical and empirical results suggest that the normalized test tends to achieve a larger type-I error and a larger power. As such, it is more likely to reject the null, leading to these inconsistencies.

To address such inconsistency, we further outline two approaches in Section A.3. The first approach chooses one out of the three tests, depending on the application scenarios. The second approach aggregates results from all three tests to produce a final p-value. This approach leverages the advantages of the three tests and outperforms each of them individually, according to our empirical study; see Figure A.2.

Given an offline dataset, we focus on detecting the most recent change point. That is, regardless of how many change points there are in the past, we aim to identify the most recent one. Meanwhile, our procedure can be easily adapted to identify all past change points. Specifically, as described in Section 3.4, given a pre-specified monotonically increasing sequence $\{\kappa_j\}_j \subseteq (0, T)$, our proposed test is applied to each interval $[T - \kappa_j, T]$. We define the most recent change point as $\widehat{T}^* = T - \kappa_{j_0-1}$ where the test is first rejected at κ_{j_0}. In general when there are multiple change points, we can continue applying our procedure to the interval $(0, \widehat{T}^*)$ and identify the second most recent change point $\widehat{T}_2^*$. This process can be repeated until the remaining interval does not contain other change points. When the change points are dense, we recommend to specify as many κ_j's as possible at which the test is applied, to ensure they can be precisely identified.

Acknowledgements

We thank the Editor, the Associate Editor, and the anonymous referees for their insightful suggestions and comments, which largely enhanced the quality of our paper. This work is partly supported by EPSRC grants EP/W014971/1 (CS), EP/V053639/1 (PF), NIH Grants R01 MH101459 (ZW), R01 NR013658 (ZW), and a Precision Health Investigator Award at University of Michigan (ZW, ML). The authors are grateful for the contributions of the researchers, administrators, and participants involved in the Intern Health Study (PI: Srijan Sen, https://clinicaltrials.gov/study/NCT03972293).

References

Alekh Agarwal, Nan Jiang, Sham M Kakade, and Wen Sun. Reinforcement learning: Theory and algorithms. *CS Dept., UW Seattle, Seattle, WA, USA, Tech. Rep*, 32, 2019.

Lucas N. Alegre, Ana L. C. Bazzan, and Bruno C. da Silva. Minimum-delay adaptation in non-stationary reinforcement learning via online high-confidence change-point detection. In *Proceedings of the 20th International Conference on Autonomous Agents and MultiAgent Systems*, AAMAS '21, page 97–105, Richland, SC, 2021. International Foundation for Autonomous Agents and Multiagent Systems. ISBN 9781450383073.

Pierre Alquier, Paul Doukhan, and Xiequan Fan. Exponential inequalities for nonstationary Markov chains. *Dependence Modeling*, 7(1):150–168, 2019.

S. Aminikhanghahi and D. Cook. A survey of methods for time series change point detection. *Knowledge and Information Systems*, 51:339–367, 2017.

Alexandre Belloni and Roberto I Oliveira. A high dimensional central limit theorem for martingales, with applications to context tree models. *arXiv preprint arXiv:1809.02741*, 2018.

Alexandre Belloni, Victor Chernozhukov, Denis Chetverikov, and Kengo Kato. Some new asymptotic theory for least squares series: Pointwise and uniform results. *Journal of Econometrics*, 186(2):345–366, 2015.

Zeyu Bian, Chengchun Shi, Zhengling Qi, and Lan Wang. Off-policy evaluation in doubly inhomogeneous environments. *Journal of the American Statistical Association*, to appear, 2025.

Zygmunt Wilhelm Birnbaum. An inequality for Mill's ratio. *The Annals of Mathematical Statistics*, 13(2):245–246, 1942.

Prabir Burman and Keh-Wei Chen. Nonparametric estimation of a regression function. *The Annals of Statististics*, 17(4):1567–1596, 1989. ISSN 0090-5364.

Bernard Cazelles, Clara Champagne, and Joseph Dureau. Accounting for non-stationarity in epidemiology by embedding time-varying parameters in stochastic models. *PLoS Computational Biology*, 14(8):e1006211, 2018.

Bibhas Chakraborty, Susan Murphy, and Victor Strecher. Inference for non-regular parameters in optimal dynamic treatment regimes. *Statistical Methods in Medical Research*, 19(3):317–343, 2010.

Bibhas Chakraborty, Eric B Laber, and Yingqi Zhao. Inference for optimal dynamic treatment regimes using an adaptive m-out-of-n bootstrap scheme. *Biometrics*, 69(3):714–723, 2013.

Bin Chen and Yongmiao Hong. Testing for the markov property in time series. *Econometric Theory*, 28(1):130–178, 2012.

Elynn Y Chen, Rui Song, and Michael I Jordan. Reinforcement learning with heterogeneous data: estimation and inference. *Journal of the American Statistical Association*, accepted, 2024.

Jinglin Chen and Nan Jiang. Information-theoretic considerations in batch reinforcement learning. In *International Conference on Machine Learning*, pages 1042–1051. PMLR, 2019.

Xi Chen, Yining Wang, and Yuan Zhou. Dynamic assortment optimization with changing contextual information. *Journal of machine learning research*, 21:1–44, 2020.

Xiaohong Chen and Timothy M Christensen. Optimal uniform convergence rates and asymptotic normality for series estimators under weak dependence and weak conditions. *Journal of Econometrics*, 188(2):447–465, 2015.

Xiaohong Chen and Timothy M Christensen. Optimal sup-norm rates and uniform inference on nonlinear functionals of nonparametric IV regression. *Quantitative Economics*, 9(1):39–84, 2018.

Victor Chernozhukov, Denis Chetverikov, and Kengo Kato. Gaussian approximation of suprema of empirical processes. *Ann. Statist.*, 42(4):1564–1597, 2014. ISSN 0090-5364.

Victor Chernozhukov, Denis Chetverikov, and Kengo Kato. Detailed proof of nazarov's inequality. *arXiv preprint arXiv:1711.10696*, 2017.

Wang Chi Cheung, David Simchi-Levi, and Ruihao Zhu. Reinforcement learning for non-stationary Markov decision processes: The blessing of (more) optimism. In *International Conference on Machine Learning*, pages 1843–1854. PMLR, 2020.

H. Cho and P. Fryzlewicz. Multiple change-point detection for high-dimensional time series via sparsified binary segmentation. *Journal of the Royal Statistical Society: Series B*, 77: 475–507, 2015.

Haeran Cho and Piotr Fryzlewicz. Multiscale and multilevel technique for consistent segmentation of nonstationary time series. *Statistica Sinica*, pages 207–229, 2012.

Linda M Collins, Susan A Murphy, and Victor Strecher. The multiphase optimization strategy (most) and the sequential multiple assignment randomized trial (smart): new methods for more potent ehealth interventions. *American journal of preventive medicine*, 32(5):S112–S118, 2007.

Matthew R Cooperberg, Jeanette M Broering, Mark S Litwin, Deborah P Lubeck, Shilpa S Mehta, James M Henning, Peter R Carroll, and CaPSURE Investigators. The contemporary management of prostate cancer in the united states: lessons from the cancer of the prostate strategic urologic research endeavor (capsure), a national disease registry. *The Journal of urology*, 171(4):1393–1401, 2004.

Miklós Csörgő, Miklós Csörgő, and Lajos Horváth. *Limit theorems in change-point analysis*. John Wiley & Sons, 1997.

Jérôme Dedecker and Xiequan Fan. Deviation inequalities for separately Lipschitz functionals of iterated random functions. *Stochastic Processes and their Applications*, 125(1):60–90, 2015.

Omar Darwiche Domingues, Pierre Ménard, Matteo Pirotta, Emilie Kaufmann, and Michal Valko. A kernel-based approach to non-stationary reinforcement learning in metric spaces. In *International Conference on Artificial Intelligence and Statistics*, pages 3538–3546. PMLR, 2021.

Hamid Eftekhari, Debarghya Mukherjee, Moulinath Banerjee, and Ya'acov Ritov. Markovian snd non-Markovian processes with active decision making strategies for addressing the COVID-19 pandemic. *arXiv preprint arXiv:2008.00375*, 2020.

Martin S Eichenbaum, Sergio Rebelo, and Mathias Trabandt. The macroeconomics of epidemics. Technical report, National Bureau of Economic Research, 2020.

Damien Ernst, Pierre Geurts, and Louis Wehenkel. Tree-based batch mode reinforcement learning. *Journal of Machine Learning Research*, 6:503–556, 2005. ISSN 1532-4435.

Ashkan Ertefaie and Robert L. Strawderman. Constructing dynamic treatment regimes over indefinite time horizons. *Biometrika*, 105(4):963–977, 2018. ISSN 0006-3444.

Jianqing Fan, Zhaoran Wang, Yuchen Xie, and Zhuoran Yang. A theoretical analysis of deep q-learning. In *Learning for Dynamics and Control*, pages 486–489. PMLR, 2020.

Ethan X Fang, Zhaoran Wang, and Lan Wang. Fairness-oriented learning for optimal individualized treatment rules. *Journal of the American Statistical Association*, 118(543):1733–1746, 2023.

Yingjie Fei, Zhuoran Yang, Zhaoran Wang, and Qiaomin Xie. Dynamic regret of policy optimization in non-stationary environments. In *Advances in Neural Information Processing Systems*, pages 6743–6754, 2020.

Songtao Feng, Ming Yin, Ruiquan Huang, Yu-Xiang Wang, Jing Yang, and Yingbin Liang. Non-stationary reinforcement learning under general function approximation. In *International Conference on Machine Learning*, pages 9976–10007. PMLR, 2023.

Ronald Aylmer Fisher. *Statistical methods for research workers*. Number 5. Oliver and Boyd, 1928.

P. Fryzlewicz. Wild binary segmentation for multiple change-point detection. *The Annals of Statistics*, 42:2243–2281, 2014.

Damien Garreau, Wittawat Jitkrittum, and Motonobu Kanagawa. Large sample analysis of the median heuristic. *arXiv preprint arXiv:1707.07269*, 2017.

Ulf Grenander. *Abstract inference*. Wiley Series, New York, 1981.

Xinzhou Guo and Xuming He. Inference on selected subgroups in clinical trials. *Journal of the American Statistical Association*, 116(535):1498–1506, 2021.

Botao Hao, Xiang Ji, Yaqi Duan, Hao Lu, Csaba Szepesvari, and Mengdi Wang. Bootstrapping fitted q-evaluation for off-policy inference. In *International Conference on Machine Learning*, pages 4074–4084. PMLR, 2021.

Hado V Hasselt. Double Q-learning. In *Advances in Neural Information Processing Systems*, pages 2613–2621, 2010.

Xinyu Hu, Min Qian, Bin Cheng, and Ying Kuen Cheung. Personalized policy learning using longitudinal mobile health data. *Journal of the American Statistical Association*, 116(533): 410–420, 2021.

Yuchen Hu and Stefan Wager. Off-policy evaluation in partially observed Markov decision processes under sequential ignorability. *The Annals of Statistics*, 51(4):1561–1585, 2023.

Jianhua Z. Huang. Projection estimation in multiple regression with application to functional ANOVA models. *The Annals of Statistics*, 26(1):242–272, 1998. ISSN 0090-5364.

Jianhua Z Huang. Local asymptotics for polynomial spline regression. *The Annals of Statistics*, 31(5):1600–1635, 2003.

Kenneth L Judd. *Numerical methods in economics*. MIT press, 1998.

Samer Kharroubi and Fatima Saleh. Are lockdown measures effective against covid-19? *Frontiers in public health*, 8:549692, 2020.

R. Killick, P. Fearnhead, and I. Eckley. Optimal detection of changepoints with a linear computational cost. *Journal of the American Statistical Association*, 107(500):1590–1598, 2012.

Predrag Klasnja, Shawna Smith, Nicholas J Seewald, Andy Lee, Kelly Hall, Brook Luers, Eric B Hekler, and Susan A Murphy. Efficacy of contextually tailored suggestions for physical activity: A micro-randomized optimization trial of Heartsteps. *Annals of Behavioral Medicine*, 53(6):573–582, 2019.

Varun Kompella, Roberto Capobianco, Stacy Jong, Jonathan Browne, Spencer Fox, Lauren Meyers, Peter Wurman, and Peter Stone. Reinforcement learning for optimization of COVID-19 mitigation policies. *arXiv preprint arXiv:2010.10560*, 2020.

Michael R Kosorok and Eric B Laber. Precision medicine. *Annual review of statistics and its application*, 6:263–286, 2019.

Balaji Lakshminarayanan, Alexander Pritzel, and Charles Blundell. Simple and scalable predictive uncertainty estimation using deep ensembles. *Advances in neural information processing systems*, 30, 2017.

Hoang Le, Cameron Voloshin, and Yisong Yue. batch policy learning under constraints. In *International Conference on Machine Learning*, pages 3703–3712, 2019.

Erwan Lecarpentier and Emmanuel Rachelson. Non-stationary Markov decision processes, a worst-case approach using model-based reinforcement learning. *Advances in Neural Information Processing Systems*, 32, 2019.

Gen Li, Laixi Shi, Yuxin Chen, Yuejie Chi, and Yuting Wei. Settling the sample complexity of model-based offline reinforcement learning. *The Annals of Statistics*, 52(1):233–260, 2024.

Yuxi Li. Reinforcement learning applications. *arXiv preprint arXiv:1908.06973*, 2019.

Peng Liao, Kristjan Greenewald, Predrag Klasnja, and Susan Murphy. Personalized HeartSteps: A reinforcement learning algorithm for optimizing physical activity. *Proceedings of the ACM on Interactive, Mobile, Wearable and Ubiquitous Technologies*, 4(1):1–22, 2020.

Peng Liao, Predrag Klasnja, and Susan Murphy. Off-policy estimation of long-term average outcomes with applications to mobile health. *Journal of the American Statistical Association*, 116(533):382–391, 2021.

Peng Liao, Zhengling Qi, Runzhe Wan, Predrag Klasnja, and Susan A Murphy. Batch policy learning in average reward Markov decision processes. *Annals of statistics*, 50(6):3364, 2022.

Weidong Liu, Jiyuan Tu, Yichen Zhang, and Xi Chen. Online estimation and inference for robust policy evaluation in reinforcement learning. *arXiv preprint arXiv:2310.02581*, 2023.

Y Liu and J. Xie. Cauchy combination test: a powerful test with analytic p-value calculation under arbitrary dependency structures. *Journal of the American Statistical Association*, 115: 393–402, 2020.

Luís Carlos Lopes-Júnior, Emiliana Bomfim, Denise Sayuri Calheiros da Silveira, Raphael Manhães Pessanha, Sara Isabel Pimentel Carvalho Schuab, and Regina Aparecida Garcia Lima. Protocol: Effectiveness of mass testing for control of covid-19: a systematic review protocol. *BMJ open*, 10(8), 2020.

Daniel J Luckett, Eric B Laber, Anna R Kahkoska, David M Maahs, Elizabeth Mayer-Davis, and Michael R Kosorok. Estimating dynamic treatment regimes in mobile health using V-learning. *Journal of the American Statistical Association*, 115(530):692–706, 2020.

Alexander R. Luedtke and Mark J. van der Laan. Statistical inference for the mean outcome under a possibly non-unique optimal treatment strategy. *The Annals of Statistics*, 44(2): 713–742, 2016. ISSN 0090-5364.

Hamid Reza Maei, Csaba Szepesvári, Shalabh Bhatnagar, and Richard S Sutton. Toward off-policy learning control with function approximation. In *ICML*, pages 719–726, 2010.

Cindy Marling and Razvan Bunescu. The OhioT1DM dataset for blood glucose level prediction: Update 2020. In *CEUR Workshop Proceedings*, volume 2675, page 71, 2020.

D. L. McLeish. Dependent central limit theorems and invariance principles. *Ann. Probability*, 2:620–628, 1974. ISSN 0091-1798.

Nicolai Meinshausen, Lukas Meier, and Peter Bühlmann. P-values for high-dimensional regression. *Journal of the American Statistical Association*, 104(488):1671–1681, 2009.

Shahar Mendelson, Alain Pajor, and Nicole Tomczak-Jaegermann. Uniform uncertainty principle for Bernoulli and sub-Gaussian ensembles. *Constructive Approximation*, 28(3):277–289, 2008.

Volodymyr Mnih, Koray Kavukcuoglu, David Silver, Andrei A Rusu, Joel Veness, Marc G Bellemare, Alex Graves, Martin Riedmiller, Andreas K Fidjeland, Georg Ostrovski, et al. Human-level control through deep reinforcement learning. *Nature*, 518(7540):529–533, 2015.

Rémi Munos and Csaba Szepesvári. Finite-time bounds for fitted value iteration. *Journal of Machine Learning Research*, 9(5), 2008.

S. A. Murphy. Optimal dynamic treatment regimes. *Journal of the Royal Statistical Society. Series B. Statistical Methodology*, 65(2):331–366, 2003. ISSN 1369-7412.

Anthony J Myles, Robert N Feudale, Yang Liu, Nathaniel A Woody, and Steven D Brown. An introduction to decision tree modeling. *Journal of Chemometrics: A Journal of the Chemometrics Society*, 18(6):275–285, 2004.

Timothy NeCamp, Srijan Sen, Elena Frank, Maureen A Walton, Edward L Ionides, Yu Fang, Ambuj Tewari, and Zhenke Wu. Assessing real-time moderation for developing adaptive mobile health interventions for medical interns: micro-randomized trial. *Journal of Medical Internet Research*, 22(3):e15033, 2020.

Xinkun Nie, Emma Brunskill, and Stefan Wager. Learning when-to-treat policies. *Journal of the American Statistical Association*, 116(533):392–409, 2021.

Farzad Niroui, Kaicheng Zhang, Zendai Kashino, and Goldie Nejat. Deep reinforcement learning robot for search and rescue applications: Exploration in unknown cluttered environments. *IEEE Robotics and Automation Letters*, 4(2):610–617, 2019.

Sindhu Padakandla, KJ Prabuchandran, and Shalabh Bhatnagar. Reinforcement learning algorithm for non-stationary environments. *Applied Intelligence*, 50(11):3590–3606, 2020.

K.J. Prabuchandran, Nitin Singh, Pankaj Dayama, Ashutosh Agarwal, and Vinayaka Pandit. Change point detection for compositional multivariate data. *Applied Intelligence*, 52(2): 1930–1955, 2022.

Martin L Puterman. *Markov decision processes: discrete stochastic dynamic programming*. John Wiley & Sons, 2014.

Zhengling Qi, Dacheng Liu, Haoda Fu, and Yufeng Liu. Multi-armed angle-based direct learning for estimating optimal individualized treatment rules with various outcomes. *Journal of the American Statistical Association*, 115(530):678–691, 2020.

Min Qian and Susan A. Murphy. Performance guarantees for individualized treatment rules. *The Annals of Statistics*, 39(2):1180–1210, 2011. ISSN 0090-5364.

Tianchen Qian, Ashley E Walton, Linda M Collins, Predrag Klasnja, Stephanie T Lanza, Inbal Nahum-Shani, Mashfiqui Rabbi, Michael A Russell, Maureen A Walton, Hyesun Yoo, et al. The microrandomized trial for developing digital interventions: Experimental design and data analysis considerations. *Psychological Methods*, 2022.

Ali Rahimi and Benjamin Recht. Random features for large-scale kernel machines. In J. Platt, D. Koller, Y. Singer, and S. Roweis, editors, *Advances in Neural Information Processing Systems*, volume 20. Curran Associates, Inc., 2007. URL https://proceedings.neurips.cc/paper/2007/file/013a006f03dbc5392effeb8f18fda755-Paper.pdf.

Pratik Ramprasad, Yuantong Li, Zhuoran Yang, Zhaoran Wang, Will Wei Sun, and Guang Cheng. Online bootstrap inference for policy evaluation in reinforcement learning. *arXiv preprint arXiv:2108.03706*, 2021.

James M Robins. Optimal structural nested models for optimal sequential decisions. In *Proceedings of the Second Seattle Symposium in Biostatistics*, pages 189–326. Springer, 2004.

Chengchun Shi, Ailin Fan, Rui Song, and Wenbin Lu. High-dimensional A-learning for optimal dynamic treatment regimes. *Ann. Statist.*, 46(3):925–957, 2018a. ISSN 0090-5364.

Chengchun Shi, Rui Song, Wenbin Lu, and Bo Fu. Maximin projection learning for optimal treatment decision with heterogeneous individualized treatment effects. *Journal of Royal Statistical Society: Series B*, 80(4):681–702, 2018b.

Chengchun Shi, Wenbin Lu, and Rui Song. Breaking the curse of nonregularity with dubagging—inference of the mean outcome under optimal treatment regimes. *Journal of Machine Learning Research*, 21(176):1–67, 2020a.

Chengchun Shi, Runzhe Wan, Rui Song, Wenbin Lu, and Ling Leng. Does the Markov decision process fit the data: testing for the Markov property in sequential decision making. In *International Conference on Machine Learning*, pages 8807–8817. PMLR, 2020b.

Chengchun Shi, Sheng Zhang, Wenbin Lu, and Rui Song. Statistical inference of the value function for reinforcement learning in infinite-horizon settings. *Journal of the Royal Statistical Society Series B: Statistical Methodology*, 84(3):765–793, 2022.

Chengchun Shi, Shikai Luo, Yuan Le, Hongtu Zhu, and Rui Song. Statistically efficient advantage learning for offline reinforcement learning in infinite horizons. *Journal of the American Statistical Association*, 119(545):232–245, 2024a.

Chengchun Shi, Zhengling Qi, Jianing Wang, and Fan Zhou. Value enhancement of reinforcement learning via efficient and robust trust region optimization. *Journal of the American Statistical Association*, 119(547):2011–2025, 2024b.

Daniel L Silver, Qiang Yang, and Lianghao Li. Lifelong machine learning systems: Beyond learning algorithms. In *2013 AAAI spring symposium series*, 2013.

Rui Song, Weiwei Wang, Donglin Zeng, and Michael R Kosorok. Penalized Q-learning for dynamic treatment regimens. *Statistica Sinica*, 25(3):901–920, 2015.

Richard S. Sutton and Andrew G. Barto. *Reinforcement Learning: An Introduction*. Adaptive Computation and Machine Learning. MIT Press, Cambridge, MA, second edition, 2018. ISBN 978-0-262-03924-6.

Joel Tropp. Freedman's inequality for matrix martingales. *Electronic Communications in Probability*, 16:262–270, 2011.

C. Truong, L. Oudre, and N. Vayatis. Selective review of offline change point detection methods. *Signal Processing*, 167, 2020. 107299.

Anastasios A Tsiatis, Marie Davidian, Shannon T Holloway, and Eric B Laber. *Dynamic Treatment Regimes: Statistical Methods for Precision Medicine*. CRC press, 2019.

Masatoshi Uehara, Masaaki Imaizumi, Nan Jiang, Nathan Kallus, Wen Sun, and Tengyang Xie. Finite sample analysis of minimax offline reinforcement learning: Completeness, fast rates and first-order efficiency. *arXiv preprint arXiv:2102.02981*, 2021.

Aad W. van der Vaart and Jon A. Wellner. *Weak convergence and empirical processes*. Springer Series in Statistics. Springer-Verlag, New York, 1996. ISBN 0-387-94640-3.

Michael P. Wallace and Erica E. M. Moodie. Doubly-robust dynamic treatment regimen estimation via weighted least squares. *Biometrics*, 71(3):636–644, 2015. ISSN 0006-341X.

Runzhe Wan, Xinyu Zhang, and Rui Song. Multi-objective reinforcement learning for infectious disease control with application to covid-19 spread. *arXiv preprint arXiv:2009.04607*, 2020.

Jiayi Wang, Zhengling Qi, and Raymond KW Wong. Projected state-action balancing weights for offline reinforcement learning. *The Annals of Statistics*, 51(4):1639–1665, 2023a.

Jitao Wang, Chengchun Shi, and Zhenke Wu. A robust test for the stationarity assumption in sequential decision making. In *International Conference on Machine Learning*, pages 36355–36379. PMLR, 2023b.

Lan Wang, Yu Zhou, Rui Song, and Ben Sherwood. Quantile-optimal treatment regimes. *J. Amer. Stat. Assoc.*, 113(523):1243–1254, 2018.

T. Wang and R. Samworth. High dimensional change point estimation via sparse projection. *Journal of the Royal Statistical Society: Series B*, 80:57–83, 2018.

Christopher JCH Watkins and Peter Dayan. Q-learning. *Machine learning*, 8(3-4):279–292, 1992.

Chen-Yu Wei and Haipeng Luo. Non-stationary reinforcement learning without prior knowledge: An optimal black-box approach. In *Conference on Learning Theory*, pages 4300–4354. PMLR, 2021.

Chien-Fu Jeff Wu. Jackknife, bootstrap and other resampling methods in regression analysis. *the Annals of Statistics*, 14(4):1261–1295, 1986.

Annie Xie, James Harrison, and Chelsea Finn. Deep reinforcement learning amidst continual structured non-stationarity. In *International Conference on Machine Learning*, pages 11393–11403. PMLR, 2021.

Mengjia Yu and Xiaohui Chen. Finite sample change point inference and identification for high-dimensional mean vectors. *Journal of the Royal Statistical Society: Series B*, 83(2): 247–270, 2021.

Baqun Zhang, Anastasios A Tsiatis, Eric B Laber, and Marie Davidian. Robust estimation of optimal dynamic treatment regimes for sequential treatment decisions. *Biometrika*, 100(3): 681–694, 2013.

Yichi Zhang, Eric B. Laber, Marie Davidian, and Anastasios A. Tsiatis. Estimation of optimal treatment regimes using lists. *Journal of American Statistical Association*, 113(524):1541–1549, 2018. ISSN 0162-1459.

Ying-Qi Zhao, Donglin Zeng, Eric B. Laber, and Michael R. Kosorok. New statistical learning methods for estimating optimal dynamic treatment regimes. *Journal of American Statistical Association*, 110(510):583–598, 2015. ISSN 0162-1459.

Han Zhong, Zhuoran Yang, and Zhaoran Wang Csaba Szepesvári. Optimistic policy optimization is provably efficient in non-stationary MDPs. *arXiv preprint arXiv:2110.08984*, 2021.

Wenzhuo Zhou, Ruoqing Zhu, and Annie Qu. Estimating optimal infinite horizon dynamic treatment regimes via pt-learning. *Journal of the American Statistical Association*, 119(545): 625–638, 2024.

Yunzhe Zhou, Chengchun Shi, Lexin Li, and Qiwei Yao. Testing for the markov property in time series via deep conditional generative learning. *Journal of the Royal Statistical Society Series B: Statistical Methodology*, 85(4):1204–1222, 2023.

Ruoqing Zhu, Ying-Qi Zhao, Guanhua Chen, Shuangge Ma, and Hongyu Zhao. Greedy outcome weighted tree learning of optimal personalized treatment rules. *Biometrics*, 73(2): 391–400, 2017.

This supplement is organized as follows. We begin with a list of commonly used notations in the supplement. We next compare model-free tests against mode-based tests, and discuss some extensions in Section A. In Section B, we present the proofs of our theorems. Finally, in Section C, we detail the simulation setting and present some additional empirical results.

For a J-tuple $\alpha = (\alpha_1, \ldots, \alpha_J)^\top$ of nonnegative integers and a given function h on $\mathcal{S}$, let D^α denote the differential operator:

$$D^\alpha h(s) = \frac{\partial^{\|\alpha\|_1} h(s)}{\partial s_1^{\alpha_1} \cdots \partial s_J^{\alpha_J}}.$$

Here, s_j denotes the jth element of s. For any $p > 0$, let $\lfloor p \rfloor$ denote the largest integer that is smaller than p. The class of p-smooth functions is defined as follows:

$$\Lambda(p, c) = \left\{ h : \sup_{\|\alpha\|_1 \le \lfloor p \rfloor} \sup_{s \in \mathcal{S}} |D^\alpha h(s)| \le c, \sup_{\|\alpha\|_1 = \lfloor p \rfloor} \sup_{\substack{s_1, s_2 \in \mathcal{S} \\ s_1 \neq s_2}} \frac{|D^\alpha h(s_1) - D^\alpha h(s_2)|}{\|s_1 - s_2\|_2^{p - \lfloor p \rfloor}} \le c \right\},$$

for some constant $c > 0$.

A Additional Discussions

A.1 Model-free Tests vs. Model-based Tests

As commented in the main text, we focus on model-free tests in this paper, constructing the test statistic without directly estimating the reward and transition functions. Alternatively, one may study model-based tests [see e.g., Alegre et al., 2021, Wang et al., 2023b], which directly evaluate the stationarity of the MDP model (i.e., reward and transition functions). Both model-based and model-free methods have their own advantages. For example, model-free RL focuses on learning a one-dimensional optimal Q-function, eliminating the need to model a complex transition function that has an output dimension equal to the state's. This is particularly beneficial given the challenges in modeling transition functions, which can be prone to misspecification, as demonstrated in our simulation studies. More specifically, consider the case where the future state follows a conditional Gaussian distribution. Specifying the d-dimensional mean and $d \times d$-dimensional covariance functions of the state-action pair can be quite complex. Conversely, the estimation the Q-function is challenging. A limited number of visits to certain state-action pairs can lead to inaccurate estimations of the Q-function's value across other pairs.

A.2 Extensions to Settings with Varying Termination Times

Our proposed method is readily adaptable to scenarios where subjects have varying termination times. To elaborate, let $T^{(i)}$ represent the termination time for the ith subject, and

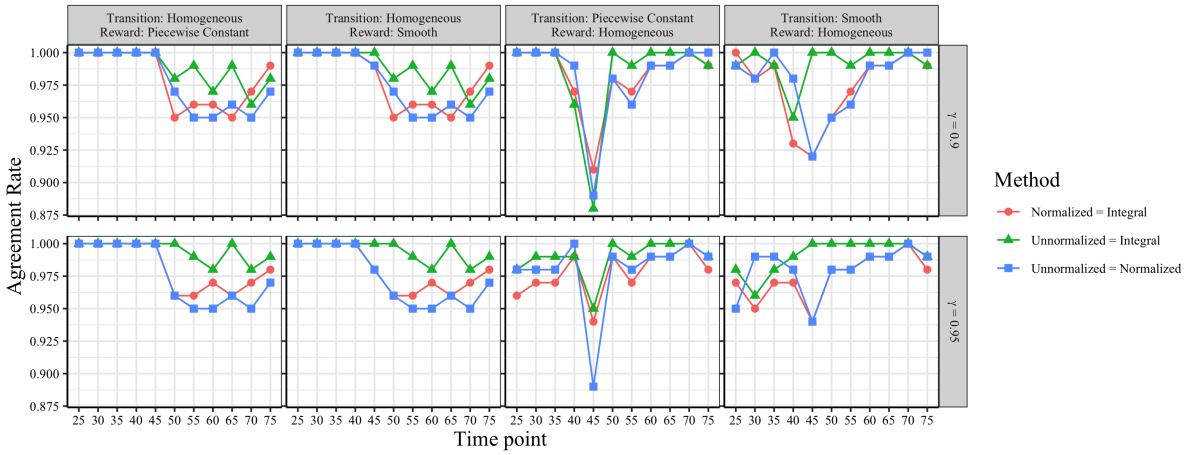

Figure A.1: Agreements rates of the three tests under settings in Section 5.1 with $N = 25$.

$T = \max_i T^{(i)}$ be the maximum of these times. In estimating $\widehat{\beta}_{[T_1,T_2]}$, we can modify the empirical sum operator $\sum_{i=1}^{N}\sum_{t=T_1}^{T_2-1}$ to $\sum_{i:1\le i\le N, T^{(i)}>T_1}\sum_{t=T_1}^{T^{(i)}-1}$. Similarly, for the construction of the ℓ_1-type test, the empirical average operator $1/(N(T-T_0))\sum_{i=1}^{N}\sum_{t=T_0}^{T-1}$ can be substituted with $n^{-1}(T_0)\sum_{i:1\le i\le N, T^{(i)}>T_0}\sum_{t=T_0}^{T^{(i)}-1}$, where $n(T_0)$ denotes the total count of observations in the interval between T_0 and T.

A.3 Inconsistency, Comparison and Aggregation of the Three Tests

For each time point that is a candidate change point, we calculate the percentage of times any of the two tests produce consistent results – both rejecting or both not rejecting the null hypothesis – out of 100 replications and visualize the results in Figure A.1. All three tests agree in most cases. In particular, the unnormalized and ℓ_1-type tests have the highest agreement rates in most scenarios. The normalized test has a relatively lower agreement rates, since it is more likely to reject the null hypothesis compared to the other two.

To address such inconsistency, we outline two approaches below. The first approach chooses one out of the three tests, depending on the application scenarios. In scenarios where our goal lies in identifying meaningful change points in scientific discoveries, the ℓ_1-type or unnormalized maximum-type test is preferable for lower type-I errors (see Remark 6). For instance, in biomedical applications like mobile health, type-I errors are more detrimental than type-II errors. In scenarios where our goal is to train an optimal policy that maximizes the cumulative reward, the normalized test will be preferred. This is because overlooking a potential change point (type-II error) may lead to a sub-optimal policy and can be more critical than incorrectly identifying a non-change point as a change (type-I error), which still uses stationary data, leading to consistent, though inefficient policy learning.

The second approach aggregates results from all three tests to produce a final p-value. This approach leverages the advantages of the three tests and is expected to outperform each of

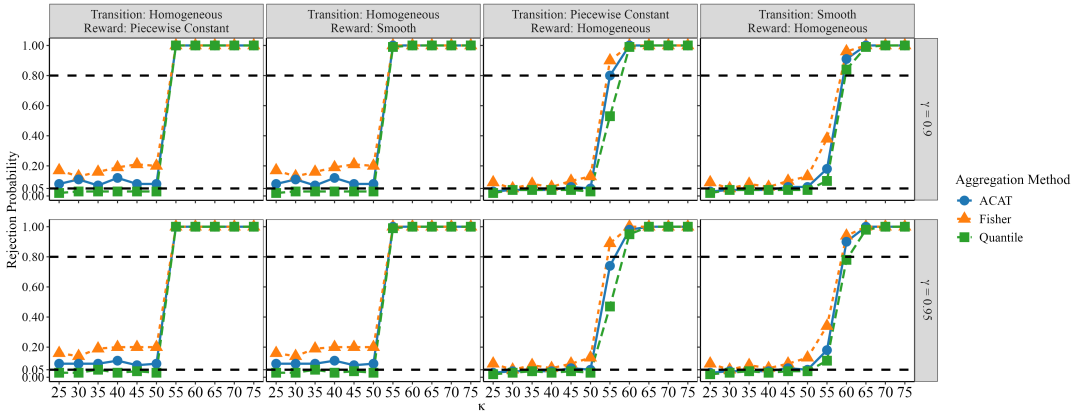

(a) Rejection probabilities under $N = 25$.

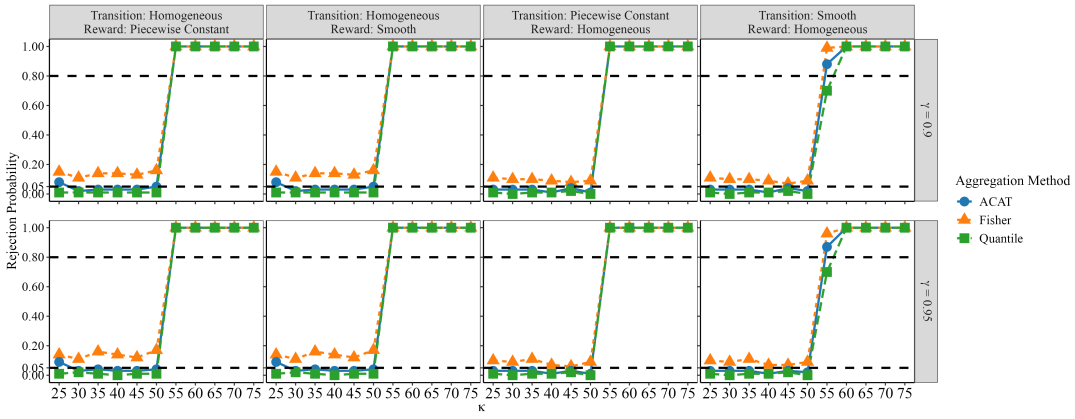

(b) Rejection probabilities under $N = 100$.

Figure A.2: Test results by aggregating p-values from the three tests using Fisher's method, the Cauchy combination method, and quantile-based method (with 0.1 quantile), under simulation settings in Section 5.1 with $N = 25$ and 100. True change point is 50 in all scenarios.

them individually. Various p-value aggregation methods are applicable, including the Fisher's method [Fisher, 1928], the quantile-based method [Meinshausen et al., 2009] and the Cauchy combination method [ACAT; Liu and Xie, 2020]. We implement these three methods under settings in Section 5.1 and report the results in Figure A.2. It can be seen that while the Fisher's method is subject to inflated type-I errors, both the quantile method and ACAT asymptotically control type-I errors and achieve comparable or better power to that of the individual tests in all scenarios. Notably, in the last two settings with nonstationary transition functions, ACAT and the quantile methods are more powerful when the change point is near the endpoint of the interval being tested (i.e., κ is close to 50). These results empirically verify the benefits of combining the three tests.

Finally, as commented in Remark 6 of the main paper, the normalized test statistic requires to compute the estimated variance $\widehat{\sigma}_u^2$, which slightly increases the computational time. Here

we investigate the time required to compute each test statistic in Scenario 4 of the synthetic data simulation, with smooth transition function and homogeneous reward function. Specifically, we focus on the test when $\kappa = 25, 50$, and 75 with sample size $N = 100$. Table A.3 reports the average time used to calculate the three test statistics over 10 replications. The experiments were conducted on Apple M4 Pro chip with 24GB memory. It can be seen that the normalized test is indeed the most computationally expensive among the three tests, even though all three tests are computed very fast.

B Proofs

Throughout the proof, we use c, $\bar{c}$, C, $\bar{C}$ to denote some generic constants whose values are allowed to vary from place to place. Additionally, the discount factor γ is set to a fixed constant that is less than 1. This is to simplify our finite-sample error bounds by omitting some higher-order remainder terms, which are more heavily dependent on $(1-\gamma)^{-1}$. However, for the leading remainder terms, we will explicitly allow them to depend on $(1-\gamma)^{-1}$ to illustrate their dependence with the horizon. Finally, recall that for any two positive sequences $\{a_{N,T}\}_{N,T}, \{b_{N,T}\}_{N,T}$, the notation $a_{N,T} \preceq b_{N,T}$ means that there exists some constant $C > 0$ such that $a_{N,T} \leq C b_{N,T}$ for any N and T.

B.1 Proof of Theorem 2.1

The derivation of SA2 from SA1 is straightforward, given the definition of Q_t^{π}. Similarly, the derivation from SA3 to SA4 is straightforward, as it directly follows from Equation (2.3). Therefore, we aim to show SA3 under SA2 in the rest of the proof.

Without loss of generality, assume $T_0 = 0$. The main idea of our proof lies in the use of policy iteration [Sutton and Barto, 2018] to establish the connection between a (non-optimal) Q-function and its optimal counterpart. We initiate this process with an arbitrarily chosen stationary policy π_1. Subsequently, we define π_2 as the greedy policy with respect to $Q_t^{\pi_1}$, i.e.,

$$\pi_{2,t}(a|s) = \begin{cases} 1, & \text{if } a = \arg\max_{a'} Q_t^{\pi_1}(a', s); \\ 0, & \text{otherwise.} \end{cases}$$

When the argmax is non-unique, we select the smallest maximizer. Under SA2, $Q_t^{\pi_1}$ is stationary, so is π_2. We next repeat this process by defining π_k to the greedy policy with respect

Table A.3: Mean (SD) computation time ($\times 10^{-3}$ seconds) for three test statistics in synthetic data simulation across 10 replicates

κ	Integral	Normalized	Unnormalized
25	35.42 (15.19)	51.7 (5.35)	35.16 (5.11)
50	54.2 (11.21)	68.54 (7.73)	49.46 (6.77)
75	72.17 (10.26)	73.02 (9.43)	52.1 (6.61)

to $Q_t^{\pi_{k-1}}$ for $k = 3, 4, \cdots$. Similarly, we can show that all these policies and Q-functions are stationary. To ease the notation, we remove the subscript t from $\pi_{k,t}$ and $Q_t^{\pi_{k-1}}$. Thus, they are represented as π_k and $Q^{\pi_{k-1}}$, respectively.

According to the policy improvement theorem [see e.g., Sutton and Barto, 2018, Equation 4.8], we obtain $V_t^{\pi_k}(s) \geq V_t^{\pi_{k-1}}(s)$ for any k, t and s. Here, $V_t^{\pi}(\bullet)$ denotes the (state) value function $\mathbb{E}^{\pi}(\sum_{k \geq t} \gamma^{k-t} R_k | S_t = s)$ starting from a given state s at time t. Additionally, the Q-function is connected to the value function through the following equation:

$$Q_t^{\pi}(a, s) = \mathbb{E}[R_t + \gamma V_{t+1}^{\pi}(S_{t+1}) | A_t = a, S_t = s]. \tag{B.1}$$

As such, we obtain that $Q^{\pi_k}(a, s) \geq Q^{\pi_{k-1}}(a, s)$ for any k, a and s. For a given state-action pair, the sequence $\{Q^{\pi_k}(a, s)\}_k$ is monotonically non-decreasing. Since all rewards are uniformly bounded, so are these Q-function. Consequently, Q^{π_k} converges to a bounded function Q^*. The convergence is uniform given that the state-action space is finite.

To complete the proof, we aim to show that $Q^* = Q_t^{opt}$ for any t. According to Theorem 6.2.10 of Puterman [2014], π^{opt} maximizes the value function among all policies, i.e., $V_t^{\pi_{opt}}(s) \geq V_t^{\pi}(s)$ for any t, s and π. This together with (B.1) yields

$$Q^{\pi_k} \leq Q_t^{opt}, \tag{B.2}$$

for any k, t. Additionally, it follows from (B.1) that

$$Q^{\pi_k}(a, s) = \mathbb{E}[R_t + \gamma Q^{\pi_k}(\pi_k(S_{t+1}), S_{t+1}) | A_t = a, S_t = s].$$

Since Q^{π_k} is monotonically non-decreasing, we obtain

$$\begin{aligned} Q^{\pi_k}(a, s) &\geq \mathbb{E}[R_t + \gamma Q^{\pi_{k-1}}(\pi_k(S_{t+1}), S_{t+1}) | A_t = a, S_t = s] \\ &= \mathbb{E}[R_t + \gamma \max_{a'} Q^{\pi_{k-1}}(a', S_{t+1}) | A_t = a, S_t = s]. \end{aligned}$$

This together with the Bellman optimality equation yields,

$$Q^{\pi_k}(a, s) - Q_t^{opt}(a, s) \geq \gamma \mathbb{E}[\max_{a'} Q^{\pi_{k-1}}(a', S_{t+1}) - \max_{a'} Q_{t+1}^{opt}(a', S_{t+1}) | A_t = a, S_t = s].$$

In view of (B.2), we obtain

$$\begin{aligned} |Q^{\pi_k}(a, s) - Q_t^{opt}(a, s)| &\leq \gamma \mathbb{E}[|\max_{a'} Q^{\pi_{k-1}}(a', S_{t+1}) - \max_{a'} Q_{t+1}^{opt}(a', S_{t+1})| | A_t = a, S_t = s] \\ &\leq \gamma \max_{a', s'} |Q^{\pi_{k-1}}(a', s') - Q_{t+1}^{opt}(a', s')|, \end{aligned}$$

and hence

$$\max_{a,s} |Q^{\pi_k}(a, s) - Q_t^{opt}(a, s)| \leq \gamma \max_{a,s} |Q^{\pi_{k-1}}(a, s) - Q_{t+1}^{opt}(a, s)|.$$

Notice that Q^{π_k} converges uniformly to Q^*. By letting $k \to \infty$, we obtain

$$\max_{a,s} |Q^*(a, s) - Q_t^{opt}(a, s)| \leq \gamma \max_{a,s} |Q^*(a, s) - Q_{t+1}^{opt}(a, s)| \leq \gamma^K \max_{a,s} |Q^*(a, s) - Q_{t+K}^{opt}(a, s)|,$$

for any $K > 1$. Under the bounded reward assumption, by letting $K \to \infty$, we obtain $Q^* = Q_t^{opt}$ for any t. This yields SA3. The proof is hence completed.

B.2 Proof of Theorem 4.1

We begin by introducing the following auxiliary lemmas. Specifically, Lemma B.1 lists the properties of B-spline basis function. Lemma B.2 derives the uniform rate of convergence of $\{\widehat{Q}_{[T_1,T_2]}\}_{T_1,T_2}$ and obtain their asymptotic linear representations. It in turn implies the asymptotic normality of these estimated Q-functions. Lemma B.3 provides a uniform upper error bound on $\|\widehat{W}_{[T_1,T_2]} - W_{[T_1,T_2]}\|_2$. Without loss of generality, assume $T_0 = 0$. Their proofs are provided in Sections B.3 and B.4, respectively.

Lemma B.1. *Under the null hypothesis defined in (2.6) that $Q_t^{opt} = Q^{opt}$ for all $t \geq T_0$, there exists some $\beta^* \in \mathbb{R}^L$ such that*

$$\sup_{a,s} |Q^{opt}(a,s) - \phi_L^\top(a,s)\beta^*| = O\Big(\frac{L^{-p/d}}{(1-\gamma)^2}\Big). \tag{B.3}$$

Additionally, we have

$$\max_a \lambda_{\max}\Big[\int_s \phi_L(a,s)\phi^\top(a,s)ds\Big] = O(1), \tag{B.4}$$

$$1 \leq \|\phi_L(a,s)\|_2 \leq \|\phi_L(a,s)\|_1 = \sqrt{L}, \quad \forall a,s, \tag{B.5}$$

and

$$\max_a \sup_{s_1 \neq s_2} \frac{\|\phi_L(a,s_1) - \phi_L(a,s_2)\|_2}{\|s_1 - s_2\|_2} = O(\sqrt{L}). \tag{B.6}$$

Lemma B.2. *Under the null hypothesis, the set of Q-estimators $\{\phi_L^\top(a,s)\widehat{\beta}_{[T_1,T_2]}\}$ are uniformly consistent in ℓ_∞ norm and satisfy the following uniform rate of convergence*

$$\max_{\substack{[T_1,T_2]\subseteq[T_0,T]\\ T_2-T_1>\epsilon T}} \sup_{a,s} |\phi_L^\top(a,s)\widehat{\beta}_{[T_1,T_2]} - Q^{opt}(a,s)| = O\Big(\frac{L^{-p/d}}{(1-\gamma)^2}\Big) + O\Big(\frac{\sqrt{L\log(NT)}}{(1-\gamma)^2\sqrt{\epsilon NT}}\Big), \tag{B.7}$$

with probability at least $1 - O(N^{-1}T^{-1})$. Additionally,

$$\begin{aligned}\phi_L^\top(a,s)\widehat{\beta}_{[T_1,T_2]} - Q^{opt}(a,s) = \frac{\phi_L^\top(a,s)}{N(T_2-T_1)} W_{[T_1,T_2]}^{-1} \sum_{i=1}^{N}\sum_{t=T_1}^{T_2-1} \phi_L(A_{i,t},S_{i,t})\delta_{i,t}^* \\ + O\Big(\frac{L^{-p/d}}{(1-\gamma)^3}\Big) + O\Big(\frac{L^{3/2}\log(NT)}{(1-\gamma)^3\epsilon NT}\Big),\end{aligned} \tag{B.8}$$

where the big-O terms hold uniformly for any pair (T_1,T_2) such that $T_2 - T_1 \geq \epsilon T$ with probability at least $1 - O(N^{-1}T^{-1})$, and we recall that $\delta_{i,t}^*$ denotes the temporal difference error $R_{i,t} + \gamma \max_a Q^{opt}(a, S_{i,t+1}) - Q^{opt}(A_{i,t}, S_{i,t})$.

Lemma B.3. *Under the null hypothesis, there exists some constant $\bar{c} > 0$ such that $\|W_{[T_1,T_2]}^{-1}\|_2 \leq \bar{c}(1-\gamma)^{-1}$ and that $\max_{T_2-T_1\geq\epsilon T} \|\widehat{W}_{[T_1,T_2]} - W_{[T_1,T_2]}\| = O\{(\epsilon NT)^{-1/2}\sqrt{L\log(NT)}\}$ with probability at least $1 - O(N^{-1}T^{-1})$. Here, $\|W_{[T_1,T_2]}^{-1}\|_2$ corresponds to the matrix operator norm of $W_{[T_1,T_2]}^{-1}$.*

B.2.1 Unnormalized Maximum-type Tests

We first provide an outline of the proof. Define TS_∞^* to be a version of TS_∞ with $\widehat{Q}_{[T_1,T_2]}(a,s)$ replaced by the leading terms in the asymptotic expansion (B.8), i.e.,

$$\frac{1}{N(T_2-T_1)}\sum_{i=1}^{N}\sum_{t=T_1}^{T_2-1}\phi_L^\top(a,s)W_{[T_1,T_2]}^{-1}\phi_L(A_{i,t},S_{i,t})\delta_{i,t}^*.$$

It follows from (B.8) that

$$\mathbb{P}\Big(|\text{TS}_\infty-\text{TS}_\infty^*|\le\frac{CL^{-p/d}}{(1-\gamma)^3}+\frac{CL^{3/2}\log(NT)}{(1-\gamma)^3\epsilon NT}\Big)=1-O\Big(\frac{1}{NT}\Big), \tag{B.9}$$

for some constant $C>0$.

The rest of the proof is divided into three steps. In the first step, we establish a uniform upper error bound for $\max_{i,t,T_1,T_2}|\widehat{Q}^b_{[T_1,T_2]}(A_{i,t},S_{i,t})-\widehat{Q}^{b,0}_{[T_1,T_2]}(A_{i,t},S_{i,t})|$, where

$$\widehat{Q}^{b,0}_{[T_1,T_2]}(a,s)=\frac{1}{N(T_2-T_1)}\phi_L^\top(a,s)W_{[T_1,T_2]}^{-1}\sum_{i=1}^{N}\sum_{t=T_1}^{T_2-1}\phi_L(A_{i,t},S_{i,t})\delta_{i,t}^*e_{i,t},\quad\forall T_1,T_2,$$

a version of $\widehat{Q}^b_{[T_1,T_2]}(a,s)$ with $\widehat{W}^{-1}_{[T_1,T_2]}$ and $\delta_{i,t}(\widehat{\beta}_{[T_1,T_2]})$ replaced by their oracle values. This in turn leads to the following bound for the difference between TS_∞^b and $\text{TS}_\infty^{b,*}$,

$$\mathbb{P}\Big(|\text{TS}_\infty^b-\text{TS}_\infty^{b,*}|\le\frac{CL^{3/2}\log(NT)}{(1-\gamma)^3\epsilon NT}+\frac{CL^{-p/d}\sqrt{\log(NT)}}{(1-\gamma)^3\sqrt{\epsilon NT}}\Big)=1-O\Big(\frac{1}{NT}\Big), \tag{B.10}$$

for some constant $C>0$, where

$$\text{TS}_\infty^{b,*}=\max_{\epsilon T<u<(1-\epsilon)T}\max_{a,s}\sqrt{\frac{u(T-u)}{T^2}}|\widehat{Q}^{b,0}_{[0,u]}(a,s)-\widehat{Q}^{b,0}_{[u,T]}(a,s)|.$$

Notice that in the test statistic, the maximum is taken over all state-action pairs. Recall that the state space is $[0,1]^d$. In the second step, we discretize the state space by considering an ε-net of $[0,1]^d$ – denoted by $\mathcal{S}_\varepsilon$ – with $\varepsilon=\sqrt{d}/(NT)^4$ so that for any $s\in[0,1]^d$, there exists some s' in the ε-net such that $\|s-s'\|_2\le\varepsilon$. Let TS_∞^{**} and $\text{TS}_\infty^{b,**}$ be versions of TS_∞^* and $\text{TS}_\infty^{b,*}$ where the maximum is taken over the ε-net. The focus of this step is to upper bound $|\text{TS}_\infty^*-\text{TS}_\infty^{**}|$ and $|\text{TS}_\infty^{b,*}-\text{TS}_\infty^{b,**}|$. Due to the choice of ε, these bounds are minimal. Together with (B.9) and (B.10), we can show that

$$\begin{aligned}
&\mathbb{P}\Big(|\text{TS}_\infty-\text{TS}_\infty^{**}|\le\frac{cL^{-p/d}}{(1-\gamma)^3}+\frac{cL^{3/2}\log(NT)}{(1-\gamma)^3\epsilon NT}\Big)=1-O\Big(\frac{1}{NT}\Big),\\
&\mathbb{P}\Big(|\text{TS}_\infty^b-\text{TS}_\infty^{b,**}|\le\frac{cL^{-p/d}}{(1-\gamma)^3}+\frac{cL^{3/2}\log(NT)}{(1-\gamma)^3\epsilon NT}\Big)=1-O\Big(\frac{1}{NT}\Big).
\end{aligned} \tag{B.11}$$

In the last step, we aim to show the proposed test controls the type-I error. A key step in our proof is to bound the Kolmogorov distance between TS_∞^{**} and $\text{TS}_\infty^{b,**}$, which together with (B.11) yields the validity of the proposed test. Notice that TS_∞^{**} can be viewed as the maximum of a set of mean zero random vectors

$$\Big\{Z_{u,a,s,j} \triangleq (-1)^j \tau_u \phi_L^\top(a,s)\Big[\frac{W_{[0,u]}^{-1}}{Nu}\sum_{i=1}^{N}\sum_{t=0}^{u-1}\phi_L(A_{i,t},S_{i,t})\delta_{i,t}^* - \frac{W_{[u,T]}^{-1}}{N(T-u)} \times \sum_{i=1}^{N}\sum_{t=u}^{T-1}\phi_L(A_{i,t},S_{i,t})\delta_{i,t}^*\Big] : j\in\{0,1\}, \epsilon T < u < (1-\epsilon)T, a\in\mathcal{A}, s\in\mathcal{S}_\varepsilon\Big\}, \tag{B.12}$$

Similarly, $\text{TS}_\infty^{b,*}$ can be represented as a function of the bootstrapped samples

$$\Big\{Z_{u,a,s,j}^b \triangleq (-1)^j \tau_u \Big[\frac{W_{[0,u]}^{-1}}{Nu}\sum_{i=1}^{N}\sum_{t=0}^{u-1}\phi_L(A_{i,t},S_{i,t})\delta_{i,t}^* e_{i,t} - \frac{W_{[u,T]}^{-1}}{N(T-u)}\sum_{i=1}^{N}\sum_{t=u}^{T-1}\phi_L(A_{i,t},S_{i,t}) \times\delta_{i,t}^* e_{i,t}\Big] : j\in\{0,1\}, \epsilon T < u < (1-\epsilon)T, a\in\mathcal{A}, s\in\mathcal{S}_\varepsilon\Big\}. \tag{B.13}$$

When T and L are fixed, the classical continuous mapping theorem can be applied to establish the weak convergence results. However, in our setting, L needs to diverge with the number of observations to alleviate the model misspecification error. We also allow T to approach infinity. Hence, classical weak convergence results cannot be applied. Toward that end, we establish a nonasymptotic error bound for the Kolmogorov distance as a function of N, T and L, and show that this bound decays to zero under the given conditions. The proof is based on the high-dimensional martingale central limit theorem (CLT) developed by Belloni and Oliveira [2018]; see also the high-dimensional CLT by Chernozhukov et al. [2014].

We next detail the proof for each step.

Step 1. By definition, $\widehat{Q}_{[T_1,T_2]}^{b,0}(a,s) - \widehat{Q}_{[T_1,T_2]}^{b}(a,s)$ is equal to the sum of

$$\frac{1}{N(T_2-T_1)}\phi_L^\top(a,s)(\widehat{W}_{[T_1,T_2]}^{-1} - W_{[T_1,T_2]}^{-1})\sum_{i=1}^{N}\sum_{t=T_1}^{T_2-1}\phi_L(A_{i,t},S_{i,t})\delta_{i,t}(\widehat{\beta}_{[T_1,T_2]})e_{i,t} \tag{B.14}$$

and

$$\frac{1}{N(T_2-T_1)}\phi_L^\top(a,s)W_{[T_1,T_2]}^{-1}\sum_{i=1}^{N}\sum_{t=T_1}^{T_2-1}\phi_L(A_{i,t},S_{i,t})(\delta_{i,t}(\widehat{\beta}_{[T_1,T_2]}) - \delta_{i,t}^*)e_{i,t}. \tag{B.15}$$

Consider the first term. In Lemma B.3, we establish a uniform upper error bound for $\|\widehat{W}_{[T_1,T_2]} - W_{[T_1,T_2]}\|_2$ and show that $(1-\gamma)\|W_{[T_1,T_2]}^{-1}\|_2$ is upper bounded by some constant. Using similar arguments in Part 3 of the proof of Lemma 3 in Shi et al. [2022], we can show that $\|\widehat{W}_{[T_1,T_2]}^{-1} - W_{[T_1,T_2]}^{-1}\|_2$ is of the same order of magnitude to $(1-\gamma)^{-2}\|\widehat{W}_{[T_1,T_2]} - W_{[T_1,T_2]}\|_2$. The boundedness of rewards (implied by A2) implies that the Q-function is bounded by $O((1-\gamma)^{-1})$.

This together with Lemma B.2 implies the estimated Q-function is bounded by $O((1-\gamma)^{-1})$ as well, and so is $\delta_{i',t'}(\widehat{\beta}_{[T_1,T_2]})$. By (B.4), the conditional variance of (B.14) given the data is upper bounded by

$$\frac{CL^2\log(NT)}{\epsilon^2N^2T^2(1-\gamma)^6}\lambda_{\max}\left\{\frac{1}{N(T_2-T_1)}\sum_{i=1}^{N}\sum_{t=T_1}^{T_2-1}\phi_L(A_{i,t},S_{i,t})\phi_L^\top(A_{i,t},S_{i,t})\right\}.$$

Similar to Lemma B.3, we can show that the maximum eigenvalue of the matrix inside the curly brackets converges to $\lambda_{\max}\{(T_2-T_1)^{-1}\sum_{t=T_1}^{T_2-1}\mathbb{E}\phi_L(A_t,S_t)\phi_L^\top(A_t,S_t)\}$, which is bounded by some finite constant according to (B.4) and the boundedness of the transition function p_ts in Condition A4(iii). Hence, the conditional variance of (B.14) given the data is of the order $O(L^2\epsilon^{-2}N^{-2}T^{-2}(1-\gamma)^{-6}\log(NT))$, with probability at least $1-O(N^{-1}T^{-1})$.

Notice that the probability of a standard normal random variable exceeding z is bounded by $\exp(-z^2/2)$ for any $z>1$; see e.g., the inequality for the Gaussian Mill's ratio [Birnbaum, 1942]. Since (B.14) is a mean-zero Gaussian random variable given the data, it is of the order

$$O\Big(\frac{L\log(NT)}{(1-\gamma)^3\epsilon NT}\Big),$$

with probability at least $1-O\{(NT)^{-C}\}$ for any sufficiently large constant $C>0$. This together with Bonferroni's inequality yields the desired uniform upper error bound for the first term.

As for the second term, notice that according to the finite-sample error bound established in Lemma B.2, the difference $\delta_{i,t}(\widehat{\beta}_{[T_1,T_2]})-\delta_{i,t}^*$ decays to zero at a rate of

$$O\Big(\frac{L^{-p/d}}{(1-\gamma)^2}\Big)+O\Big(\frac{\sqrt{L\log(NT)}}{(1-\gamma)^2\sqrt{\epsilon NT}}\Big),$$

uniformly in i,t,T_1,T_2, with probability at least $1-O(N^{-1}T^{-1})$. Based on this result and Condition A5(ii), we can similarly derive the upper error bound for the second term. This completes the proof of this step.

Step 2. Recall that $\mathcal{S}_\varepsilon$ is an ε-net of $\mathcal{S}=[0,1]^d$ such that for any $s\in[0,1]^d$, there exists some $s'\in\mathcal{S}_\varepsilon$ that satisfies $\|s-s'\|_2\le\varepsilon=\sqrt{d}/(NT)^4$. It follows from Lemma 2.2 of Mendelson et al. [2008] that there exist some $\mathcal{S}_\varepsilon^0$ that is an ε-net of the ball $\{s:\|s\|_2\le\sqrt{d}\}$ with number of elements upper bounded by $5^d(NT)^{4d}$. For any $s^0=(s_1,\cdots,s_d)^\top\in\mathcal{S}_\varepsilon^0$, consider its restriction to $\mathcal{S}$, denoted by $s'=(\max(\min(s_1,1),0),\cdots,\max(\min(s_d,1),0))^\top$. It is immediate to see that for any $s\in\mathcal{S}$, $\|s^0-s\|_2\le\|s'-s\|_2$. Let $\mathcal{S}_\varepsilon$ denote the set of these restricted vectors, i.e., $\{s':s^0\in\mathcal{S}_\varepsilon^0\}$. It follows that $\mathcal{S}_\varepsilon$ corresponds to an ε-net of $\mathcal{S}$ as well. Using similar arguments to Step 1 of the proof, we can show that

$$\max_{(T_1,T_2):T_2-T_1\ge\epsilon T}\Big\|\frac{W_{[T_1,T_2]}^{-1}}{N(T_2-T_1)}\sum_{i=1}^{N}\sum_{t=T_1}^{T_2-1}\phi_L(A_{i,t},S_{i,t})\delta_{i,t}^*\Big\|_2\preceq\frac{\sqrt{L}}{(1-\gamma)^2},$$

Combining this together with (B.5) yields that $|Z_{u,a,s,j} - Z_{u,a,s',j}| = O((1-\gamma)^{-2}L\|s-s'\|_2)$ where the big-O term is uniform in u, a, s, s', j and $Z_{u,a,s,j}$ is defined in (B.12). Consequently, for any $s \in \mathcal{S}$, there exists some $s' \in \mathcal{S}_\varepsilon$ such that $|Z_{u,a,s,j} - Z_{u,a,s',j}|$ is upper bounded by

$$O\Big(\frac{L}{(1-\gamma)^2(NT)^4}\Big). \tag{B.16}$$

This allows us to upper bound $|\mathrm{TS}_\infty^* - \mathrm{TS}_\infty^{**}|$ by (B.16) as well.

Using similar arguments, we can show that $|\mathrm{TS}_\infty^{b,*} - \mathrm{TS}_\infty^{b,**}|$ is of the order (B.16) as well, with probability at least $1 - O(N^{-1}T^{-1})$. This completes the proof of this step.

Step 3. As we have commented in the outline, the proof is based on the high-dimensional martingale central limit theorem developed by Belloni and Oliveira [2018]. Let Z and Z^b denote the high-dimensional random vectors formed by stacking the random vectors in the set (B.12) and (B.13), respectively. Notice that Z can be represented as $\sum_{i,t} Z_{i,t}$ where each $Z_{i,t}$ depends on the data tuple $(S_{i,t}, A_{i,t}, R_{i,t}, S_{i,t+1})$. We first observe that it corresponds to a sum of high-dimensional martingale difference. Specifically, for any integer $1 \le g \le NT$, let $i(g)$ and $t(g)$ be the quotient and the remainder of $g + T - 1$ divided by T that satisfy

$$g = \{i(g) - 1\}T + t(g) + 1 \quad \text{and} \quad 0 \le t(g) < T.$$

Let $\mathcal{F}^{(0)} = \{S_{1,0}, A_{1,0}\}$. Then we recursively define $\{\mathcal{F}^{(g)}\}_{1\le g\le NT}$ as follows:

$$\mathcal{F}^{(g)} = \begin{cases} \mathcal{F}^{(g-1)} \cup \{R_{i(g),t(g)}, S_{i(g),t(g)+1}, A_{i(g),t(g)+1}\}, & \text{if } t(g) < T-1; \\ \mathcal{F}^{(g-1)} \cup \{R_{i(g),T-1}, S_{i(g),T}, S_{i(g)+1,0}, A_{i(g)+1,0}\}, & \text{otherwise.} \end{cases}$$

This allows us to rewrite Z as $\sum_{g=1}^{NT} Z^{(g)} = \sum_{g=1}^{NT} Z_{i(g),t(g)}$. Similarly, we can rewrite Z^b as $\sum_{g=1}^{NT} Z^{b,(g)}$. Under the Markov assumption and the conditional (mean) independence assumptions in (2.1) and (2.2) (e.g., the future state and the conditional mean of the immediate reward are independent of the history given the current state-action pair), Z corresponds to a sum of martingale difference sequence with respect to the filtration $\{\sigma(\mathcal{F}^{(g)})\}_{g\ge 0}$ where $\sigma(\mathcal{F})$ denotes the σ-algebra generated by $\mathcal{F}$.

Due to the existence of the max operator, TS_1^{**} is a non-smooth function of Z. We next approximate the maximum using a smooth surrogate. Let θ be a sufficiently large real number. Consider the following smooth approximation of the maximum function,

$$F_\theta(\{Z_{u,a,s,j}\}_{u,a,s,j}) = \frac{1}{\theta}\log\Big(\sum_{u,a,s,j} \exp(\theta Z_{u,a,s,j})\Big).$$

As we have restricted the state space to $\mathcal{S}_\varepsilon$, the number of cardinality of the quadruples (u, a, s, j) can be upper bounded by $O(N^cT^c)$ for some constant $c > 0$. It can be shown that

$$\max_{u,a,s,j} Z_{u,a,s,j} \le F_\theta(\{Z_{u,a,s,j}\}_{u,a,s,j}) \le \max_{u,a,s,j} Z_{u,a,s,j} + \frac{C\log(NT)}{\theta}, \tag{B.17}$$

for some constant $C > 0$. See e.g., Equation (37) of Chernozhukov et al. [2014].

For a given z, consider the probability $\mathbb{P}(\text{TS}_\infty^{**} \leq z)$. According to Section B.1 of Belloni and Oliveira [2018], for any $\delta > 0$, there exists a thrice differentiable function h that satisfies $|h'| \leq \delta^{-1}$, $|h''| \leq \delta^{-2}K$ and $|h'''| \leq \delta^{-3}K$ for some universal constant $K > 0$ such that

$$\mathbb{I}(x \leq z + \delta) \leq h(x) \leq \mathbb{I}(x \leq z + 4\delta). \tag{B.18}$$

Define a composite function $m(\{Z_{u,a,s,j}\}_{u,a,s,j}) = h \circ F_\theta(\{Z_{u,a,s,j}\}_{u,a,s,j})$. By setting δ to $C\log(NT)/\theta$, it follows from (B.17) and (B.18) that

$$\mathbb{P}(\text{TS}_\infty^{**} \leq z) \leq \mathbb{E}m(\{Z_{u,a,s,j}\}_{u,a,s,j}) \leq \mathbb{P}(\text{TS}_\infty^{**} \leq z + 4\delta). \tag{B.19}$$

Similarly, we have

$$\mathbb{P}(\text{TS}_\infty^{b,**} \leq z|\text{Data}) \leq \mathbb{E}[m(\{Z^b_{u,a,s,j}\}_{u,a,s,j})|\text{Data}] \leq \mathbb{P}(\text{TS}_\infty^{b,**} \leq z + 4\delta|\text{Data}),$$

where Z_u^b is defined in (B.13). This together with (B.19) yields that

$$\begin{aligned} &\max\{\max_z |\mathbb{P}(\text{TS}_\infty^{b,**} \leq z|\text{Data}) - \mathbb{P}(\text{TS}_\infty^{**} \leq z - 4\delta)|, \\ &\qquad \max_z |\mathbb{P}(\text{TS}_\infty^{b,**} \leq z|\text{Data}) - \mathbb{P}(\text{TS}_\infty^{**} \leq z + 4\delta)|\} \\ &\leq |\mathbb{E}m(\{Z_{u,a,s,j}\}_{u,a,s,j}) - \mathbb{E}[m(\{Z^b_{u,a,s,j}\}_{u,a,s,j})|\text{Data}]|. \end{aligned} \tag{B.20}$$

We next apply Corollary 2.1 of Belloni and Oliveira [2018] to establish an upper bound for the last line of (B.20). Similar to Lemma 4.3 of Chernozhukov et al. [2014], we can show that $c_0 \equiv \sup_{z,z'} |m(z) - m(z')| \leq 1$,

$$\begin{aligned} c_2 &\equiv \sup_z \sum_{j_1,j_2} \left| \frac{\partial^2 m(z)}{\partial z_{j_1} \partial z_{j_2}} \right| \preceq \delta^{-2} + \delta^{-1}\theta, \\ c_3 &\equiv \sup_z \sum_{j_1,j_2,j_3} \left| \frac{\partial^3 m(z)}{\partial z_{j_1} \partial z_{j_2} \partial z_{j_3}} \right| \preceq \delta^{-3} + \delta^{-2}\theta + \delta^{-1}\theta^2. \end{aligned}$$

In addition, similar to Lemma B.3, we can show that the quadratic variation process $\sum_g \mathbb{E}\{Z^{(g)}(Z^{(g)})^\top | \mathcal{F}^{(g-1)}\}$ will converge to some deterministic matrix with elementwise approximation error upper bounded by $O((1-\gamma)^{-4}L^{3/2}\sqrt{\log(NT)}/(NT)^{3/2})$, with probability at least $1 - O(N^{-1}T^{-1})$. So is the conditional covariance matrix of Z^b given the data, e.g.,

$$\sum_g \mathbb{E}[Z^{b,(g)}(Z^{b,(g)})^\top | \{S_{i,t}, A_{i,t}, R_{i,t}\}_{1 \leq i \leq N, 0 \leq t \leq T}].$$

Moreover, by (B.4), the sum of third absolute moments of each element in $Z^{(g)}$ is upper bounded by $O((1-\gamma)^{-6}\epsilon^{-1/2}(NT)^{-2}L^2)$. It follows from Corollary 2.1 of Belloni and Oliveira [2018] that the last line of (B.20) is upper bounded by

$$\frac{\theta^2 L^{3/2}\sqrt{\log(NT)}\log^2(NT)}{(1-\gamma)^4(NT)^{3/2}} + \frac{\theta^3 L^2 \log^3(NT)}{(1-\gamma)^6\sqrt{\epsilon}(NT)^2}$$

with probability at least $1 - O(N^{-1}T^{-1})$.

Meanwhile, under Assumption A4(iv) that the conditional variance of temporal difference error $\delta^*_{i,t}$ is lower bounded by $c(1-\gamma)^{-2}$ for some constant $c > 0$. Additionally, by setting γ' in A5(ii) to 0, we obtain that the minimum eigenvalue of $\mathbb{E}[\phi_L(A_t, S_t)\phi_L^\top(A_t, S_t)]$ is bounded away from zero. Using similar arguments to Step 1 of the proof, we can show that the conditional variance of each $Z^b_{u,a,s,j}$ given the data is lower bounded by $C(1-\gamma)^{-2}\|\phi_L(a,s)\|_2^2/(NT)$. By (B.5), it can be uniformly lower bounded by $C(1-\gamma)^{-2}/(NT)$ for some constant $C > 0$. As such, it follows from the anti-concentration inequality for the maximum of Gaussian random vector [Chernozhukov et al., 2017, Theorem 1] that

$$\sup_z |\mathbb{P}(\mathrm{TS}^{b,**}_\infty \le z - 4\delta|\mathrm{Data}) - \mathbb{P}(\mathrm{TS}^{b,**}_\infty \le z + 4\delta|\mathrm{Data})| \preceq \frac{\sqrt{NT}\log^{3/2}(NT)}{(1-\gamma)^{-1}\theta},$$

with probability at least $1 - O(N^{-1}T^{-1})$.

In view of (B.20), by setting $\theta = (1-\gamma)^{7/4}L^{-1/2}\epsilon^{1/8}(NT)^{3/8}\log^{-3/8}(NT)$, we have

$$\sup_z |\mathbb{P}(\mathrm{TS}^{b,**}_\infty \le z|\mathrm{Data}) - \mathbb{P}(\mathrm{TS}^{**}_\infty \le z)| \preceq \frac{\sqrt{L}\log^{15/8}(NT)}{(1-\gamma)^{3/4}(\epsilon NT)^{1/8}},$$

with probability at least $1 - O(N^{-1}T^{-1})$. Similarly, based on (B.11), we can show that

$$\sup_z |\mathbb{P}(\mathrm{TS}^b_1 \le z|\mathrm{Data}) - \mathbb{P}(\mathrm{TS}_1 \le z)| \preceq \frac{\sqrt{L}\log^{15/8}(NT)}{(1-\gamma)^{3/4}(\epsilon NT)^{1/8}} + \frac{L^{-p/d}\sqrt{NT\log(NT)}}{(1-\gamma)^2}.$$

The proof is hence completed.

B.2.2 Normalized Maximum-Type Tests

For any u, a and s, define the variance estimator $\widehat{\sigma}^2_u(a,s)$ by

$$\frac{\phi_L^\top(a,s)\widehat{W}^{-1}_{[T-\kappa,T-u]}}{N^2(\kappa-u)^2}\left[\sum_{i=1}^N\sum_{t=T-\kappa}^{T-u-1}\phi_L(A_{i,t},S_{i,t})\phi_L^\top(A_{i,t},S_{i,t})\delta^2_{i,t}(\widehat{\beta}_{[T-\kappa,T-u]})\right]\{\widehat{W}^{-1}_{[T-\kappa,T-u]}\}^\top\phi_L^\top(a,s)$$
$$+\frac{1}{N^2u^2}\phi_L^\top(a,s)\widehat{W}^{-1}_{[T-u,T]}\left[\sum_{i=1}^N\sum_{t=T-u}^{T-1}\phi_L(A_{i,t},S_{i,t})\phi_L^\top(A_{i,t},S_{i,t})\delta^2_{i,t}(\widehat{\beta}_{[T-u,T]})\right]\{\widehat{W}^{-1}_{[T-u,T]}\}^\top\phi_L^\top(a,s).$$

We next show that the normalized maximum-type test has good size property. The proof is very similar to that in Section B.2.1. We provide a sketch of the proof and outline a key step only. Define TS^*_n and $\mathrm{TS}^{b,*}_n$ to be versions of TS_n and TS^b_n, respectively, where the variance estimator $\widehat{\sigma}^2_u(a,s)$ is replaced with its oracle value $\sigma^2_u(a,s)$. The key step here is to upper bound the differences $|\mathrm{TS}^*_n - \mathrm{TS}_n|$ and $|\mathrm{TS}^{b,*}_n - \mathrm{TS}^b_n|$.

Toward that end, we first upper bound the difference between $\widehat{\sigma}^2_u(a,s)$ and $\sigma^2_u(a,s)$. Using similar arguments to Step 1 of the proof in Section B.2.1, we can show that with probability at least $1-O(N^{-1}T^{-1})$, (i)$\max_{T_2-T_1\ge\epsilon T}\|\widehat{W}^{-1}_{[T_1,T_2]} - W^{-1}_{[T_1,T_2]}\|_2 = O((1-\gamma)^{-2}\sqrt{L(\epsilon NT)^{-1}\log(NT)})$;

(ii) $|\delta_{i,t}^2(\widehat{\beta}_{[T_1,T_2]}) - (\delta_{i,t}^*)^2| = O((1-\gamma)^{-3}L^{-p/d}) + O((1-\gamma)^{-3}\sqrt{L(\epsilon NT)^{-1}\log(NT)})$ where the bound is uniform in i, t, T_1, T_2;

$$\text{(iii)} \max_{T_2-T_1\geq\epsilon T} \lambda_{\max}\left\{\frac{1}{N(T_2-T_2)}\sum_{i=1}^{N}\sum_{t=T_1}^{T_2-1}\phi_L(A_{i,t},S_{i,t})\phi_L^\top(A_{i,t},S_{i,t})\right\} = O(1),$$

(iv) the matrix $N^{-1}(T_2-T_2)^{-1}\sum_{i=1}^{N}\sum_{t=T_1}^{T_2-1}\phi_L(A_{i,t},S_{i,t})\phi_L^\top(A_{i,t},S_{i,t})(\delta_{i,t}^*)^2$ converges uniformly to its expectation across all pairs (T_1,T_2) such that $T_2-T_1\geq\epsilon T$, with the uniform approximation error given by $O((1-\gamma)^{-2}\sqrt{L(\epsilon NT)^{-1}\log(NT)})$. These allow us to establish the following error bound

$$|\widehat{\sigma}_u^2(a,s)-\sigma_u^2(a,s)| \leq \frac{\|\phi_L(a,s)\|_2^2}{NT\tau_u^2}\Big[O\Big(\frac{L^{-p/d}}{(1-\gamma)^5}\Big)+O\Big(\frac{\sqrt{L(\epsilon NT)^{-1}\log(NT)}}{(1-\gamma)^5}\Big)\Big], \quad \text{(B.21)}$$

with probability at least $1-O(N^{-1}T^{-1})$, where the big-O terms on the RHS are uniform in a, s, u.

Similar to Step 3 of the proof for the unnormalized test in Section B.2.1, we can show that $\sigma_u^2(a,s)\geq c(1-\gamma)^{-2}\|\phi_L(a,s)\|_2^2/(NT\tau_u^2)$ for some constant $c>0$ and hence

$$\sup_{a,s,u}\frac{|\widehat{\sigma}_u^2(a,s)-\sigma_u^2(a,s)|}{\sigma_u^2(a,s)} = O\Big(\frac{L^{-p/d}}{(1-\gamma)^3}\Big)+O\Big(\frac{\sqrt{L(\epsilon NT)^{-1}\log(NT)}}{(1-\gamma)^3}\Big),$$

with probability at least $1-O(N^{-1}T^{-1})$, and hence,

$$\sup_{a,s,u}\frac{|\widehat{\sigma}_u(a,s)-\sigma_u(a,s)|}{\sigma_u(a,s)} = O\Big(\frac{L^{-p/d}}{(1-\gamma)^3}\Big)+O\Big(\frac{\sqrt{L(\epsilon NT)^{-1}\log(NT)}}{(1-\gamma)^3}\Big). \quad \text{(B.22)}$$

Meanwhile, it follows from (B.21) that there exists some constant $C>0$ such that $\widehat{\sigma}_u^2(a,s)\geq C(1-\gamma)^{-2}\|\phi_L(a,s)\|_2^2/(NT\tau_u^2)$ for any u,a,s, with probability at least $1-O(N^{-1}T^{-1})$.

In view of these, using similar arguments to Steps 1 and 2 of the proof for the unnormalized test, we can show that the bootstrapped normalized test statistics can be upper bounded by

$$O(\sqrt{\log(NT)}), \quad \text{(B.23)}$$

with probability at least $1-O(N^{-1}T^{-1})$. Additionally, as discussed in Step 3 of the proof for the unnormalized test, each $Z_{u,a,s,j}/\sigma_u(a,s)$ can be represented as a sum of high-dimensional martingale difference sequence. We can first discretize the state space in a manner similar to Step 2 of the proof, and then apply the martingale concentration inequality [see e.g., Tropp, 2011, Theorem 1.1] and the Bonferroni's inequality to obtain a uniform upper error bound for $\{Z_{u,a,s,j}/\sigma_u(a,s)\}_{u,a,s,j}$. This implies that the normalized test statistics is of the order of magnitude (B.23) as well, with probability at least $1-O(N^{-1}T^{-1})$.

To the contrary, the scaled unnormalized test $(1-\gamma)^2\sqrt{NT}\text{TS}_\infty$ and its bootstrap version $(1-\gamma)^2\sqrt{NT}\text{TS}_\infty^b$ are of the order of magnitude $O(\sqrt{L\log(NT)})$. When compared to the

error bound in (B.23), it can be seen that the normalized test achieves a smaller order of magnitude by a factor of $L^{-1/2}$. This reduction results from the normalization, which makes the order of each $Z_{u,a,s,j}$ independent of $\phi_L(a,s)$, thus avoiding multiplying with an additional supremum term $\sup_{a,s}\|\phi_L(a,s)\|_2$ (which is of the order $O(\sqrt{L})$ according to (B.4)) when taking the maximum over $Z_{u,a,s,j}$.

Combining (B.23) together with (B.22), we obtain that

$$|\mathrm{TS}_n - \mathrm{TS}_n^*| = O\Big(\frac{L^{-p/d}\sqrt{\log(NT)}}{(1-\gamma)^3}\Big) + O\Big(\frac{\sqrt{L(\epsilon NT)^{-1}}\log(NT)}{(1-\gamma)^3}\Big).$$

With this upper bound, the rest of the proof can be established in a similar manner to the proof for the unnormalized test. We omit the details to save space.

B.2.3 ℓ_1-type Test

The proof for the ℓ_1-type test is more involved. It is divided into three steps.

In Step 1, we show there exists some constant $C > 0$ such that

$$\mathbb{P}(|\mathrm{TS}_1 - \mathrm{TS}_1^*| \le C\kappa\sqrt{LN^{-1}T^{-1}\log(NT)}) = 1 - O\Big(\frac{1}{NT}\Big). \tag{B.24}$$

where

$$\mathrm{TS}_1^* = \max_{\epsilon T<u<(1-\epsilon)T} \sqrt{\frac{u(T-u)}{T^2}} \left\{ \frac{1}{T}\sum_{t=0}^{T-1}\sum_a \int_s |\widehat{Q}_{[0,u]}(a,s) - \widehat{Q}_{[u,T]}(a,s)|\pi_t^b(a|s)p_t^b(s)ds \right\},$$

where π_t^b denotes the behavior policy at time t, p_t^b denotes the marginal distribution of S_t under the behavior policy, and κ is a shorthand for $(1-\gamma)^{-2}L^{-p/d} + (1-\gamma)^{-2}\sqrt{L\log(NT)/(\epsilon NT)}$. By definition, TS_1^* corresponds to a version of TS_1 assuming the marginal distribution of the observed state-action pairs is known to us.

In the second step, we notice that we have established a uniform upper error bound for $\max_{i,t,T_1,T_2}|\widehat{Q}^b_{[T_1,T_2]}(A_{i,t},S_{i,t}) - \widehat{Q}^{b,0}_{[T_1,T_2]}(A_{i,t},S_{i,t})|$ in Step 2 of the proof for the unnormalized test. This error bound in turn leads to the following bound for the difference between TS_1^b and $\mathrm{TS}_1^{b,0}$,

$$\mathbb{P}\Big(|\mathrm{TS}_1^b - \mathrm{TS}_1^{b,0}| \le \frac{CL^{3/2}\log(NT)}{(1-\gamma)^3\epsilon NT} + \frac{CL^{-p/d}\sqrt{\log(NT)}}{(1-\gamma)^3\sqrt{\epsilon NT}}\Big) = 1 - O\Big(\frac{1}{NT}\Big), \tag{B.25}$$

for some constant $C > 0$, where

$$\mathrm{TS}_1^{b,0} = \max_{\epsilon T<u<(1-\epsilon)T} \sqrt{\frac{u(T-u)}{T^2}} \left\{ \frac{1}{NT}\sum_{i=1}^{N}\sum_{t=0}^{T-1} |\widehat{Q}^{b,0}_{[0,u]}(A_{i,t},S_{i,t}) - \widehat{Q}^{b,0}_{[u,T]}(A_{i,t},S_{i,t})| \right\}.$$

Using similar arguments to the proof of (B.24) in Step 1, we can show that $|\mathrm{TS}_1^b - \mathrm{TS}_1^{b,0}|$ is of the order $O(\kappa\sqrt{LN^{-1}T^{-1}\log(NT)})$ as well, with probability at least $1 - O(N^{-1}T^{-1})$, where

$$\mathrm{TS}_1^{b,*} = \max_{\epsilon T<u<(1-\epsilon)T} \sqrt{\frac{u(T-u)}{T^2}} \left\{ \frac{1}{T} \sum_{t=0}^{T-1} \sum_a \int_s |\widehat{Q}^{b,0}_{[0,u]}(a,s) - \widehat{Q}^{b,0}_{[u,T]}(a,s)| \pi_t^b(a|s) p_t^b(s) ds \right\}.$$

This together with (B.25) yields that

$$\mathbb{P}\Big(|\mathrm{TS}_1^b - \mathrm{TS}_1^{b,*}| \le \frac{cL^{3/2}\log(NT)}{(1-\gamma)^3\epsilon NT} + \frac{cL^{-p/d}\sqrt{L\log(NT)}}{(1-\gamma)^3\sqrt{NT}}\Big) = 1 - O\Big(\frac{1}{NT}\Big), \tag{B.26}$$

for some constants $c > 0$, under the given conditions on L (see A9) and ϵ (see A1).

Meanwhile, we define TS_1^{**} to be a version of TS_1^* with $\widehat{Q}_{[T_1,T_2]}(a,s)$ replaced by

$$\frac{1}{N(T_2-T_1)} \sum_{i=1}^{N} \sum_{t=T_1}^{T_2-1} \phi_L^\top(a,s) W^{-1}_{[T_1,T_2]} \phi_L(A_{i,t}, S_{i,t}) \delta^*_{i,t}.$$

By (B.8), we have

$$\mathbb{P}\Big(|\mathrm{TS}_1^* - \mathrm{TS}_1^{**}| \le \frac{CL^{-p/d}}{(1-\gamma)^3} + \frac{CL^{3/2}\log(NT)}{(1-\gamma)^3\epsilon NT}\Big) = 1 - O\Big(\frac{1}{NT}\Big), \tag{B.27}$$

for some constant $C > 0$.

Combining the results in (B.24)-(B.27), we have shown that

$$\begin{aligned}
&\mathbb{P}\Big(|\mathrm{TS}_1 - \mathrm{TS}_1^{**}| \le \frac{cL^{-p/d}}{(1-\gamma)^3} + \frac{cL^{3/2}\log(NT)}{(1-\gamma)^3\epsilon NT}\Big) = 1 - O\Big(\frac{1}{NT}\Big), \\
&\mathbb{P}\Big(|\mathrm{TS}_1^b - \mathrm{TS}_1^{b,*}| \le \frac{cL^{-p/d}}{(1-\gamma)^3} + \frac{cL^{3/2}\log(NT)}{(1-\gamma)^3\epsilon NT}\Big) = 1 - O\Big(\frac{1}{NT}\Big),
\end{aligned} \tag{B.28}$$

for some constant $c > 0$. Define

$$\Big\{ Z_u \triangleq \tau_u \Big[\frac{W^{-1}_{[0,u]}}{Nu} \sum_{i=1}^{N} \sum_{t=0}^{u-1} \phi_L(A_{i,t}, S_{i,t}) \delta^*_{i,t} - \frac{W^{-1}_{[u,T]}}{N(T-u)} \sum_{i=1}^{N} \sum_{t=u}^{T-1} \phi_L(A_{i,t}, S_{i,t}) \delta^*_{i,t} \Big] : u \Big\}, \tag{B.29}$$

$$\Big\{ Z_u^b \triangleq \tau_u \Big[\frac{W^{-1}_{[0,u]}}{Nu} \sum_{i=1}^{N} \sum_{t=0}^{u-1} \phi_L(A_{i,t}, S_{i,t}) \delta^*_{i,t} e_{i,t} - \frac{W^{-1}_{[u,T]}}{N(T-u)} \sum_{i=1}^{N} \sum_{t=u}^{T-1} \phi_L(A_{i,t}, S_{i,t}) \delta^*_{i,t} e_{i,t} \Big] : u \Big\}. \tag{B.30}$$

Notice that TS_1^{**} and $\mathrm{TS}_1^{b,*}$ can be represented as functions of $\{Z_u\}_u$ and $\{Z_u^b\}_u$, respectively. The last step is again to apply the high-dimensional martingale central limit theorem to bound their Kolmogorov distance.

We next detail the proofs for Steps 1 and 3.

Step 1. For each u, we aim to develop a concentration inequality to bound the difference

$$\left|\sqrt{\frac{u(T-u)}{T^2}}\left\{\frac{1}{NT}\sum_{t=0}^{T-1}\sum_{i=1}^{N}\sum_{a}\int_s[|\widehat{Q}_{[0,u]}(A_{i,t},S_{i,t})-\widehat{Q}_{[u,T]}(A_{i,t},S_{i,t})| - |\widehat{Q}_{[0,u]}(a,s)-\widehat{Q}_{[u,T]}(a,s)|]\pi_t^b(a|s)p_t^b(s)ds\right\}\right|. \tag{B.31}$$

According to Lemma B.2 (see (B.56)), we have that $\sup_{T_2-T_1\geq\epsilon T}\|\widehat{\beta}_{[T_1,T_2]}-\beta^*\|_2=O(\kappa)$, with probability at least $1-O(N^{-1}T^{-1})$.

Define the set $\mathcal{B}(C)=\{\beta\in\mathbb{R}^L:\|\beta-\beta^*\|_2\leq C\kappa\}$. It follows that there exists some sufficiently large constant $C>0$ such that $\widehat{\beta}_{[T_1,T_2]}\in\mathcal{B}(C)$ with probability at least $1-O(N^{-1}T^{-1})$. (B.31) can thus be upper bounded by

$$\sup_{\substack{\beta_1\in\mathcal{B}(C)\\ \beta_2\in\mathcal{B}(C)}}\left|\frac{1}{2NT}\sum_{t=0}^{T-1}\sum_{i=1}^{N}\{|\phi_L^\top(A_{i,t},S_{i,t})(\beta_1-\beta_2)|-\mathbb{E}|\phi_L^\top(A_{i,t},S_{i,t})(\beta_1-\beta_2)|\}\right|. \tag{B.32}$$

The upper bound for (B.32) can be established using similar arguments to in the proof of Lemma B.3. To save space, we only provide a sketch of the proof here. Please refer to the proof of Lemma B.3 for details.

Notice that the suprema in (B.32) are taken with respect to infinitely many βs. As such, standard concentration inequalities are not applicable to bound (B.32). Toward that end, we first take an ε-net of $\mathcal{B}(C)$ for some sufficiently small $\varepsilon>0$, denote by $\mathcal{B}^*(C)$, such that for any $\beta\in\mathcal{B}(C)$, there exists some $\beta^*\in\mathcal{B}^*(C)$ that satisfies $\|\beta-\beta^*\|_2\leq\varepsilon$. The purpose of introducing an ε-net is to approximate these sets by collections of finitely many βs so that concentration inequalities are applicable to establish the upper bound. Set $\varepsilon=C\kappa(NT)^{-2}$. It follows from Lemma 2.2 of Mendelson et al. [2008] that there exist some $\mathcal{B}^*(C)$ with number of elements upper bounded by $5^L(NT)^{2L}$.

By Lemma B.1, we have $\sup_{a,s}\|\phi_L(a,s)\|_2=O(\sqrt{L})$. Thanks to this uniform bound, the quantity within the absolute value symbol in (B.32) is a Lipschitz continuous function of (β_1,β_2), with the Lipschitz constant upper bounded by $O(\sqrt{L})$. As such, (B.32) can be approximated by

$$\sup_{\beta_1,\beta_2\in\mathcal{B}^*(C)}\left|\underbrace{\frac{1}{2NT}\sum_{t=0}^{T-1}\sum_{i=1}^{N}\sum_{a}\{|\phi_L^\top(A_{i,t},S_{i,t})(\beta_1-\beta_2)|-\mathbb{E}|\phi_L^\top(A_{i,t},S_{i,t})(\beta_1-\beta_2)|\}}_{I(\beta_1,\beta_2)\ \text{(without absolute value)}}\right| \tag{B.33}$$

with the approximation error given by $O(C\sqrt{L}N^{-2}T^{-2}\kappa)$.

It remains to develop a concentration inequality for (B.33). Since the number of elements in $\mathcal{B}^*(C)$ are bounded, we could develop a tail inequality for the quantity within the absolute value symbol in (B.33) for each combination of β_1 and β_2, and then apply Bonferroni's inequality to establish a uniform upper error bound. More specifically, for each pair (β_1,β_2), let

$$I^*(\beta_1,\beta_2)=\frac{1}{2NT}\sum_{t=0}^{T-1}\sum_{i=1}^{N}[\mathbb{E}\{|\phi_L^\top(A_{i,t},S_{i,t})(\beta_1-\beta_2)||S_{i,t-1}\}-\mathbb{E}|\phi_L^\top(A_{i,t},S_{i,t})(\beta_1-\beta_2)|],$$

with the convention that $S_{i,-1} = \emptyset$. Notice that $I(\beta_1, \beta_2) - I^*(\beta_1, \beta_2)$ forms a mean-zero martingale under (2.1) and (2.2), we can first apply the martingale concentration inequality to show that

$$|I(\beta_1, \beta_2) - I^*(\beta_1, \beta_2)| = O(\varepsilon\sqrt{LN^{-1}T^{-1}\log(NT)}), \tag{B.34}$$

with probability at least $1-O\{(NT)^{-CL}\}$ for some sufficiently large constant $C > 0$. Here, the upper bound $O(\kappa\sqrt{LN^{-1}T^{-1}\log(NT)})$ decays faster than the parametric rate, due to the fact that the variance of the summand decays to zero. Specifically, notice that $\text{Var}\{\phi_L^\top(A_t, S_t)(\beta_1 - \beta_2)|S_{t-1}\}$ is upper bounded by

$$\max_{a,a',s} \lambda_{\max}\left\{\int_{s'} \phi_L(a', s')\phi_L^\top(a', s')p(s'|a, s)ds'\right\} \|\beta_1 - \beta_2\|_2^2 = O(\kappa^2),$$

where the equality is due to Lemma B.1 and the fact that p_ts are uniformly bounded.

Next, under A4(i) and (ii), the transition functions $\{\mathcal{T}_t\}_t$ satisfy the conditions in the statement of Theorem 3.1 in Alquier et al. [2019]. In addition, each summand in the definition of $I^*(\beta_1, \beta_2)$ is upper bounded by κ. We can thus apply the concentration inequality for non-stationary Markov chains developed therein to show that $|I^*(\beta_1, \beta_2)| = O(\kappa\sqrt{LN^{-1}T^{-1}\log(NT)})$, with probability at least $1 - O\{(NT)^{-CL}\}$ for some sufficiently large constant $C > 0$. This together with the upper bound for $|I(\beta_1, \beta_2) - I^*(\beta_1, \beta_2)|$ in (B.34) and Bonferroni's inequality yields the desired uniform upper bound for (B.33). This completes Step 1 of the proof.

Step 3. The proof is very similar to that for the unnormalized test. Let Z and Z^b denote the high-dimensional random vectors formed by stacking the random vectors in the set (B.29) and (B.30), respectively. Again, Z can be represented as a sum of high-dimensional martingale difference $\sum_{g=1}^{NT} Z^{(g)}$ with respect to the filtration $\{\sigma(\mathcal{F}^{(g)})\}_{g\geq 0}$. Similarly, we can rewrite Z^b as $\sum_{g=1}^{NT} Z^{b,(g)}$ and $Z_u = \sum_{g=1}^{NT} Z_u^{(g)}$. The test statistic can be represented as

$$\text{TS}_1^{**} = \max_{\epsilon T<u<(1-\epsilon)T} \underbrace{\frac{1}{T}\sum_{t=0}^{T-1}\sum_a \int_s |\phi_L^\top(a, s)Z_u| p_t^b(s)\pi_t^b(a|s)ds}_{\psi_u}.$$

Next, we approximate the absolute value function $|x| = \max(x, 0) + \max(-x, 0)$ by $\theta^{-1}\{\log(1+\exp(\theta x))+\log(1+\exp(-\theta x))\}$. Define the corresponding smooth function $f_\theta(Z_u)$ as

$$\sqrt{\frac{u(T-u)}{T^2}}\frac{1}{T\theta}\sum_{t=0}^{T-1}\sum_a \int_s \{\log(1+\exp(\theta\phi_L^\top(a, s)Z_u)) + \log(1+\exp(-\theta\phi_L^\top(a, s)Z_u))\} \times p_t^b(s)\pi_t^b(a|s)ds.$$

Similarly, we have $\psi_u \leq f_\theta(Z_u) \leq \psi_u + \theta^{-1}\log 2$. This together with (B.17) yields

$$\text{TS}_1^{**} \leq F_\theta(\{f_\theta(Z_u)\}_u) \leq F_\theta(\{\psi_u + \theta^{-1}\log 2\}_u) \leq \text{TS}_1^{**} + \frac{\log(2T)}{\theta}. \tag{B.35}$$

Define a composite function $m(\{Z_u\}_u) = h \circ F_\theta(\{f_\theta(Z_u)\}_u)$ where the smooth function h is defined in Step 3 of the proof for the unnormalized test. By setting δ to $\log(2T)/\theta$, it follows from (B.35) and (B.18) that

$$\mathbb{P}(\mathrm{TS}_1^{**} \le z) \le \mathbb{E}m(\{Z_u\}_u) \le \mathbb{P}(\mathrm{TS}_1^{**} \le z + 4\delta). \tag{B.36}$$

Similarly, we have

$$\mathbb{P}(\mathrm{TS}_1^{b,*} \le z|\mathrm{Data}) \le \mathbb{E}[m(\{Z_u^b\}_u)|\mathrm{Data}] \le \mathbb{P}(\mathrm{TS}_1^{b,*} \le z + 4\delta|\mathrm{Data}),$$

where Z_u^b is defined in (B.30). This together with (B.36) yields that

$$\begin{aligned} \max\{\max_z |\mathbb{P}(\mathrm{TS}_1^{b,*} \le z|\mathrm{Data}) - \mathbb{P}(\mathrm{TS}_1^{**} \le z - 4\delta)|, \\ \max_z |\mathbb{P}(\mathrm{TS}_1^{b,*} \le z|\mathrm{Data}) - \mathbb{P}(\mathrm{TS}_1^{**} \le z + 4\delta)|\} \\ \le |\mathbb{E}m(\{Z_u\}) - \mathbb{E}[m(\{Z_u^b\}_u)|\mathrm{Data}]|. \end{aligned} \tag{B.37}$$

Meanwhile, we can show that for this choice of m, $c_0 \equiv \sup_{z,z'} |m(z) - m(z')| \le 1$,

$$\begin{aligned} c_2 &\equiv \sup_z \sum_{j_1,j_2} \left| \frac{\partial^2 m(z)}{\partial z_{j_1} \partial z_{j_2}} \right| \preceq \delta^{-2} L + \delta^{-1}\theta L, \\ c_3 &\equiv \sup_z \sum_{j_1,j_2,j_3} \left| \frac{\partial^3 m(z)}{\partial z_{j_1} \partial z_{j_2} \partial z_{j_3}} \right| \preceq \delta^{-3} L^{3/2} + \delta^{-2}\theta L^{3/2} + \delta^{-1}\theta^2 L^{3/2}. \end{aligned}$$

In addition, similar to Lemma B.3, we can show that both $\sum_g \mathbb{E}\{Z^{(g)}(Z^{(g)})^\top|\mathcal{F}^{(g-1)}\}$ and $\sum_g \mathbb{E}\{Z^{b,(g)}(Z^{b,(g)})^\top|\mathrm{Data}\}^\top$ will converge to the same deterministic matrix with elementwise approximation error upper bounded by $C(1-\gamma)^{-4}\sqrt{L\log(NT)}/(NT)^{3/2}$ for some constant $C > 0$, with probability at least $1 - O(N^{-1}T^{-1})$.

However, the anti-concentration inequality is not applicable here, since the test statistic is no longer a maximum of $\{Z_u\}_u$. Toward that end, assuming $(1-\gamma)\sqrt{NT}\mathrm{TS}_1^{b,*}/\sqrt{\log(NT)}$ has a bounded density function, it follows that

$$\sup_z |\mathbb{P}(\mathrm{TS}_1^{b,*} \le z - 4\delta|\mathrm{Data}) - \mathbb{P}(\mathrm{TS}_1^{b,*} \le z + 4\delta|\mathrm{Data})| \preceq \frac{\sqrt{NT}\log^{3/2}(NT)}{(1-\gamma)^{-1}\theta}.$$

In view of (B.37), by similarly setting $\theta = (1-\gamma)^{7/4}L^{-1/2}\epsilon^{1/8}(NT)^{3/8}\log^{-3/8}(NT)$, we obtain

$$\sup_z |\mathbb{P}(\mathrm{TS}_1^{b,**} \le z|\mathrm{Data}) - \mathbb{P}(\mathrm{TS}_1^{**} \le z)| \preceq \frac{\sqrt{L}\log^{15/8}(NT)}{(1-\gamma)^{3/4}(\epsilon NT)^{1/8}}.$$

Finally, based on (B.28), one can show that

$$\sup_z |\mathbb{P}(\mathrm{TS}_1^b \le z|\mathrm{Data}) - \mathbb{P}(\mathrm{TS}_1 \le z)| \preceq \frac{\sqrt{L}\log^{15/8}(NT)}{(1-\gamma)^{3/4}(\epsilon NT)^{1/8}} + \frac{L^{-p/d}\sqrt{NT\log(NT)}}{(1-\gamma)^2}.$$

The proof is hence completed.

B.3 Proof of Lemmas B.1 and B.2

First, we notice that (B.4) can be proven based on the proof of Theorem 3.3 of Burman and Chen [1989]. Second, the B-spline basis function is non-negative and sum up to 1. Following Chen and Christensen [2015], we rescale the basis by multiplying it by $L^{1/2}$. This leads to the equality in (B.5). Next, according to Cauchy-Schwarz inequality, the ℓ_2-norm of $\phi_L(a,s)$ is lower bounded by its ℓ_1-norm divided by $\sqrt{L}$. This yields the inequality in (B.5). Additionally, each function in Φ is Lipschitz continuous. This yields (B.6).

The rest of the proof is organized as follows. We first outline the challenge in establishing the uniform convergence rate of the Q-function estimators under the nonstandard stationarity assumption SA3 where the reward and transition functions may remain nonstationary over time and illustrate our main idea in addressing this challenge. Next, we conduct a population-level analysis with infinitely many data to prove (B.3). Next, we consider the finite-sample scenario and formally establish the uniform convergence rate of the Q-estimators in (B.7). Finally, we conduct an asymptotic analysis to prove (B.8).

Challenge: In FQI, we iteratively update the Q-function according to the following formula,

$$Q^{(k+1)} = \arg\min_{Q} \sum_{i=1}^{N} \sum_{t=T_1}^{T_2-1} \Big[R_{i,t} + \gamma \max_a Q^{(k)}(a, S_{i,t+1}) - Q(A_{i,t}, S_{i,t}) \Big]^2.$$

Our goal is to establish the uniform rate of convergence of these estimators across different time intervals $[T_1, T_2]$, under the nonstandard stationarity assumption SA3 where the reward and transition functions can remain nonstationary over time.

Under the more conventional stationarity assumption SA1, it is immediate to see that $Q^{(k+1)}(a,s)$ is to converge to

$$g_t(a, s, Q^{(k)}) \triangleq r_t(a,s) + \gamma \int_{s'} \max_a Q^{(k)}(a, s') p_t(s'|a,s) ds', \tag{B.38}$$

where the subscript t could be removed due to the stationarity of the reward and transition functions. However, this no longer holds under SA3 where the reward and state transition functions may remain nonstationary over time. Our key insight is that although $Q^{(k+1)}(a,s)$ might not converge to (B.38), it converges to its weighted average with weights $w_t(a,s) = \pi_t^b(a|s) p_t^b(s)$ dependent upon the state-action visitation probability (recall that p_t^b denotes the density function of S_t), given by

$$Q^{(k+1),*}(a,s) = \Big[\sum_{t=T_1}^{T_2-1} w_t(a,s) \Big]^{-1} \Big[\sum_{t=T_1}^{T_2-1} g_t(a, s, Q^{(k)}) w_t(a,s) \Big]. \tag{B.39}$$

Meanwhile, under SA3, the optimal Q-function Q^{opt} is stationary and satisfies $Q^{opt}(a,s) = g_t(a, s, Q^{opt})$ for any t, and hence, we have

$$Q^{opt}(a,s) = \Big[\sum_{t=T_1}^{T_2-1} w_t(a,s) \Big]^{-1} \Big[\sum_{t=T_1}^{T_2-1} g_t(a, s, Q^{opt}) w_t(a,s) \Big].$$

This together with (B.39) enables us to apply the standard error analysis in FQI to show that

$$\sup_{a,s}|Q^{opt}(a,s)-\widehat{Q}_{[T_1,T_2]}(a,s)|\leq\sum_{1\leq k\leq K}\gamma^{K-k}\sup_{a,s}|Q^{(k),*}(a,s)-Q^{(k)}(a,s)| \\ +\gamma^K\sup_{a,s}|Q^{opt}(a,s)-Q^{(0)}(a,s)|, \tag{B.40}$$

where the first term on the right-hand-side (RHS) denotes the finite-sample estimation error between the Q-function estimator $Q^{(k)}$ and its population-level target $Q^{(k),*}$, and the second term measures the bias due to initialization.

In the following, we first conduct a population-level analysis by assuming $N=\infty$. We next conduct the finite-sample analysis to formally establish the rate of convergence.

Population-level analysis. Recall that $\Sigma_{[T_1,T_2]}=(T_2-T_1)^{-1}\sum_{t=T_1}^{T_2-1}\mathbb{E}\phi_L(A_t,S_t)\phi_L^\top(A_t,S_t)$. As $N=\infty$, the regression coefficients $\beta^{(k)}$ computed at each kth iteration equals

$$\beta^{(k)}=\Sigma_{[T_1,T_2]}^{-1}\Big[\frac{1}{T_2-T_1}\sum_{t=T_1}^{T_2-1}\mathbb{E}\phi_L(A_t,S_t)\{r_t(A_t,S_t)+\gamma\max_a\phi_L^\top(a,S_{t+1})\beta^{(k-1)}\}\Big], \tag{B.41}$$

with $\beta^{(0)}$ initialized to a zero vector. This yields the Q-function estimator $Q^{(k)}(a,s)=\phi_L^\top(a,s)\beta^{(k)}$.

To illustrate the rationale behind the definition of $Q^{(k),*}$ in (B.39), consider what would occur if we replace $r_t(A_t,S_t)+\gamma\max_a\phi_L^\top(a,S_{t+1})\beta^{(k-1)}$ in (B.41) with $Q^{(k),*}(A_t,S_t)$. Equation (B.41) remains true. In other words, we have

$$\beta^{(k)}=\Sigma_{[T_1,T_2]}^{-1}\Big[\frac{1}{T_2-T_1}\sum_{t=T_1}^{T_2-1}\mathbb{E}\phi_L(A_t,S_t)Q^{(k),*}(A_t,S_t)\Big]. \tag{B.42}$$

This implies that $\phi_L^\top\beta^{(k)}$ is the projection of $Q^{(k),*}$ onto the linear function class. Consequently, $Q^{(k),*}$ is indeed the population limit of $\phi_L^\top\beta^{(k)}$ in the presence of nonstationary reward and transition functions.

To effectively control the difference between $Q^{(k)}$ and $Q^{(k)*}$, we need to approximate $Q^{(k)*}$ using the linear function class. This can be achieved using the realizability assumption in A2 and the completeness assumption in A3. Specifically, under the p-smoothness condition in A2, there exists some β_t^* such that $\phi_L^\top\beta_t^*$ can approximate r_t uniformly with the uniform approximation error upper bounded by $O(L^{-p/d})$ [see Huang, 1998, Section 2.2]. Similarly, under A3, there exists some $\beta_t^{(k)*}$ whose ℓ_2-norm is bounded by $\|\beta^{(k-1)}\|_2$ such that $\phi_L^\top\beta_t^{(k)*}$ can approximate $\mathcal{B}_t\phi_L^\top\beta^{(k-1)}$ uniformly with the error upper bounded by $O(L^{-p/d}\|\beta^{(k-1)}\|_2)$. This allows us to use $\phi_L^\top(\beta_t^*+\gamma\beta_t^{(k)*})$ to approximate $g_t(a,s,Q^{(k-1)})$, which further leads to the approximation of $Q^{(k)*}$ by $\phi_L^\top\beta^{(k)*}$ where

$$\beta^{(k)*}=\Big[\sum_{t=T_1}^{T_2-1}w_t(a,s)\Big]^{-1}\Big[\sum_{t=T_1}^{T_2-1}(\beta_t^*+\gamma\beta_t^{(k)*})w_t(a,s)\Big],$$

such that

$$\text{err}(a,s) \triangleq |\phi_L^\top(a,s)\beta^{(k)*} - Q^{(k)*}(a,s)| = O\{L^{-p/d}(1+\|\beta^{(k-1)}\|_2)\},$$

where the big-O term is uniform in (a,s). It follows from Equation (B.42) that

$$\beta^{(k)} - \beta^{(k)*} = \frac{1}{T_2-T_1}\sum_{t=T_1}^{T_2-1}\mathbb{E}\Sigma_{[T_1,T_2]}^{-1}\phi_L(A_t,S_t)\{Q^{(k),*}(A_t,S_t) - \phi_L^\top(A_t,S_t)\beta^{(k)*}\}, \quad \text{(B.43)}$$

and hence, $\|\beta^{(k)} - \beta^{(k)*}\|_2$ can be upper bounded by

$$\sup_{\theta\in\mathbb{R}^{mL}:\|\theta\|_2=1}\left|\frac{1}{T_2-T_1}\sum_{t=T_1}^{T_2-1}\mathbb{E}\theta^\top\Sigma_{[T_1,T_2]}^{-1}\phi_L(A_t,S_t)\{Q^{(k),*}(A_t,S_t) - \phi_L^\top(A_t,S_t)\beta^{(k)*}\}\right|$$
$$\le \sup_{a,s}\text{err}(a,s) \times \sup_{\theta\in\mathbb{R}^{mL}:\|\theta\|_2=1}\frac{1}{T_2-T_1}\sum_{t=T_1}^{T_2-1}\mathbb{E}|\theta^\top\Sigma_{[T_1,T_2]}^{-1}\phi_L(A_t,S_t)|$$

Using Cauchy-Schwarz inequality, the second term in the last line can be upper bounded by

$$\sup_{\theta\in\mathbb{R}^{mL}:\|\theta\|_2=1}\sqrt{\frac{1}{T_2-T_1}\sum_{t=T_1}^{T_2-1}\mathbb{E}|\theta^\top\Sigma_{[T_1,T_2]}^{-1}\phi_L(A_t,S_t)|^2} = \sup_{\theta\in\mathbb{R}^{mL}:\|\theta\|_2=1}\sqrt{\theta^\top\Sigma_{[T_1,T_2]}^{-1}\theta}.$$

Under A5(ii), the minimum eigenvalue of $\Sigma_{[T_1,T_2]}$ is bounded away from zero, which in turn suggests that the maximum eigenvalue of $\Sigma_{[T_1,T_2]}^{-1}$ is bounded away from infinity. It follows that the above expression is of the order $O(1)$, and hence

$$\|\beta^{(k)} - \beta^{(k)*}\|_2 = O\{L^{-p/d}(1+\|\beta^{(k-1)}\|_2)\}. \quad \text{(B.44)}$$

Next, we focus on providing an upper bound for $\sup_k\|\beta^{(k)}\|_2$ to further simplify the RHS of (B.44). To begin with, we first provide an uniform upper bound for $\sup_t\|\beta_t^*\|_2$. Notice that

$$\begin{aligned}\beta_t^* = \Sigma_{[t,t+1]}^{-1}\Sigma_{[t,t+1]}\beta_t^* = \Sigma_{[t,t+1]}^{-1}\mathbb{E}[\phi_L(A_t,S_t)r_t(A_t,S_t)] \\ -\Sigma_{[t,t+1]}^{-1}\mathbb{E}\phi_L(A_t,S_t)[r_t(A_t,S_t) - \phi_L^\top(A_t,S_t)\beta_t^*].\end{aligned} \quad \text{(B.45)}$$

As r_ts are uniformly bounded (implied by A2), using similar arguments to the proof of (B.44), it can be shown that both the rightmost term in the first line of (B.45) and the term in the second line of (B.45) are upper bounded by $O(1)$ and $O(L^{p/d})$, respectively. Consequently, we have $\sup_t\|\beta_t^*\|_2 = O(1)$. Under the completeness assumption in A3, combining this together with the definition of $\beta^{(k)*}$ yields that $\|\beta^{(k)*}\|_2 \le C + \gamma\|\beta^{(k-1)}\|_2$ for some constant $C > 0$. It follows from (B.44) that

$$\|\beta^{(k)}\|_2 \le \bar{C} + \gamma(1+\bar{C}L^{-p/d})\|\beta^{(k-1)}\|_2,$$

for some constant $\bar{C} > 0$. As $\beta^{(0)}$ is initialized to a zero vector, we obtain that $\sup_k \|\beta^{(k)}\|_2 \leq c(1-\gamma)^{-1}$ for some constant $c > 0$. It follows that the uppper bound in (B.44) can be simplified into

$$\|\beta^{(k)} - \beta^{(k)*}\|_2 = O\Big(\frac{L^{-p/d}}{1-\gamma}\Big). \tag{B.46}$$

Finally, we focus on providing an upper bound for $\sup_{a,s} |\phi_L^\top(a,s)(\beta^{(k)} - \beta^{(k)*})|$. A naïve approach is to employ the Cauchy-Schwarz inequality to show that

$$\sup_{a,s} |\phi_L^\top(a,s)(\beta^{(k)} - \beta^{(k)*})| \leq \sup_{a,s} \|\phi_L^\top(a,s)\|_2 \|\beta^{(k)} - \beta^{(k)*}\|_2 = O\Big(\frac{L^{1/2-p/d}}{1-\gamma}\Big),$$

by (B.4) and (B.46). However, this bound is not sharp. In the following, we conduct a refined analysis to show that the upper bound can be sharpened to

$$\sup_{a,s} |\phi_L^\top(a,s)(\beta^{(k)*} - \beta^{(k)})| = O\Big(\frac{L^{-p/d}}{1-\gamma}\Big), \tag{B.47}$$

which is faster by a factor of $L^{-1/2}$. This together with the upper bound on the approximation error $\sup_{a,s} |Q^{(k),*}(a,s) - \phi_L^\top(a,s)\beta^{(k)*}| = O((1-\gamma)^{-1}L^{-p/d})$ yields the following error bound for the difference between $Q^{(k)}$ and its population limit $Q^{(k),*}$,

$$\sup_{a,s} |Q^{(k),*}(a,s) - Q^{(k)}(a,s)| = O\Big(\frac{L^{-p/d}}{1-\gamma}\Big). \tag{B.48}$$

Notice that the boundedness of r_ts yields that $\sup_{a,s} |Q^{opt}(a,s)| = O((1-\gamma)^{-1})$. As the initial Q-estimator is initialized to zero, it follows from (B.48) and the error analysis in (B.40) that

$$\sup_{a,s} |Q^{opt}(a,s) - Q^{(k)}(a,s)| = O\Big(\frac{L^{-p/d}}{(1-\gamma)^2}\Big) + O\Big(\frac{\gamma^k}{1-\gamma}\Big).$$

By letting $k \to \infty$, we obtain (B.3).

It remains to prove (B.47). The main idea is to employ the bias control techniques developed by Huang [2003] (see Lemma 5.1 and Theorem A.1 therein), based on which we can show that the basis function ϕ_L satisfies

$$\Big[\sup_{a,s} |h(A_t,S_t)|\Big]^{-1} \sup_{a,s} \Big|\phi_L^\top(a,s) \frac{\Sigma_{[T_1,T_2]}^{-1}}{T_2 - T_1} \sum_{t=T_1}^{T_2-1} \mathbb{E}\phi_L(A_t,S_t)h(A_t,S_t)\Big| = O(1), \tag{B.49}$$

where the big-O term on the RHS is uniform in any nonzero function h.

Notice that our setting differs from the one considered in Huang [2003] in two ways: (i) the basis function is not only a function of the continuous state, but a function of the discrete action as well; (ii) the state-action pairs at different times may have nonstationary distribution

functions. Despite these differences, (B.49) remains valid as (i) we estimate the coefficients for different actions separately using different data subsets grouped by the action; (ii) we can treat the data as if it were sampled from a stationary distribution, in which each state-action pair follows a mixture of distributions of $\{(S_t, A_t) : T_1 \le t < T_2 - 1\}$with equal weights.

Now, in view of (B.43), (B.47) can be readily obtained by setting the function h in (B.49) to err. This completes the population-level analysis.

Finite-sample analysis. Next, we proceed to conduct the finite-sample analysis by considering a finite N. The arguments are very similar to those used in the population-level analysis. The difference lies in that, with a finite N, the equality in (B.42) no longer holds. Rather, the estimator $\beta^{(k)}$ is defined by

$$\frac{\widehat{\Sigma}_{[T_1,T_2]}^{-1}}{N(T_2-T_1)}\Big[\sum_{i=1}^{N}\sum_{t=T_1}^{T_2-1}\phi_L(A_{i,t},S_{i,t})\{R_{i,t}+\gamma\max_{a'}\phi_L^\top(a',S_{i,t+1})\beta^{(k-1)}\}\Big], \tag{B.50}$$

where we recall that

$$\widehat{\Sigma}_{[T_1,T_2]} = \frac{1}{N(T_2-T_1)}\sum_{i=1}^{N}\sum_{t=T_1}^{T_2-1}\phi_L(A_{i,t},S_{i,t})\phi_L^\top(A_{i,t},S_{i,t}).$$

As such, we have

$$\begin{aligned}\beta^{(k)}-\beta^{(k)*} = \widehat{\Sigma}_{[T_1,T_2]}^{-1}\Big[&\frac{1}{N(T_2-T_1)}\sum_{i=1}^{N}\sum_{t=T_1}^{T_2-1}\phi_L(A_{i,t},S_{i,t})\{R_{i,t}\\ &+\gamma\max_{a'}\phi_L^\top(a',S_{i,t+1})\beta^{(k-1)}-\phi_L(A_{i,t},S_{i,t})\beta^{(k)*}\}\Big],\end{aligned} \tag{B.51}$$

where the population limit $\beta^{(k)*}$ is defined in the population-level analysis.

Using similar arguments to the proof of Lemma B.3, we can show that

$$\Big\|\widehat{\Sigma}_{[T_1,T_2]}-\Sigma_{[T_1,T_2]}\Big\|_2 \le c\sqrt{L(\epsilon NT)^{-1}\log(NT)}, \tag{B.52}$$

for some constant $c > 0$, where the inequality holds uniformly across all pairs (T_1, T_2) with probability at least $1 - O(N^{-1}T^{-1})$. Under A5(ii), $\lambda_{\min}[\Sigma_{[T_1,T_2]}]$ is uniformly bounded away from zero. On the event set defined by (B.52), for sufficiently large NT, there exists some $\bar{c} > 0$ such that $\lambda_{\min}[\widehat{\Sigma}_{[T_1,T_2]}] \ge \bar{c}$. This together with (B.51) yields that

$$\begin{aligned}\|\beta^{(k)}-\beta^{(k)*}\|_2 \le \bar{c}^{-1}\Big\|\sum_{i=1}^{N}\sum_{t=T_1}^{T_2-1}\frac{\phi_L(A_{i,t},S_{i,t})}{N(T_2-T_1)}\{&R_{i,t}+\gamma\max_{a'}\phi_L^\top(a',S_{i,t+1})\beta^{(k-1)}\\ &-\phi_L^\top(A_{i,t},S_{i,t})\beta^{(k)*}\}\Big\|_2.\end{aligned} \tag{B.53}$$

Assume for now,

$$\sup_k\|\beta^{(k)}\|_2 \le \frac{c}{1-\gamma} \text{ and } \sup_k\|\beta^{(k)*}\|_2 \le \frac{c}{1-\gamma}, \tag{B.54}$$

for some constant $c > 0$. These assertions can be proven using similar arguments to the population-level analysis.

By definition, if $\beta^{(k-1)}$ and $\beta^{(k)*}$ were computed using an independent dataset, the expected value of the vector on the RHS of (B.53) would be of the order $O((1-\gamma)^{-1}L^{-p/d})$, based on our population-level analysis. However, since they are computed by the same dataset, they become dependent upon each other. To handle such dependence, we upper bound the ℓ_2-norm in the RHS of (B.53) by

$$\sup_{\beta_1,\beta_2} \Big\| \sum_{i=1}^{N} \sum_{t=T_1}^{T_2-1} \frac{\phi_L(A_{i,t},S_{i,t})}{N(T_2-T_1)} \{R_{i,t} + \gamma \max_{a'} \phi_L^\top(a',S_{i,t+1})\beta_1 - \phi_L^\top(A_{i,t},S_{i,t})\beta_2\} \Big\|_2 \quad \text{(B.55)}$$

where the supremum is taken over all the pairs (β_1,β_2) such that $\|\beta_1\|_2 \le (1-\gamma)^{-1}c$, $\|\beta_2\|_2 \le (1-\gamma)^{-1}c$ and that

$$\Big| \frac{1}{T_2-T_1} \mathbb{E}\Big[\sum_{t=T_1}^{T_2-1} \phi_L(A_t,S_t)\{R_t + \gamma \max_{a'} \phi_L^\top(a',S_{t+1})\beta_1 - \phi_L^\top(A_t,S_t)\beta_2\} \Big] \Big|_2 = O\Big(\frac{L^{-p/d}}{1-\gamma}\Big),$$

as the above equation would have been satisfied if we were to set $\beta_1 = \beta^{(k-1)}$ and $\beta_2 = \beta^{(k)*}$. Using similar arguments to Step 3 of the proof of Theorem 4.1, we can show that (B.55) is upper bounded by $O((1-\gamma)^{-1}\sqrt{L(\epsilon NT)^{-1}\log(NT)}) + O((1-\gamma)^{-1}L^{-p/d})$ where the big-O terms are uniform in (T_1,T_2), with probability at least $1 - O((NT)^{-1})$.

This together with (B.53) yields the following upper bound for the difference $\beta^{(k)*} - \beta^{(k)}$,

$$\|\beta^{(k)*} - \beta^{(k)}\|_2 = O\Big(\frac{\sqrt{L(\epsilon NT)^{-1}\log(NT)}}{1-\gamma}\Big) + O\Big(\frac{L^{-p/d}}{1-\gamma}\Big).$$

Notice that compared to the error bound in the population-level analysis (B.44), the RHS above includes an additional term $O((1-\gamma)^{-1}\sqrt{L(\epsilon NT)^{-1}\log(NT)})$, which accounts for the finite-sample estimation error.

Finally, to upper bound $\sup_{a,s} |\phi_L^\top(a,s)(\beta^{(k)*} - \beta^{(k)})|$, we define two intermediate quantities

$$I_1 = \frac{\Sigma_{[T_1,T_2]}^{-1}}{N(T_2-T_1)} \sum_{i=1}^{N} \sum_{t=T_1}^{T_2-1} \phi_L(A_{i,t},S_{i,t})\{R_{i,t} + \gamma \max_{a'} \phi_L^\top(a',S_{i,t+1})\beta^{(k-1)} - \phi_L(A_{i,t},S_{i,t})\beta^{(k)*}\},$$

$$I_2 = \frac{\Sigma_{[T_1,T_2]}^{-1}}{T_2-T_1} \sum_{t=T_1}^{T_2-1} \mathbb{E}\phi_L(A_t,S_t)\{R_t + \gamma \max_{a'} \phi_L^\top(a',S_{t+1})\beta^{(k-1)} - \phi_L(A_t,S_t)\beta^{(k)*}\}.$$

It follows from (B.52) that

$$\|\beta^{(k)*} - \beta^{(k)} - I_1\|_2 = O\Big(\frac{L(\epsilon NT)^{-1}\log(NT)}{(1-\gamma)^2}\Big) + O\Big(\frac{L^{1/2-p/d}\sqrt{(\epsilon NT)^{-1}\log(NT)}}{(1-\gamma)^2}\Big),$$

with probability at least $1 - O(N^{-1}T^{-1})$.

Meanwhile, using similar arguments to bounding the ℓ_2 norm in the RHS of (B.53), we obtain with probability at least $1 - O(N^{-1}T^{-1})$ that

$$\|I_1 - I_2\|_\infty = O\Big(\frac{\sqrt{L(\epsilon NT)^{-1}\log(NT)}}{1-\gamma}\Big).$$

Combining these bounds together with (B.5), we obtain that

$$\sup_{a,s}|\phi_L^\top(a,s)(\beta^{(k)*} - \beta^{(k)})| \le \sup_{a,s}\|\phi_L(a,s)\|_2\|\beta^{(k)*} - \beta^{(k)} - I_1\|_2 + \sup_{a,s}\|\phi_L(a,s)\|_1\|I_1 - I_2\|_\infty$$
$$+ \sup_{a,s}|\phi_L^\top(a,s)I_2| = O\Big(\frac{\sqrt{L(\epsilon NT)^{-1}\log(NT)}}{1-\gamma}\Big) + \sup_{a,s}|\phi_L^\top(a,s)I_2|,$$

under the conditions on L in A9.

Finally, it follows from the arguments used to the proof of (B.47) in the population-level analysis that $\sup_{a,s}|\phi_L^\top(a,s)I_2| = O((1-\gamma)^{-1}L^{-p/d})$. Consequently, we have

$$\sup_{a,s}|\phi_L^\top(a,s)(\beta^{(k)*} - \beta^{(k)})| = O\Big(\frac{\sqrt{L(\epsilon NT)^{-1}\log(NT)}}{1-\gamma}\Big) + O\Big(\frac{L^{-p/d}}{1-\gamma}\Big),$$

and hence $\sup_{a,s}|Q^{(k)*}(a,s) - Q^{(k)}(a,s)|$ is of the same order of magnitude. It follows from the error analysis in (B.40) that

$$\sup_{a,s}|Q^{opt}(a,s) - Q^{(k)}(a,s)| = O\Big(\frac{\sqrt{L(\epsilon NT)^{-1}\log(NT)}}{(1-\gamma)^2}\Big) + O\Big(\frac{L^{-p/d}}{(1-\gamma)^2}\Big) + O\Big(\frac{\gamma^k}{1-\gamma}\Big),$$

with probability at least $1 - O(N^{-1}T^{-1})$. This establishes the rate of convergence in (B.7) by noting that the number of FQI iterations much larger than $\log(NT)$ (see Assumption A9).

To conclude this part, notice that

$$\beta^{(k)} - \beta^* = \frac{\Sigma_{[T_1,T_2]}^{-1}}{T_2 - T_1}\sum_{t=T_1}^{T_2-1}\mathbb{E}\phi_L(A_t,S_t)\phi_L^\top(A_t,S_t)(\beta^{(k)} - \beta^*)$$
$$= \frac{\Sigma_{[T_1,T_2]}^{-1}}{T_2 - T_1}\sum_{t=T_1}^{T_2-1}\mathbb{E}\phi_L(A_t,S_t)\{\phi_L^\top(A_t,S_t)\beta^{(k)} - Q^{opt}(A_t,S_t)\}$$
$$+ \frac{\Sigma_{[T_1,T_2]}^{-1}}{T_2 - T_1}\sum_{t=T_1}^{T_2-1}\mathbb{E}\phi_L(A_t,S_t)\{Q^{opt}(A_t,S_t) - \phi_L^\top(A_t,S_t)\beta^*\}.$$

Based on the established rate of convergence and (B.3), one can similarly prove that

$$\|\beta^{(k)} - \beta^*\|_2 = O\Big(\frac{L^{-p/d}}{(1-\gamma)^2}\Big) + O\Big(\frac{\sqrt{L(\epsilon NT)^{-1}\log(NT)}}{(1-\gamma)^2}\Big) + O\Big(\frac{\gamma^k}{1-\gamma}\Big), \qquad \text{(B.56)}$$

We omit the detailed proof to save space.

Asymptotic analysis. To begin with, we notice that

$$\beta^* = \frac{\Sigma_{[T_1,T_2]}^{-1}}{T_2-T_1}\mathbb{E}\Big[\sum_{t=T_1}^{T_2-1}\phi_L(A_t,S_t)\phi_L^\top(A_t,S_t)\beta^*\Big] = \frac{\Sigma_{[T_1,T_2]}^{-1}}{T_2-T_1}\mathbb{E}\Big[\sum_{t=T_1}^{T_2-1}\phi_L(A_t,S_t)Q^*(A_t,S_t)\Big] - \underbrace{\frac{\Sigma_{[T_1,T_2]}^{-1}}{T_2-T_1}\mathbb{E}\Big[\sum_{t=T_1}^{T_2-1}\phi_L(A_t,S_t)\text{reminder}(A_t,S_t)\Big]}_{\theta_r^{(1)}},$$

where the reminder function is bounded by $O((1-\gamma)^{-2}L^{-p/d})$, due to (B.3). This together with the Bellman optimality equation $Q^{opt} = r_t + \gamma\mathcal{B}_t Q^{opt}$ implies that β^* is equal to

$$\underbrace{\frac{\Sigma_{[T_1,T_2]}^{-1}}{T_2-T_1}\mathbb{E}\Big[\sum_{t=T_1}^{T_2-1}\phi_L(A_t,S_t)r_t(A_t,S_t)\Big]}_{\beta_r} + \frac{\gamma\Sigma_{[T_1,T_2]}^{-1}}{T_2-T_1}\mathbb{E}\Big[\sum_{t=T_1}^{T_2-1}\phi_L(A_t,S_t)Q^{opt}(\pi^{opt}(S_{t+1}),S_{t+1})\Big] - \theta_r^{(1)},$$

and hence,

$$\beta^* = \beta_r + \gamma\underbrace{\frac{\Sigma_{[T_1,T_2]}^{-1}}{T_2-T_1}\mathbb{E}\Big[\sum_{t=T_1}^{T_2-1}\phi_L(A_t,S_t)\phi_L^\top(\pi^{opt}(S_{t+1}),S_{t+1})\Big]}_{\mathcal{P}}\beta^* - \theta_r^{(1)} + \gamma\underbrace{\frac{\Sigma_{[T_1,T_2]}^{-1}}{T_2-T_1}\mathbb{E}\Big[\sum_{t=T_1}^{T_2-1}\phi_L(A_t,S_t)\text{reminder}(\pi^{opt}(S_{t+1}),S_{t+1})\Big]}_{\theta_r^{(2)}}.$$

Using the same arguments, we obtain that $\beta^* = \beta_r + \gamma\mathcal{P}\beta_r + \gamma^2\mathcal{P}^2\beta^* - \theta_r - \mathcal{P}\theta_r$ where $\theta_r = \theta_r^{(1)} - \gamma\theta_r^{(2)}$. Repeating this process, we obtain that $\beta^* = \sum_{j=1}^{k}(\gamma\mathcal{P})^{j-1}\beta_r + \gamma^k\mathcal{P}^k\beta^* - \sum_{j=1}^{k-1}(\gamma\mathcal{P})^j\theta_r$ and hence

$$\phi_L^\top(a,s)\beta^* = \sum_{j=1}^{k}\gamma^{j-1}\phi_L^\top(a,s)\mathcal{P}^{j-1}\beta_r + \gamma^k\phi_L^\top(a,s)\mathcal{P}^k\beta^* - \sum_{j=1}^{k-1}\gamma^j\phi_L^\top(a,s)\mathcal{P}^j\theta_r \quad \text{(B.57)}$$

Below, we focus on providing an upper bound on the rightmost reminder term in (B.57). First, as the reminder function is of the order $O((1-\gamma)^{-2}L^{-p/d})$, it follows from (B.49) that $\sup_{a,s}|\phi_L^\top(a,s)\theta_r^{(1)}| = O((1-\gamma)^{-2}L^{-p/d})$. Second, when upper bounding the function $\phi_L^\top(a,s)\theta_r^{(2)}$, we notice that it can be represented as

$$\phi_L^\top(a,s)\frac{\Sigma_{[T_1,T_2]}^{-1}}{T_2-T_1}\mathbb{E}\Big[\sum_{t=T_1}^{T_2-1}\phi_L(A_t,S_t)(\mathcal{B}_t^*\text{reminder})(A_t,S_t)\Big], \quad \text{(B.58)}$$

where $\mathcal{B}_t^*$ is defined such that $\mathcal{B}_t^* g(a,s) = \int_{s'} g(\pi^{opt}(s'), s') p_t(s'|a,s) ds'$.

However, $\mathcal{B}_t$reminder can vary over time, as the transition function may not be stationary. As a result, (B.49) is not directly applicable to upper bound (B.58). Nonetheless, we may apply the techniques in (B.42) to stationarize the reminder term in (B.58). Specifically, define

$$\text{reminder}^*(a,s) = \Big[\sum_{t=T_1}^{T_2-1} w_t(a,s)\Big]^{-1}\Big[\sum_{t=T_1}^{T_2-1} w_t(a,s)(\mathcal{B}_t\text{reminder})(a,s)\Big]$$

With some calculations, it can be shown that (B.58) is equal to

$$\phi_L^\top(a,s)\frac{\Sigma_{[T_1,T_2]}^{-1}}{T_2-T_1}\mathbb{E}\Big[\sum_{t=T_1}^{T_2-1}\phi_L(A_t,S_t)\text{reminder}^*(A_t,S_t)\Big],$$

with $\mathcal{B}_t$reminder being replaced by a stationary function reminder* so that we can use (B.49) to show that $\sup_{a,s}|\phi_L^\top(a,s)\theta_r^{(2)}| = O((1-\gamma)^{-2}L^{-p/d})$. Third, we will show below that

$$\sup_{\beta\in\mathbb{R}^{mL}:\|\beta\|_2=1}\|\gamma\Sigma_{[T_1,T_2]}^{1/2}\mathcal{P}\Sigma_{[T_1,T_2]}^{-1/2}\beta\|_2 \le \rho = \sqrt{1-c(1-\gamma)}, \tag{B.59}$$

for some constant $c>0$. This suggests that the operator norm of $\gamma\Sigma_{[T_1,T_2]}^{1/2}\mathcal{P}\Sigma_{[T_1,T_2]}^{-1/2}$ is strictly smaller than 1, which together with the boundedness of $\|\Sigma_{[T_1,T_2]}^{-1/2}\|_2$ (implied by A5(ii)) yields

$$\|\gamma^j\mathcal{P}^j\theta_r\|_2 \le \|\Sigma_{[T_1,T_2]}^{-1/2}\|_2\|\gamma\Sigma_{[T_1,T_2]}^{1/2}\mathcal{P}\Sigma_{[T_1,T_2]}^{-1/2}\|_2^j\|\Sigma_{[T_1,T_2]}^{1/2}\theta_r\|_2 \le C\rho^j\|\Sigma_{[T_1,T_2]}^{1/2}\theta_r\|_2. \tag{B.60}$$

Meanwhile, using similar arguments to the proof of (B.44), we can show that $\|\Sigma_{[T_1,T_2]}^{1/2}\theta_r\|_2 = O((1-\gamma)^{-2}L^{-p/d})$, which together with (B.60) yields that $\|\gamma^j\mathcal{P}^j\theta_r\|_2 \le \bar{c}(1-\gamma)^{-2}\rho^j L^{-p/d}$ for some constant $c>0$ and any $j\ge 0$. Consequently, for each j, we can represent $\gamma^j\phi_L^\top(a,s)\mathcal{P}^j\theta_r$ as $\gamma\phi_L^\top(a,s)\mathcal{P}\theta_{r,j}$, i.e.,

$$\gamma\phi_L^\top(a,s)\frac{\Sigma_{[T_1,T_2]}^{-1}}{T_2-T_1}\mathbb{E}\Big[\sum_{t=T_1}^{T_2-1}\phi_L(A_t,S_t)\mathcal{B}_t^*\phi_L^\top(A_t,S_t)\theta_{r,j}\Big] \tag{B.61}$$

for some $\theta_{r,j}$ whose ℓ_2-norm is bounded by $\bar{c}(1-\gamma)^{-2}\rho^{j-1}L^{-p/d}$. As p_ts are bounded, it follows from (B.4) that $\sup_{a,s}\|\mathcal{B}_t^*\phi_L^\top(a,s)\|_2 = O(1)$. Using similar arguments in bounding $\theta_L^\top\theta_r^{(2)}$, we can show that (B.61) is of the order $O((1-\gamma)^{-2}\rho^{j-1}L^{-p/d})$.

Hence, the rightmost reminder term in (B.57) is of the order

$$O\Big(\frac{L^{-p/d}}{(1-\gamma)^2(1-\rho)}\Big) = O\Big(\frac{L^{-p/d}}{(1-\gamma)^3}\Big), \tag{B.62}$$

since

$$\frac{1}{1-\rho} = \frac{1+\sqrt{1-c(1-\gamma)}}{[1-\sqrt{1-c(1-\gamma)}][1+\sqrt{1-c(1-\gamma)}]} = \frac{1+\sqrt{1-c(1-\gamma)}}{c(1-\gamma)} \le \frac{2}{c(1-\gamma)}.$$

It remains to prove (B.59). Toward that end, notice that the left-hand-side of (B.59) can be represented by

$$\sup_{\substack{\beta_1\in\mathbb{R}^{mL}:\|\beta_1\|_2=1\\ \beta_2\in\mathbb{R}^{mL}:\|\beta_2\|_2=1}} \left\|\gamma\beta_1^\top \frac{\Sigma_{[T_1,T_2]}^{-1/2}}{T_2-T_1}\sum_{t=T_1}^{T_2-1}\mathbb{E}\phi_L(A_t,S_t)\phi_L^\top(\pi^{opt}(S_{t+1}),S_{t+1})\Sigma_{[T_1,T_2]}^{-1/2}\beta_2\right\|_2.$$

It follows from the Cauchy-Schwarz inequality that the ℓ_2 norm of in the above expression can be upper bounded by

$$\begin{aligned}&\frac{\gamma}{T_2-T_1}\sum_{t=T_1}^{T_2-1}\mathbb{E}|\beta_1^\top\Sigma_{[T_1,T_2]}^{-1/2}\phi_L(A_t,S_t)||\phi_L^\top(\pi^{opt}(S_{t+1}),S_{t+1})\Sigma_{[T_1,T_2]}^{-1/2}\beta_2|\\ &\qquad\le\gamma\sqrt{\frac{1}{T_2-T_1}\sum_{t=T_1}^{T_2-1}\mathbb{E}|\beta_1^\top\Sigma_{[T_1,T_2]}^{-1/2}\phi_L(A_t,S_t)|^2}\\ &\qquad\times\sqrt{\frac{1}{T_2-T_1}\sum_{t=T_1}^{T_2-1}\mathbb{E}|\phi_L^\top(\pi^{opt}(S_{t+1}),S_{t+1})\Sigma_{[T_1,T_2]}^{-1/2}\beta_2|^2}.\end{aligned}$$

By the definition of $\Sigma_{[T_1,T_2]}$, the second line equals γ. Hence, to prove (B.59), it suffices to show the maximum eigenvalue of the matrix

$$\frac{\gamma^2}{T_2-T_1}\Sigma_{[T_1,T_2]}^{-1/2}\sum_{t=T_1}^{T_2-1}\Big[\mathbb{E}\phi_L(\pi^{opt}(S_{t+1}),S_{t+1})\phi_L^\top(\pi^{opt}(S_{t+1}),S_{t+1})\Big]\Sigma_{[T_1,T_2]}^{-1/2} \tag{B.63}$$

is strictly smaller than 1, or equivalently, the matrix

$$\frac{\Sigma_{[T_1,T_2]}^{-1/2}}{T_2-T_1}\sum_{t=T_1}^{T_2-1}\Big[\mathbb{E}\phi_L(A_t,S_t)\phi_L^\top(A_t,S_t)-\gamma^2\mathbb{E}\phi_L(\pi^{opt}(S_{t+1}),S_{t+1})\phi_L^\top(\pi^{opt}(S_{t+1}),S_{t+1})\Big]\Sigma_{[T_1,T_2]}^{-1/2}$$

is positive semi-definite. The latter condition is implied by (B.4), the boundedness of p_t and A5(ii), which suggest that (i) the maximum eigenvalue of $\Sigma_{[T_1,T_2]}$ is bounded away from infinity, or equivalently, the minimum eigenvalue of $\Sigma_{[T_1,T_2]}^{-1}$ is bounded away from zero, and (ii) the minimum eigenvalue of the matrix

$$\frac{1}{T_2-T_1}\sum_{t=T_1}^{T_2-1}\Big[\mathbb{E}\phi_L(A_t,S_t)\phi_L^\top(A_t,S_t)-\gamma^2\mathbb{E}\phi_L(\pi^{opt}(S_{t+1}),S_{t+1})\phi_L^\top(\pi^{opt}(S_{t+1}),S_{t+1})\Big]$$

is lower bounded by $C(1-\gamma)$ for some constant $C>0$. Consequently, the maximum eigenvalue of (B.63) is upper bounded by $1-c(1-\gamma)$ for some constant $c>0$. This completes the proof of (B.59).

To summarize, so far, we have shown that

$$\phi_L^\top(a,s)\beta^* = \sum_{j=1}^{k} \gamma^{j-1}\phi_L^\top(a,s)\mathcal{P}^{j-1}\beta_r + \gamma^k \phi_L^\top(a,s)\mathcal{P}^k\beta^* + O\Big(\frac{L^{-p/d}}{(1-\gamma)^3}\Big), \tag{B.64}$$

by (B.57) and (B.62).

Next, we aim to obtain a similar expression for $\beta^{(k)}$. Let m_0 denote the margin defined in A7. Under the condition on ϵ in A1 and that on L in A9, it follows from the uniform rate of convergence derived in the finite-sample analysis and the condition $K \gg \log(NT)$ that

$$\mathbb{P}\Big(\max_{k\geq K/2}\max_{(T_1,T_2):T_2-T_1\geq \epsilon T}\sup_{a,s}|\phi_L^\top(a,s)\beta^{(k)} - Q^{opt}(a,s)| \leq \frac{m_0}{3}\Big) \geq 1 - O\Big(\frac{1}{NT}\Big). \tag{B.65}$$

Under the event defined in (B.65), it follows from the uniqueness of the optimal policy (see A6) that

$$\begin{aligned} &\phi_L^\top(\pi^{opt}(s),s))\widehat{\beta}_{[T_1,T_2]} - \max_{a\neq\pi^{opt}(s)}\phi_L^\top(a,s))\widehat{\beta}_{[T_1,T_2]} \\ \geq\ & Q^{opt}(\pi^{opt}(s),s) - \max_{a\neq\pi^{opt}(s)} Q^{opt}(a,s) - \frac{2m_0}{3} \geq \frac{m_0}{3}, \end{aligned}$$

for any a, s, T_1 and T_2. This leads to

$$\pi^{opt}(s) = \pi_{\beta^{(k)}}(s) = \arg\max_a \phi_L^\top(a,s)\beta^{(k)}, \qquad \forall k \geq K/2, \tag{B.66}$$

with probability $1 - O(N^{-1}T^{-1})$. On the event defined in (B.66), it follows from the definition of $\beta^{(k)}$ (see (B.50)) that

$$\begin{aligned} \beta^{(k)} =& \underbrace{\sum_{i=1}^{N}\sum_{t=T_1}^{T_2-1}\frac{\widehat{\Sigma}^{-1}_{[T_1,T_2]}}{N(T_2-T_1)}\phi_L(A_{i,t},S_{i,t})R_{i,t}}_{\widehat{\beta}_r} \\ +\ & \underbrace{\gamma\sum_{i=1}^{N}\sum_{t=T_1}^{T_2-1}\frac{\widehat{\Sigma}^{-1}_{[T_1,T_2]}}{N(T_2-T_1)}\phi_L(A_{i,t},S_{i,t})\phi_L^\top(\pi^{opt}(S_{i,t+1}),S_{i,t+1})}_{\widehat{\mathcal{P}}}\,\beta^{(k-1)}, \end{aligned}$$

for all $k > K/2$. By iteratively applying this argument, we obtain that $\beta^{(K)} = \sum_{k=1}^{K/2}\gamma^{k-1}\widehat{\mathcal{P}}^{k-1}\widehat{\beta}_r + \gamma^{K/2}\widehat{\mathcal{P}}^{K/2}\beta^{(K/2)}$ and hence

$$\phi_L^\top(a,s)\beta^{(K)} = \sum_{k=1}^{K/2}\gamma^{k-1}\phi_L^\top(a,s)\widehat{\mathcal{P}}^{k-1}\widehat{\beta}_r + \gamma^{K/2}\phi_L^\top(a,s)\widehat{\mathcal{P}}^{K/2}\beta^{(K/2)}.$$

In view of (B.64), we obtain that

$$\begin{aligned}\phi_L^\top(a,s)(\beta^{(K)}-\beta^*) &= \sum_{k=1}^{K/2}\gamma^{k-1}\phi_L^\top(a,s)(\widehat{\mathcal{P}}^{k-1}\widehat{\beta}_r-\mathcal{P}^{k-1}\beta_r)\\ &+\gamma^{K/2}\phi_L^\top(a,s)(\widehat{\mathcal{P}}^{K/2}\beta^{(K/2)}-\mathcal{P}^{K/2}\beta^*)+O\Big(\frac{L^{-p/d}}{(1-\gamma)^3}\Big).\end{aligned} \tag{B.67}$$

Using similar arguments to the proof of (B.59), it can be shown that $\|\gamma\Sigma_{[T_1,T_2]}^{1/2}\widehat{\mathcal{P}}\Sigma_{[T_1,T_2]}^{-1/2}\|_2$ is also strictly smaller than 1, with probability at least $1-O(N^{-1}T^{-1})$. As $K\gg\log(NT)$ (Assumption A8) and $\beta^{(k)}$s are bounded (see (B.54)), $\beta^{(K/2)}$ in the first term on the second line of (B.67) can be replaced with β^*, and the resulting error can be made arbitrarily small, specifically of the order $O((NT)^{-c})$ for any sufficiently large constant $c>0$. In view of the condition on L in A9, we obtain that

$$\begin{aligned}\phi_L^\top(a,s)(\beta^{(K)}-\beta^*) &= \sum_{k=1}^{K/2}\gamma^{k-1}\phi_L^\top(a,s)(\widehat{\mathcal{P}}^{k-1}\widehat{\beta}_r-\mathcal{P}^{k-1}\beta_r)\\ &+\gamma^{K/2}\phi_L^\top(a,s)(\widehat{\mathcal{P}}^{K/2}\beta^*-\mathcal{P}^{K/2}\beta^*)+O\Big(\frac{L^{-p/d}}{(1-\gamma)^3}\Big).\end{aligned}$$

With some calculations, the first two terms on the RHS can be shown to equal

$$\sum_{k=1}^{K/2}\gamma^{k-1}\phi_L^\top(a,s)(\widehat{\mathcal{P}}^{k-1}\widehat{\alpha}_r-\mathcal{P}^{k-1}\alpha_r) \tag{B.68}$$

where

$$\begin{aligned}\widehat{\alpha}_r &= \sum_{i=1}^{N}\sum_{t=T_1}^{T_2-1}\frac{\widehat{\Sigma}_{[T_1,T_2]}^{-1}}{N(T_2-T_1)}\phi_L(A_{i,t},S_{i,t})[R_{i,t}+\gamma\phi_L^\top(\pi^{opt}(S_{i,t+1}),S_{i,t+1})\beta^*-\phi_L^\top(A_{i,t},S_{i,t})\beta^*],\\ \alpha_r &= \sum_{t=T_1}^{T_2-1}\frac{\Sigma_{[T_1,T_2]}^{-1}}{T_2-T_1}\mathbb{E}\phi_L(A_t,S_t)[R_t+\gamma\phi_L^\top(\pi^{opt}(S_{t+1}),S_{t+1})\beta^*-\phi_L^\top(A_t,S_t)\beta^*].\end{aligned}$$

Using similar arguments in bounding the rightmost reminder term in (B.57), it can be show that $\sup_{a,s}|\phi_L^\top(a,s)\alpha_r|=O((1-\gamma)^{-2}L^{-p/d})$ and $\sup_{a,s}|\phi_L^\top(a,s)\sum_k\gamma^{k-1}\mathcal{P}^{k-1}\alpha_r|=O((1-\gamma)^{-3}L^{-p/d})$. Similarly, we can further replace $\widehat{\alpha}_r$ in (B.68) with

$$\widehat{\alpha}_r^*=\sum_{i=1}^{N}\sum_{t=T_1}^{T_2-1}\frac{\widehat{\Sigma}_{[T_1,T_2]}^{-1}}{N(T_2-T_1)}\phi_L(A_{i,t},S_{i,t})\delta_{i,t}^*,$$

with the approximation error upper bounded by $O((1-\gamma)^{-3}L^{-p/d})$, where we recall that $\delta_{i,t}^*$ denotes the temporal difference error $R_{i,t}+\gamma Q^{opt}(\pi^{opt}(S_{i,t+1}),S_{i,t+1})-Q^{opt}(A_{i,t},S_{i,t})$. It

follows that

$$\phi_L^\top(a,s)(\beta^{(K)}-\beta^*)=\sum_{k=1}^{K/2}\gamma^{k-1}\phi_L^\top(a,s)\widehat{\mathcal{P}}^{k-1}\widehat{\alpha}_r^*+O\Big(\frac{L^{-p/d}}{(1-\gamma)^3}\Big).$$

Meanwhile, using similar arguments to bounding $\|\beta^{(k)*}-\beta^{(k)}-I_1\|_2$ in the finite-sample analysis, we can further approximate the leading term in the above expression by

$$\sum_{k=1}^{K/2}\gamma^{k-1}\phi_L^\top(a,s)\mathcal{P}^{k-1}\widehat{\alpha}_r^{**},$$

with the approximation error bounded by $O((1-\gamma)^{-3}L^{3/2}\log(NT)/(\epsilon NT))$, where

$$\widehat{\alpha}_r^{**}=\sum_{i=1}^{N}\sum_{t=T_1}^{T_2-1}\frac{\Sigma_{[T_1,T_2]}^{-1}}{N(T_2-T_1)}\phi_L(A_{i,t},S_{i,t})\delta_{i,t}^*.$$

Now, the assertion in (B.8) can be readily obtained by noting that the matrix $\sum_{k=1}^{K/2}\gamma^{k-1}\mathcal{P}^{k-1}$ can be well-approximated by $(I-\gamma\mathcal{P})^{-1}$, and that $\sup_{a,s}|\phi_L^\top(a,s)\beta^*-Q^{opt}(a,s)|=O((1-\gamma)^{-2}L^{-p/d})$.

B.4 Proof of Lemma B.3

We focus on establishing a uniform upper error bound for $\{\|\widehat{W}_{[T_1,T_2]}-W_{[T_1,T_2]}\|_2: T_2-T_1\geq\epsilon T\}$ in this section. The assertion that $\|W_{[T_1,T_2]}^{-1}\|_2\leq\bar{c}(1-\gamma)^{-1}$ can be proven by Lemma 3 of Shi et al. [2022].

In Step 3 of the proof of Theorem 4.1, we have shown that $\arg\max_a\phi_L^\top(a,s)\widehat{\beta}_{[T_1,T_2]}=\arg\max_a Q^{opt}(a,s)$ and hence $\pi_{\widehat{\beta}_{[T_1,T_2]}}=\pi^{opt}$, WPA1. It follows that

$$\widehat{W}_{[T_1,T_2]}=\frac{1}{N(T_2-T_1)}\sum_{i=1}^{N}\sum_{t=T_1}^{T_2-1}\phi_L(A_{i,t},S_{i,t})\{\phi_L(A_{i,t},S_{i,t})-\gamma\phi_L(\pi^{opt}(S_{i,t+1}),S_{i,t+1})\}^\top \quad \text{(B.69)}$$

We next provide an upper bound on the difference between the RHS of (B.69) and $W_{[T_1,T_2]}$. Define $\widehat{W}^*_{[T_1,T_2]}$ as

$$\frac{1}{N(T_2-T_1)}\sum_{i=1}^{N}\sum_{t=T_1}^{T_2-1}\sum_{a}\pi^b(a|S_{i,t})\phi_L(a,S_{i,t})[\phi_L(a,S_{i,t})-\gamma\mathbb{E}\{\phi_L(\pi^{opt}(S_{i,t+1}),S_{i,t+1})|A_{i,t}=a,S_{i,t}\}]^\top.$$

The difference $\|\widehat{W}_{[T_1,T_2]}-W_{[T_1,T_2]}\|_2$ can be upper bounded by $\|\widehat{W}_{[T_1,T_2]}-\widehat{W}^*_{[T_1,T_2]}\|_2+\|\widehat{W}^*_{[T_1,T_2]}-W_{[T_1,T_2]}\|_2$.

Under the conditional mean independent assumption on the reward (2.1), the first term $\widehat{W}_{[T_1,T_2]}-\widehat{W}^*_{[T_1,T_2]}$ corresponds to a sum of martingale difference. Using similar arguments

to the proof of Lemma 3 of Shi et al. [2022], we can show that the first term is of the order $O(\sqrt{(\epsilon NT)^{-1}L\log(NT)})$, with probability at least $1-O\{(NT^{-3})\}$, under the condition that $T_2 - T_1 \geq \epsilon T$. See also, Freedman's inequality for matrix martingales developed by Tropp [2011]. It follows from Bonferroni's inequality that $\sup_{T_1,T_2} \|\widehat{W}_{[T_1,T_2]} - \widehat{W}^*_{[T_1,T_2]}\|_2 = O(\sqrt{(\epsilon NT)^{-1}L\log(NT)})$, with probability at least $1-O\{(NT)^{-1}\}$.

It remains to bound $\|\widehat{W}^*_{[T_1,T_2]} - W_{[T_1,T_2]}\|_2$. Let Γ_0 be an ε-net of the unit sphere in $\mathbb{R}^L$ that satisfies the following: for any $\nu \in \mathbb{R}^L$ with unit ℓ_2 norm, there exists some $\nu_0 \in \Gamma_0$ such that $\|\nu - \nu_0\|_2 \leq \varepsilon$. Set $\varepsilon = (NT)^{-2}$. According to Lemma 2.3 of Mendelson et al. [2008], there exists such an ε-net Γ_0 that belongs to the unit sphere and satisfies $|\Gamma_0| \leq 5^L(NT)^{2L}$.

For any ν_1, ν_2 with unit ℓ_2 norm, define

$$\Psi_t(a,s,\nu_1,\nu_2) = \pi_t^b(a|s)\nu_1^\top \phi_L(a,s)[\phi_L(a,s) - \gamma\mathbb{E}\{\phi_L(\pi^{opt}(S_{t+1}),S_{t+1})|A_t=a,S_t=s\}]^\top\nu_2.$$

The difference $\|\widehat{W}^*_{[T_1,T_2]} - W_{[T_1,T_2]}\|_2$ can be represented as

$$\sup_{\|\nu_1\|_2=\|\nu_2\|_2=1}\left|\frac{1}{N(T_2-T_1)}\sum_{i=1}^{N}\sum_{t=T_1}^{T_2-1}\sum_a\{\Psi_t(a,S_{i,t},\nu_1,\nu_2) - \mathbb{E}\Psi_t(a,S_{i,t},\nu_1,\nu_2)\}\right|.$$

We first show that $\Psi_t(a,s,\nu_1,\nu_2)$ is a Lipschitz continuous function of ν_1 and ν_2. For any ν_1,ν_2,ν_3,ν_4, the difference $\Psi_t(a,s,\nu_1,\nu_2) - \Psi_t(a,s,\nu_3,\nu_4)$ can be decomposed into the sum of the following two terms:

$$\begin{aligned}&\pi_t^b(a|s)(\nu_1-\nu_3)^\top\phi_L(a,s)[\phi_L(a,s) - \gamma\mathbb{E}\{\phi_L(\pi^{opt}(S_{t+1}),S_{t+1})|A_t=a,S_t=s\}]^\top\nu_2\\ +&\pi_t^b(a|s_2)\nu_3^\top\phi_L(a,s)[\phi_L(a,s) - \gamma\mathbb{E}\{\phi_L(\pi^{opt}(S_{t+1}),S_{t+1})|A_t=a,S_t=s\}]^\top(\nu_2-\nu_4).\end{aligned}$$

The first term is $O(L)\|\nu_1-\nu_3\|_2$ according to (B.5). Similarly, the second term is $O(L\|\nu_2-\nu_4\|_2)$. To summarize, we have shown that

$$|\Psi_t(a,s_1,\nu_1,\nu_2) - \Psi_t(a,s_2,\nu_3,\nu_4)| \leq cL(\|\nu_1-\nu_3\|_2 + \|\nu_2-\nu_4\|_2),$$

for some constant $c>0$.

For any ν_1,ν_2 with unit ℓ_2-norm, there exist $\nu_{1,0},\nu_{2,0} \in \Gamma_0$ that satisfy $\|\nu_1-\nu_{1,0}\|_2 \leq \varepsilon$ and $\|\nu_2-\nu_{2,0}\|_2 \leq \varepsilon$. As such, $\Psi_t(a,s_1,\nu_1,\nu_2) - \Psi_t(a,s_2,\nu_1,\nu_2)$ can be upper bounded by

$$\sup_{\nu_{1,0},\nu_{2,0}\in\Gamma_0}\left|\frac{1}{N(T_2-T_1)}\sum_{i=1}^{N}\sum_{t=T_1}^{T_2-1}\sum_a\{\Psi_t(a,S_{i,t},\nu_{1,0},\nu_{2,0}) - \mathbb{E}\Psi_t(a,S_{i,t},\nu_{1,0},\nu_{2,0})\}\right| + \frac{2cL}{(NT)^2}.$$

It remains to establish a uniform upper bound for the first term. We aim to apply the concentration inequality developed by Alquier et al. [2019]. However, a direct application of Theorem 3.1 in Alquier et al. [2019] would yield a sub-optimal bound. This is because each summand $\Psi_t(a,S_t,\nu_{1,0},\nu_{2,0})$ is not bounded, since $\|\phi_L\|_2$ is proportional to $L^{1/2}$. To obtain a

sharper bound, we further decompose the first term into the sum of the following two terms:

$$\sup_{\nu_{1,0},\nu_{2,0}\in\Gamma_0}\left|\frac{1}{N(T_2-T_1)}\sum_{i=1}^{N}\sum_{t=T_1}^{T_2-1}\sum_{a}[\Psi_t(a,S_{i,t},\nu_{1,0},\nu_{2,0})-\mathbb{E}\{\Psi_t(a,S_{i,t},\nu_{1,0},\nu_{2,0})|S_{i,t-1}\}]\right| \\ +\sup_{\nu_{1,0},\nu_{2,0}\in\Gamma_0}\left|\frac{1}{N(T_2-T_1)}\sum_{i=1}^{N}\sum_{t=T_1}^{T_2-1}\sum_{a}[\mathbb{E}\{\Psi_t(a,S_{i,t},\nu_{1,0},\nu_{2,0})|S_{i,t-1}\}-\mathbb{E}\Psi_t(a,S_{i,t},\nu_{1,0},\nu_{2,0})]\right|. \tag{B.70}$$

The first term corresponds to a sum of martingale difference. Using similar arguments in showing $\sup_{T_1,T_2}\|\widehat{W}_{[T_1,T_2]}-\widehat{W}^*_{[T_1,T_2]}\|_2=O(\sqrt{(\epsilon NT)^{-1}L\log(NT)})$, we can show that the first term in (B.70) is of the order $O(\sqrt{(\epsilon NT)^{-1}L\log(NT)})$, with probability at least $1-O(N^{-1}T^{-1})$, where the big-O term is uniform in $\{(T_1,T_2):T_2-T_1\geq\epsilon T\}$.

As for the second term, notice that by definition, $\mathbb{E}\{\Psi_t(a,S_t,\nu_{1,0},\nu_{2,0})|S_{t-1}=s\}$ equals

$$\int_{s'}\pi_t^b(a|s')\nu_{1,0}^\top\phi_L(a,s')[\phi_L(a,s')-\gamma\mathbb{E}\{\phi_L(\pi^{opt}(S_{t+1}),S_{t+1})|A_t=a,S_t=s'\}]^\top\nu_{2,0}p_{t-1}(s'|a,s)ds'.$$

Given that $p_t(s'|a,\bullet)$s are Lipschitz continuous on $\mathcal{S}$, $\mathbb{E}\{\Psi_t(a,S_t,\nu_{1,0},\nu_{2,0})|S_{t-1}=s\}$ is a Lipschitz continuous function of s. However, unlike $\Psi_t(a,s,\nu_{1,0},\nu_{2,0})$, the integrand

$$|\pi_t^b(a|s')\nu_{1,0}^\top\phi_L(a,s')[\phi_L(a,s')-\gamma\mathbb{E}\{\phi_L(\pi^{opt}(S_{t+1}),S_{t+1})|A_t=a,S_t=s'\}]^\top\nu_{2,0}|$$

is upper bounded by a constant; see e.g., Equation (E.77) of Shi et al. [2022]. As such, the Lipschitz constant is uniformly bounded by some constant. Consequently, the conditions in the statement of Theorem 3.1 in Alquier et al. [2019] are satisfied. We can apply Theorem 3.1 to the mean zero random variable

$$\frac{1}{N(T_2-T_1)}\sum_{i=1}^{N}\sum_{t=T_1}^{T_2-1}\sum_{a}[\mathbb{E}\{\Psi_t(a,S_{i,t},\nu_{1,0},\nu_{2,0})|S_{i,t-1}\}-\mathbb{E}\Psi_t(a,S_{i,t},\nu_{1,0},\nu_{2,0})],$$

for each combination of $\nu_{1,0},\nu_{2,0},T_1,T_2$, and show that it is of the order $O(\sqrt{\epsilon L(NT)^{-1}\log(NT)})$ with probability at least $1-O(N^{-CL}T^{-CL})$, for some sufficiently large constant $C>0$. By Bonferroni's inequality, we can show that

$$\sup_{T_2-T_1\geq\epsilon T}\sup_{\nu_{1,0},\nu_{2,0}\in\Gamma_0}\left|\frac{1}{N(T_2-T_1)}\sum_{i=1}^{N}\sum_{t=T_1}^{T_2-1}\sum_{a}[\Psi_t(a,S_{i,t},\nu_{1,0},\nu_{2,0})-\mathbb{E}\{\Psi_t(a,S_{i,t},\nu_{1,0},\nu_{2,0})|S_{i,t-1}\}]\right|,$$

is upper bounded by $O(\sqrt{L\epsilon^{-1}(NT)^{-1}\log(NT)})$ with probability at least $1-O(N^{-1}T^{-1})$.

B.5 Proof of Theorem 4.2

Without loss of generality, assume $T_0 = 0$. We first consider the ℓ_1-type test. Under the given conditions on T^*, we have

$$\begin{aligned} \text{TS}_1 &\geq \sqrt{\frac{T^*(T-T^*)}{T^2}} \left\{ \frac{1}{NT} \sum_{i,t} |\widehat{Q}_{[0,T^*]}(A_{i,t}, S_{i,t}) - \widehat{Q}_{[T^*,T]}(A_{i,t}, S_{i,t})| \right\} \\ &\geq \sqrt{\epsilon(1-\epsilon)} \left\{ \frac{1}{NT} \sum_{i,t} |\widehat{Q}_{[0,T^*]}(A_{i,t}, S_{i,t}) - \widehat{Q}_{[T^*,T]}(A_{i,t}, S_{i,t})| \right\}. \end{aligned} \tag{B.71}$$

Similar to Lemma B.2, we can show that

$$\sup_{a,s} \max(|\widehat{Q}_{[0,T^*]}(a,s) - Q_0^{opt}(a,s)|, |\widehat{Q}_{[T^*,T]}(a,s) - Q_T^{opt}(a,s)|) = O(\kappa), \tag{B.72}$$

where we recall that $\kappa = (1-\gamma)^{-2}(L^{-p/d} + \sqrt{L(\epsilon NT)^{-1}\log(NT)})$. This together with (B.71) yields that

$$\begin{aligned} \text{TS}_1 \geq\ & \sqrt{\epsilon(1-\epsilon)} \frac{1}{NT} \sum_{i=1}^{N} \sum_{t=0}^{T-1} |Q_0^{opt}(A_{i,t}, S_{i,t}) - Q_T^{opt}(A_{i,t}, S_{i,t})| \\ & + \sqrt{\epsilon(1-\epsilon)} O\Big(\frac{\sqrt{L\log(NT)}}{(1-\gamma)^2 \sqrt{\epsilon NT}} \Big) + \sqrt{\epsilon(1-\epsilon)} O\Big(\frac{L^{-p/d}}{(1-\gamma)^2} \Big), \end{aligned} \tag{B.73}$$

with probability at least $1 - O(N^{-1}T^{-1})$. Using similar arguments to proving the size property of the ℓ_1-type test in Section B.2, we can show that

$$\begin{aligned} & \frac{1}{T} \sum_{t=0}^{T-1} \sum_{a} \int_s |Q_0^{opt}(a,s) - Q_T^{opt}(a,s)| \pi_t^b(a|s) p_t^b(s) ds \\ =\ & \frac{1}{NT} \sum_{i=1}^{N} \sum_{t=0}^{T-1} |Q_0^{opt}(A_{i,t}, S_{i,t}) - Q_T^{opt}(A_{i,t}, S_{i,t})| + O\Big(\frac{\sqrt{\log(NT)}}{(1-\gamma)NT} \Big), \end{aligned}$$

with probability at least $1 - O(N^{-1}T^{-1})$, which together with (B.73) leads to

$$\begin{aligned} \text{TS}_1 \geq\ & \frac{\sqrt{\epsilon(1-\epsilon)}}{T} \sum_{t=0}^{T-1} \sum_{a} \int_s |Q_0^{opt}(a,s) - Q_T^{opt}(a,s)| \pi_t^b(a|s) p_t^b(s) ds \\ & + O\Big(\frac{\sqrt{L(NT)^{-1}\log(NT)}}{(1-\gamma)^2} \Big) + O\Big(\frac{\sqrt{\epsilon} L^{-p/d}}{(1-\gamma)^2} \Big), \end{aligned}$$

with probability at least $1 - O(N^{-1}T^{-1})$. In addition, using similar arguments to the proof of Theorem 4.1, we can show that the bootstrapped test statistic TS_1^b is upper bounded by $O((1-\gamma)^{-2}\sqrt{L(NT)^{-1}\log(NT)})$, with probability at least $1 - O(N^{-1}T^{-1})$. Under the given

condition on Δ_1, TS_1 is much larger than the upper αth quantile of TS_1^b, with probability at least $1 - O(N^{-1}T^{-1})$. As such, the power of the proposed test is at least $1 - O(N^{-1}T^{-1})$ under the alternative hypothesis. This completes the proof for the ℓ_1-type test.

The power property of the unnormalized maximum-type test can be similarly established based on (B.72).

Finally, notice that the normalized test requires a weaker condition to detect the alternative hypothesis. This is due to normalization, which makes its bootstrapped test statistic upper bounded by $O(\sqrt{\log(NT)})$, as opposed to $O(\sqrt{L\log(NT)})$, with probability at least $1 - O(N^{-1}T^{-1})$; see the proof of the size property of the normalized test in Section B.2. Additionally, the normalized estimation error divided by the variance estimator

$$\frac{1}{\widehat{\sigma}_{T^*}(a,s)} \max(|\widehat{Q}_{[0,T^*]}(a,s) - Q_0^{opt}(a,s)|, |\widehat{Q}_{[T^*,T]}(a,s) - Q_T^{opt}(a,s)|),$$

can be upper bounded by $O(\sqrt{\log(NT)}) + O(\widehat{\sigma}_{T^*}^{-1}(a,s)L^{-p/d})$, with probability at least $1 - O(N^{-1}T^{-1})$ where the probability upper bound is uniform in a and s. Using similar arguments in proving of the size property of the normalized test in Section B.2, we can show that $\widehat{\sigma}_{T^*}(a,s)$ can be upper bounded by $\sqrt{L}(1-\gamma)^{-2}(\epsilon NT)^{-1/2}$. The proof is hence completed under the given condition on the signal strength.

C More on the numerical study

C.1 Implementation Details

To implement the proposed tests, the boundary removal parameter ϵ is set to 0.1; 2000 bootstrap samples are generated to compute p-values. The discount factor γ is chosen from $\{0.9, 0.95\}$. In our simulations, the state variables are continuous. We set the basis function Φ_L (see (3.4)) to the random Fourier features following the Random Kitchen Sinks (RKS) algorithm [Rahimi and Recht, 2007], using `RBFsampler` function from the Python `scikit-learn` module for implementation. The bandwidth in the radial basis function (RBF) kernel is selected according to the median heuristic [Garreau et al., 2017]. The number of basis functions L is selected via 5-fold cross-validation. Specifically, we first divide all data trajectories into 5 non-overlapping equal-sized data subsets. Let $\mathcal{I}_f$ denote the f-th subsample and $\mathcal{I}_f^c$ denote its complement, $f = 1, 2, 3, 4, 5$. For each combination of f, L and the specified data interval $[T_1, T_2]$, we use FQI to compute an estimated optimal Q-function $\widehat{Q}_{f,L,[T_1,T_2]}$ using L basis functions based on the data subsets in $\mathcal{I}_f^c \times [T_1, T_2]$. We next select L that minimizes the FQI objective function,

$$\sum_{f=1}^{5} \sum_{i \in \mathcal{I}_f} \sum_{t=T_1}^{T_2-1} \left\{ R_{i,t} + \gamma \max_a \widehat{Q}_{f,L,[T_1,T_2]}(a, S_{i,t+1}) - \widehat{Q}_{f,L,[T_1,T_2]}(A_{i,t}, S_{i,t}) \right\}^2. \tag{C.1}$$

When the data is stationary over $[T_1, T_2]$, this criterion balances off the bias and standard deviation of the Q-function estimator.

To mitigate the randomness introduced by the random Fourier features, for each of the 100 simulation replications, we repeat our tests four times with different random seeds. This yields p-values $\{p_r, r = 1, \ldots, 4\}$. We then employ the method developed by Meinshausen et al. [2009] to combine these p-values by defining

$$p_0 = \min\left(1, q_\tau\left\{\tau^{-1}p_r, r = 1, \ldots, 4\right\}\right), \tag{C.2}$$

to be the final p-value. Here, τ is some constant between 0 and 1, and q_τ is the empirical τ-quantile of the p-values. Compared to using a single set of Fourier features, such an aggregation method reduces the type I error and increases the power of the resulting test. Our simulation results hardly change under $\tau = 0.05, 0.1, 0.15, 0.2$; hereafter, we report results under $\tau = 0.1$. All tests are conducted at significance level $\alpha = 0.05$.

C.2 Four Synthetic Nonstationary Settings

The way we generate a smooth transition function is to first define a piecewise constant function, and smoothly connects the constant functions through a transformation. Specifically, let the piecewise constant function with two segments be $f(s,t) = f_1(s)I\{t \le T^*\} + f_2(s)I\{t > T^*\}$, where f_1 and f_2 are functions not dependent on t.

We now introduce a smooth transformation $\phi(s) = \frac{\psi(s)}{\psi(s)+\psi(1-s)}$, where $\psi(s) = e^{-1/s}I\{s > 0\}$. Then $g(s; f_1, f_2, s_0, s_1) := f_1(s) + (f_2(s) - f_1(s))\phi\left(\frac{s-s_0}{s_1-s_0}\right)$ is a smooth function from f_1 to f_2 on the interval $[s_0, s_1]$. In addition, the transformed function $\widetilde{f}(s,t) = f_1(s)I\{t \le T^* - \delta T\} + g(s; f_1, f_2, s_0, s_1)I\{T^* - \delta T < t < T^* + \delta T\} + f_2(s)I\{t > T^*\}$ is smooth in s. Here δ controls the smoothness of the transformation; smaller δ leads to more abrupt change and larger δ leads to smoother change. An example of $\widetilde{f}(s,t)$ is shown in Figure C.1.

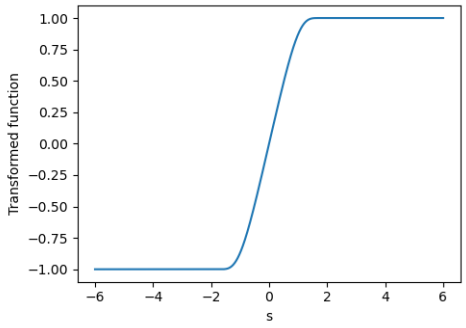

Figure C.1: Smooth transformation of piecewise constant function: $f_1(s) = -I\{s \le -2\}$ and $f_2(s) = I\{s \ge 2\}$.

The four simulations settings in Section 5.1 are specified as the following.

(1) Time-homogeneous state transition function and piecewise constant reward function:

$$S_{0,t+1} = 0.5A_{0,t}S_{0,t} + z_{0,t}, t \in [0, T].$$

$$R_{0,t} = \begin{cases} r_1(S_{0,t}, A_{0,t}; t) \equiv -1.5 A_{0,t} S_{0,t}, & \text{if } t \in [0, T^*) \\ r_2(S_{0,t}, A_{0,t}; t) \equiv A_{0,t} S_{0,t}, & \text{if } t \in [T^*, T], \end{cases}$$

(2) Time-homogeneous state transition function and smooth reward function:

$$S_{0,t+1} = 0.5 A_{0,t} S_{0,t} + z_{0,t}, t \in [0, T].$$

$$R_{0,t} = \begin{cases} r_1(S_{0,t}, A_{0,t}; t), & \text{if } t \in [0, T^* - \delta T), \\ g\left(S_{0,t}; r_1, r_2, T^* - \delta T, T^*\right), & \text{if } t \in [T^* - \delta T, T^*), \\ r_2(S_{0,t}, A_{0,t}; t), & \text{if } t \in [T^*, T]. \end{cases}$$

(3) Piecewise constant state transition and time-homogeneous reward function:

$$S_{0,t+1} = \begin{cases} F_1(S_{0,t}, A_{0,t}; t) \equiv -0.5 A_{0,t} S_{0,t} + z_{0,t}, & \text{if } t \in [0, T^*), \\ F_2(S_{0,t}, A_{0,t}; t) \equiv 0.5 A_{0,t} S_{0,t} + z_{0,t}, & \text{if } t \in [T^*, T]. \end{cases}$$

$$R_{0,t} = 0.25 A_{0,t} S_{0,t}^2 + 4 S_{0,t}, t \in [0, T].$$

(4) Smooth state transition and time-homogeneous reward function:

$$S_{0,t+1} = \begin{cases} F_1(S_{0,t}, A_{0,t}; t), & \text{if } t \in [0, T^*), \\ g\left(S_{0,t}; F_1, F_2, T^* - \delta T, T^*\right), & \text{if } t \in [T^* - \delta T, T^*), \\ F_2(S_{0,t}, A_{0,t}; t), & \text{if } t \in [T^*, T]. \end{cases}$$

$$R_{0,t} = 0.25 A_{0,t} S_{0,t}^2 + 4 S_{0,t}, t \in [0, T].$$

C.3 Details of Baseline Methods

MBCD The MBCD method tests whether $\tau \in [T_0, T_1]$ is a change point on the batch data collected on the interval $[T_0, T_1]$. Specifically, denote the conditional distribution of the next state and the current reward given the current state-action pair as $p_\theta(S_{i,t+1}, R_{i,t} \mid S_{i,t}, A_{i,t})$, where θ is a vector of model parameters. We let the parameter of the distribution of data on the left interval $[T_0, \tau]$ be θ_l, and that of data on the right interval $[\tau, T_1]$ be θ_r. The test statistic is computed as $W_\tau = \max\left\{0, \log \frac{p_{\theta_l}(S_{i,t+1}, R_{i,t} | S_{i,t}, A_{i,t}; t \in [T_0, \tau])}{p_{\theta_r}(S_{i,t+1}, R_{i,t} | S_{i,t}, A_{i,t}; t \in [\tau, T_1])}\right\}$. We reject the null hypothesis if $W_\tau > h$, where the threshold $h = |\log \alpha|$ is chosen to ensure that the false alarm rate is no larger than α. In our implementation, we specify $h = 100$ such that $\alpha \approx 10^{-43}$ is negligible.

To model the conditional distribution, we parameterize the conditional distribution $p_\theta(S_{i,t+1}, R_{i,t} | S_{i,t}, A_{i,t})$, using a multivariate normal distribution $\mathcal{N}\left(\mu(S_{i,t}, A_{i,t}), \Sigma(S_{i,t}, A_{i,t})\right)$. The parameter θ contains the mean $\mu(S_{i,t}, A_{i,t})$ and the covariance $\Sigma(S_{i,t}, A_{i,t})$, which are estimated through a bootstrap ensemble of probabilistic neural networks. The number of bootstraps is set to 5, as recommended by Lakshminarayanan et al. [2017]. Each neural network contains five layers, with 200 nodes in each hidden layer and ReLU activation function.

ODCP To implement the ODCP method [Padakandla et al., 2020], we first map the state-action pairs at each time point to compositional data, and second apply the Dirichlet likelihood test for change point detection. Specifically, for each t, we obtain transformed compositional data through the multi-dimensional expit function:

$$X_{i,t} := \left(\frac{\exp(S_{i,t})}{1+\exp(S_{i,t}+R_{i,t})}, \frac{\exp(R_{i,t})}{1+\exp(S_{i,t}+R_{i,t})}, \frac{1}{1+\exp(S_{i,t}+R_{i,t})} \right).$$

Next, for each candidate change point $\kappa_j \in (0,T)$, we test the null hypothesis H_0 that the data $\mathcal{D} = \{X_{i,1},\ldots,X_{i,T}\}_{1\le i\le N}$ comes from a single Dirichlet distribution, versus the alternative hypothesis H_1 that the two data chunks $\mathcal{D}_{:\kappa_j} = \{X_{i,1},\ldots,X_{i,\kappa_j}\}_{1\le i\le N}$ and $\mathcal{D}_{\kappa_j:} = \{X_{i,\kappa_j+1},\ldots,X_{i,T}\}_{1\le i\le N}$ come from two Dirichlet distributions. Under H_0, we compute the Dirichlet loglikelihood as $L_0 = \log p(\{X_{i,1},\ldots,X_{i,T}\}_{1\le i\le N} \mid \eta_0)$, where η_0 is the Dirichlet maximum likelihood estimate (MLE). Under H_1, we compute the sum of Dirichlet loglikelihoods as $L_1 = \log p(\{X_{i,1},\ldots,X_{i,:\kappa_j}\}_{1\le i\le N} \mid \eta_L) + \log p(\{X_{i,1},\ldots,X_{i,\kappa_j:}\}_{1\le i\le N} \mid \eta_R)$, where η_L and η_R are the MLEs for the data chunks to the left and right of κ_j. The test statistic Z_{κ_j} is given by $L_1 - L_0$.

The significance of the test is performed through a permutation test. For the w-th permutation of the time points in $(0,T)$, $w = 1,\ldots,500$, we compute a test statistic Z_w^* following the same procedure described above. We reject the null hypothesis if the fraction $\frac{|\{w:Z_w^*>Z^*\}|}{500}$ exceeds the threshold 0.05.

Kernel To implement the kernel-based method [Domingues et al., 2021], at the l-th FQI iteration, we consider the following objective function,

$$Q^{(l+1)} = \arg\min_{Q} \sum_{i,t} K\left(\frac{T-t}{Th}\right) \left\{ R_{i,t} + \gamma \max_a Q^{(l)}(a, S_{i,t+1}) - Q(A_{i,t}, S_{i,t}) \right\}^2, \quad \text{(C.3)}$$

where $K(\cdot)$ denotes the Gaussian RBF basis and h denotes the associated bandwidth parameter taken from the set $\{0, 0.1, 0.2, 0.4, 0.8, 1.6\}$. According to (C.3), the kernel-based method assigns larger weights to more recent observations to deal with nonstationarity. After we receive the kth data batch, we sample $B \gg T$ data slices across all individuals from $\{(S_{i,t}, A_{i,t}, R_{i,t}, S_{i,t+1}; 1 \le i \le N)\}_{0\le t<T+kL}$ with weights proportional to $K((T-t)/(Th))$ and apply the decision tree regression to these samples to solve (C.3).

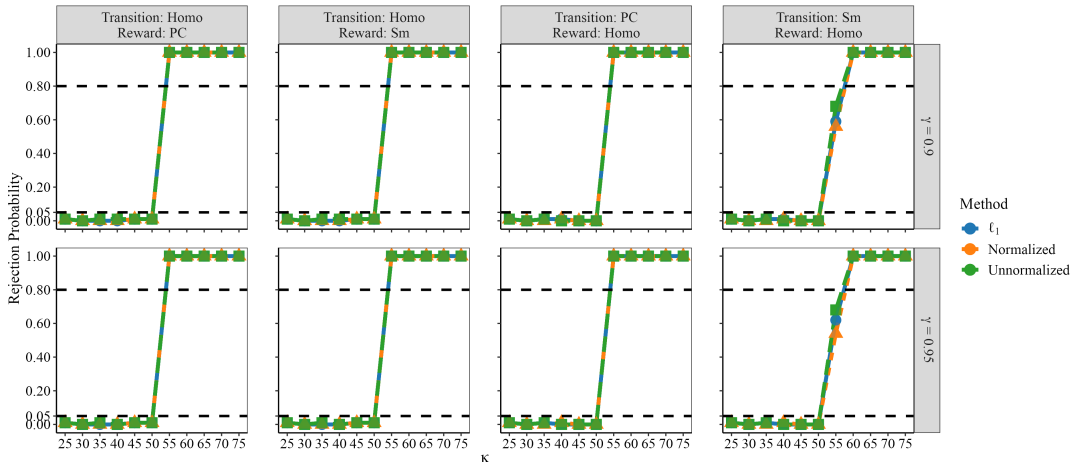

(a) Rejection probabilities.

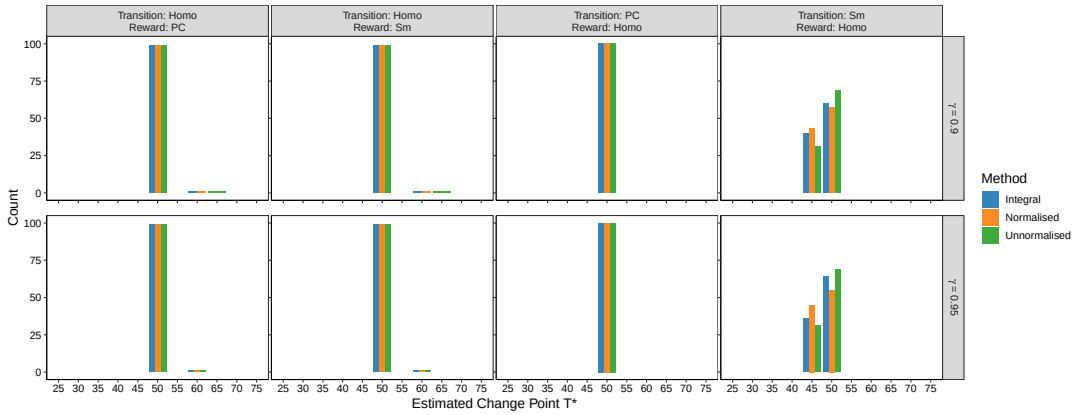

(b) Detected change points.

Figure C.2: Empirical type I errors and powers of the proposed test and their associated 95% confidence intervals under settings described in Section 5.1, with $N = 100$. Abbreviations: Homo for homogeneous, PC for piecewise constant, and Sm for smooth.

C.4 Additional Simulation Results

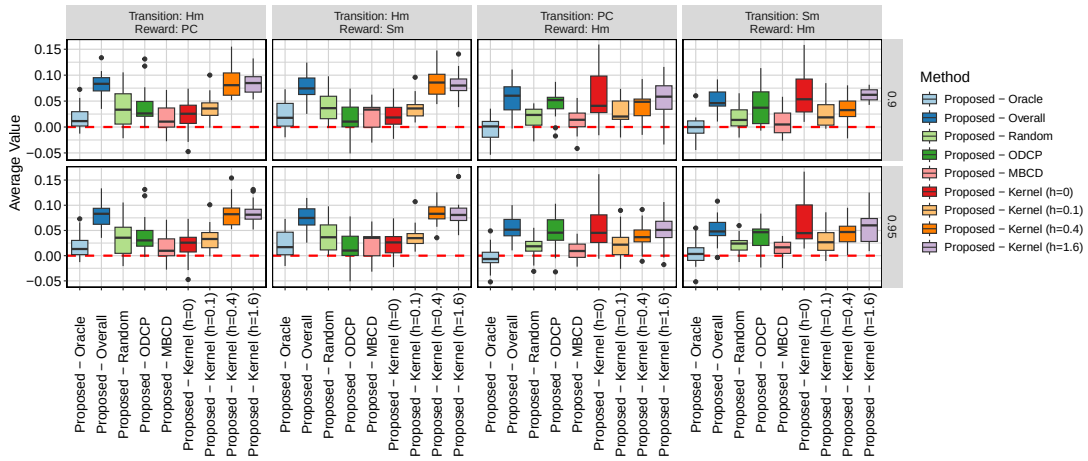

(a) Moderate signal.

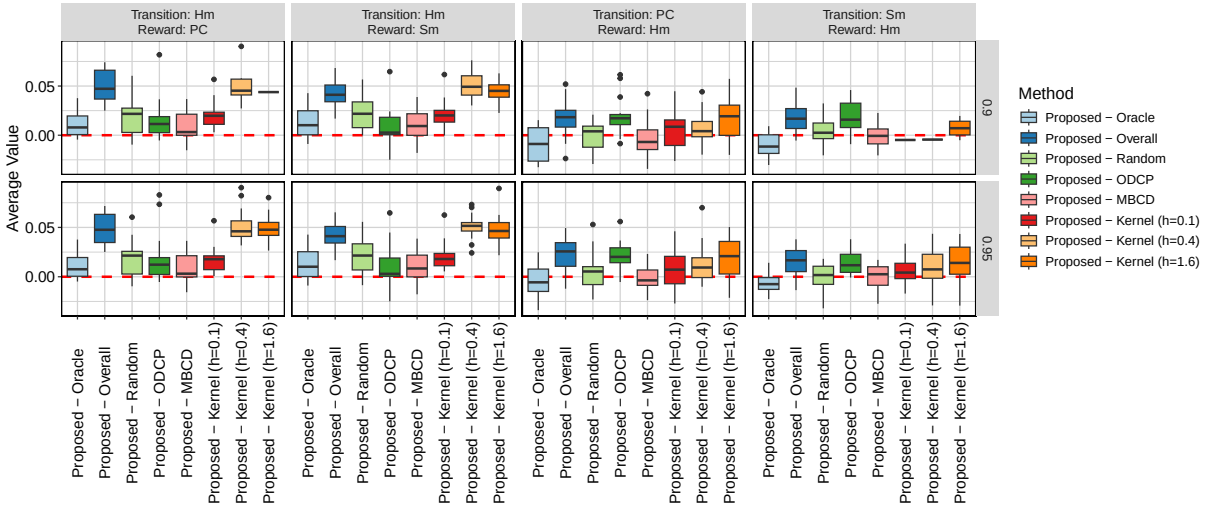

(b) Weak signal.

Figure C.3: Distribution of the difference between the expected return under the proposed policy and those under policies computed by other baseline methods, under settings in Section 5.1 with moderate and weak signal-to-noise ratios. The proposed policy is based on the change point detected by the ℓ_1 type test statistic. In all scenarios, we find the value results based on the normalized or unnormalized test statistics are similar to those of the integral test statistic.

C.5 Real-data-based Simulation

To mimic the IHS study, we simulate $N = 100$ subjects, each observed over $T = 50$ time points. Our aim is to estimate an optimal treatment policy to improve these interns' long-term

physical activity levels. See Section 6 for more details about the study background. At time t, the state vector $S_{i,t}$ comprises four variables to mimic the actual IHS study: the square root of step count at time t ($S_{i,t,1}$), cubic root of sleep minutes at time t ($S_{i,t,2}$), mood score at time t ($S_{i,t,3}$), and the square root of step count at time $t-1$ ($S_{i,t,4} = S_{i,t-1,1}$). These power transformations were applied in accordance with the approaches in NeCamp et al. [2020]. The actions are binary with $\mathbb{P}(A_{it} = 1) = 0.25$; $A_{it} = 1$ means the subject is randomized to receive activity messages at time t, and $A_{it} = 0$ means any other types of messages or no message at all. Reward $R_{i,t} = S_{i,t,1}$ is defined as the step count at time t. We assume that the state transition function has an abrupt change point at time $T^* = 25$. Specifically, we initiate the state variables as independent normal distributions with $S_{i,0,1} \sim \mathcal{N}(20, 3)$, $S_{i,0,2} \sim \mathcal{N}(20, 2)$, and $S_{i,0,3} \sim \mathcal{N}(7, 1)$, and let them evolve according to

$$\begin{pmatrix} S_{i,t+1,1} \\ S_{i,t+1,2} \\ S_{i,t+1,3} \end{pmatrix} = \boldsymbol{W}_1(A_{i,t})\widetilde{S}_{i,t} I\{t \in [0, T^*)\} + \boldsymbol{W}_2(A_{i,t})\widetilde{S}_{i,t} I\{t \in [T^*, T]\} + \boldsymbol{z}_{i,t},$$

where the transition matrices are

$$\boldsymbol{W}_1(A_{i,t}) = \begin{pmatrix} 10 + 0.6A_{i,t} & 0.4 + 0.3A_{i,t} & 0.1 - 0.1A_{i,t} & -0.04 & 0.1 \\ 11 - 0.4A_{i,t} & 0.05 & 0 & 0.4 & 0 \\ 1.2 - 0.5A_{i,t} & -0.02 & 0 & 0.03 + 0.03A_{i,t} & 0.8 \end{pmatrix},$$

$$\boldsymbol{W}_2(A_{i,t}) = \begin{pmatrix} 10 - 0.6A_{i,t} & 0.4 - 0.3A_{i,t} & 0.1 + 0.1A_{i,t} & 0.04 & -0.1 \\ 11 - 0.4A_{i,t} & 0.05 & 0 & 0.4 & 0 \\ 1.2 + 0.5A_{i,t} & -0.02 & 0 & 0.03 - 0.03A_{i,t} & 0.8 \end{pmatrix},$$

$\widetilde{S}_{i,t} = (1, S_{i,t,1}, S_{i,t,2}, S_{i,t,3}, S_{i,t-1,1})^\top$, and $\boldsymbol{z}_{i,t} \sim \mathcal{N}_3(0, \mathrm{diag}(1, 1, 0.2))$ is random noise.

Under this setting, the state transition function is nonstationary whereas the reward is a stationary function of the state. In addition, the data follow the null hypothesis when $\kappa = 1, \ldots, 25$ and follow the alternative hypothesis for $\kappa = 26, \ldots, 49$. The discount factor is set to $\gamma = 0.9$ or 0.95. We test the null hypothesis along a sequence of $\kappa = 10, 15, \ldots, 40$ for every five time points. The number of basis functions is chosen among $\{20, 30, 40, 50, 60\}$.

Figure C.4 shows the empirical rejection rates of the proposed tests as well as the distribution of the estimated change point location. Similar to the results in Section 5.1, our proposed test controls the type I error at the nominal level (see $\kappa < 25$) and is powerful to detect the alternative hypothesis (see $\kappa > 25$). At the true change point where $\kappa = 25$ however, the proposed test fails to control the type I error. We also remark that the reason the proposed test fails at the boundary is because the marginal distribution of the first few states after the change point is very different from the stationary state distribution. After an initial burn-in period of 5 points, the proposed test is able to control the type I error at $\kappa = 20$. In addition, the distribution of the estimated change point concentrates on 30, which is very close to the oracle change point location 25, implying the consistency of the proposed change point detection procedure. We remark that consistency here requires $T^{-1}|\widehat{T}^* - T^*| \xrightarrow{P} 0$ instead of $\mathbb{P}(\widehat{T}^* = T^*) \to 1$, the latter being usually impossible to achieve in change point detection. It also demonstrates the detection delay (i.e., the estimated change point occurs later than its oracle value).

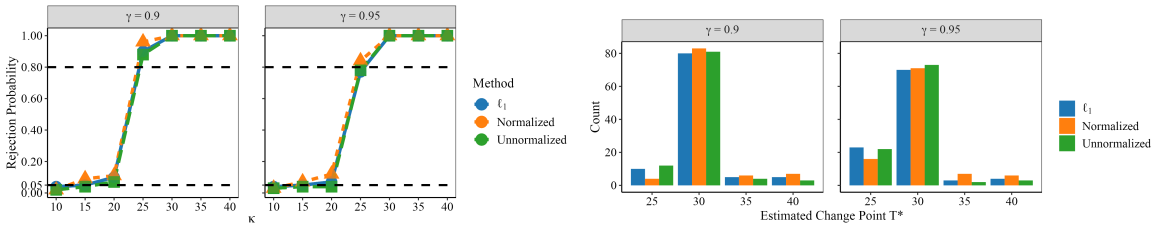

(a) Type I error ($\kappa \leq 25$) and power ($\kappa > 25$) .

(b) Estimated change point $\widehat{T}^* = T - \kappa_{j_0-1}$ where the first rejection occurs at κ_{j_0}.

Figure C.4: Real-data-based simulation: Empirical rejection rates of the proposed tests (ℓ_1-type (3.1), normalized (3.2), and unnormalized (3.3)) and the distribution of the estimated change points.

C.6 More on the IHS Data

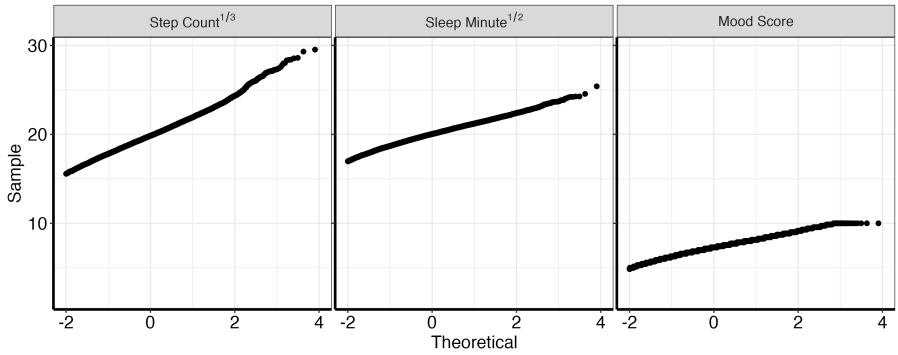

Figure C.5: Quantile-quantile plot of the state variables used in analyzing IHS data in Section 6. After cubic root transformation of weekly average step count and square root transformation of weekly average sleep minutes, the three variables are approximately normally distributed.